



Sara Daniela Filipe Santana

Licenciada em Bioquímica

Magnetic Nanoparticles for Biocatalysis and Bioseparation

Dissertação para obtenção do Grau de Mestre em
Biotecnologia

Orientadora: Prof.^a Doutora Ana Cecília Afonso Roque

Presidente: Prof. Doutor Rui Manuel Freitas Oliveira

Arguente: Doutor Pedro Miguel Vidinha Gomes



FACULDADE DE
CIÊNCIAS E TECNOLOGIA
UNIVERSIDADE NOVA DE LISBOA

Setembro 2011



Sara Daniela Filipe Santana

Licenciada em Bioquímica

Magnetic Nanoparticles for Biocatalysis and Bioseparation

Dissertação para obtenção do Grau de Mestre em
Biotecnologia

Orientadora: Prof.^a Doutora Ana Cecília Afonso Roque

Presidente: Prof. Doutor Rui Manuel Freitas Oliveira

Arguente: Doutor Pedro Miguel Vidinha Gomes



FACULDADE DE
CIÊNCIAS E TECNOLOGIA
UNIVERSIDADE NOVA DE LISBOA

Setembro 2011

Magnetic Nanoparticles for Biocatalysis and Bioseparation

A Faculdade de Ciências e Tecnologia e a Universidade Nova de Lisboa têm o direito, perpétuo e sem limites geográficos, de arquivar e publicar esta dissertação através de exemplares impressos reproduzidos em papel ou de forma digital, ou por qualquer outro meio conhecido ou que venha a ser inventado, e de a divulgar através de repositórios científicos e de admitir a sua cópia e distribuição com objectivos educacionais ou de investigação, não comerciais, desde que seja dado crédito ao autor e editor.

Agradecimentos

De uma forma geral, gostaria de agradecer a todos aqueles que contribuíram para o desenvolvimento da minha tese de mestrado durante este ano.

Em primeiro lugar gostaria de agradecer à minha orientadora Professora Ana Cecília Roque pelo seu apoio, orientação, conhecimento que me transferiu e que abriu os meus horizontes científicos e pela oportunidade de me aventurar em desafios que pensei não ser capaz de alcançar. Obrigada por toda a paciência, compreensão e conversas encorajadoras que fizeram de mim uma pessoa mais autónoma e auto-confiante permitindo-me superar quaisquer receios que eventualmente me pudessem angustiar.

Também quero agradecer aos meus colegas no laboratório pela amizade demonstrada, pelos sorrisos, pelo bom ambiente de trabalho e pela ajuda que sempre disponibilizaram. Especialmente às minhas grandes amigas Ana Pina, Íris Batalha e Telma Barroso.

À Ana Pina, um obrigada pelos almoços na companhia do "gangue do tupperware", pelas risadas que demos juntas, pelos momentos de desabafo em tempos de stress, pelas longas conversas e por alguns puxões de orelhas nos momentos certos. Sempre foste uma pessoa extremamente motivadora e quando precisei de ajuda estavas sempre lá; és uma boa amiga.

Por sua vez, à Íris Batalha quero agradecer toda a ajuda que me deu no laboratório, as úteis discussões e por me ter apresentado este mundo da nanotecnologia sempre com tanto entusiasmo. Mas também por todo o carinho, apoio e pelo positivismo que me transmitiu e que sempre me ajudou a encontrar uma solução mesmo nos momentos em que não parecia haver uma.

Também quero expressar o meus agradecimentos à Telma Barroso por iluminar sempre o meu dia com a sua alegria, força de viver, amizade e as suas histórias engraçadas que me fizeram sempre rir.

Gostaria de agradecer especialmente à minha família por todo o amor, carinho e apoio durante toda a minha vida que fizeram de mim aquilo que sou. Em particular, agradeço aos meus pais e irmã, cada um com a sua forma de carinho, que sempre me

apoiaram e me deram força para alcançar os meus objectivos e mostraram-me que o trabalho recompensa. Um obrigada porque sem o vosso esforço e dedicação eu não teria sido capaz de atingir esta nova etapa da minha vida.

Para a minha madrinha o meu especial agradecimento pelas palavras encorajadoras que sempre me deu.

A todos os meus amigos com quem tenho partilhado os momentos da minha vida e de quem eu tenho muito boas recordações, agradeço uma vez mais por estarem presentes neste momento importante da minha vida, especialmente à minha grande amiga Carolina.

Finalmente quero agradecer ao João, e embora não haja palavras suficientes que possam expressar o amor, amizade e profunda gratidão que tenho por ele e pelo que ele tem feito por mim, quero agradecer-lhe profundamente por toda a sua paciência, carinho e apoio. Um muito obrigada por me conseguires mostrar sempre as palavras certas nos momentos certos!

Resumo

Este trabalho teve como objectivo a síntese e o estudo de nanopartículas magnéticas de óxidos de ferro (MNPs) revestidas com diferentes polímeros, e a sua posterior modificação com enzimas e ligandos sintéticos de afinidade de modo a explorar as suas potenciais aplicações na área da biocatálise e bioseparação.

A adsorção dos biopolímeros - Goma arábica (Ga), Dextrano (Dex) e Polissacárido Extracelular (EPS) - foi efectuada durante a síntese das partículas e a quantidade de polímero adsorvido foi determinado e comparado com os perfis de adsorção de cada polímero. A estabilidade dos suportes magnéticos ao armazenamento e à modificação química foi estudada, tendo-se observado uma elevada estabilidade dos suportes.

A potencial aplicação destes suportes magnéticos em biocatálise foi estudada através da imobilização de uma enzima, Enterocinase (EK), por duas vias químicas distintas. Após imobilização, a actividade enzimática da EK nos suportes magnéticos foi testada com um substrato sintético e duas proteínas de fusão. Após a imobilização da enzima observou-se uma diminuição da sua actividade, que foi compensada pela sua reutilização até dez vezes. O suporte magnético mais promissor foram as MNP_Dex, apresentando uma retenção de actividade de 35% e uma percentagem de conversão de 0,4% no primeiro ciclo de reacção.

A utilização dos suportes magnéticos em processos de bioseparação de IgG foi testada através da imobilização do ligando sintético de afinidade 22/8 às partículas modificadas com biopolímeros, por três diferentes métodos. As MNP_Dex modificadas com o ligando sintetizado directamente no suporte adsorvem cerca de 130 mg IgG/g de MNP e são o suporte que apresenta menor adsorção inespecífica. Para além disso, este suporte revelou ainda especificidade e capacidade de adsorver IgG e seus fragmentos de extractos brutos de proteínas expressas por leveduras e células mamíferas.

Termos Chave: partículas magnéticas; biopolímeros; clivagem enzimática; ligandos de afinidade; purificação.

Abstract

This work aimed to prepare iron oxide magnetic nanoparticles (MNPs) coated with biopolymers and further modified with enzymes and synthetic affinity ligands in order to study their applications in biocatalysis and bioseparation areas.

The adsorption of different biopolymers - Gum Arabic (Ga), Dextran (Dex) and Extracellular Polysaccharide (EPS) - was performed during the synthesis of the particles, and the amount of polymer bound was determined and compared to the adsorption profiles of each polymer. Additionally, the storage and chemical modification stability of these supports was also evaluated. All supports showed high stability.

The eventual application of these magnetic supports in biocatalysis was evaluated through the immobilization of an enzyme, Enterokinase (EK), through two distinct chemistries. The enzyme was then tested with a synthetic substrate and two fusion proteins. After the enzyme's immobilization, its activity was observed to decrease, which was compensated by its re-utilization up to ten times. The most promising magnetic support was the MNP_Dex since it presented an activity retention of 35% and a conversion percentage of 0.4% in the first reaction cycle.

The utilization of magnetic supports for the purification of IgG was tested through the immobilization of the synthetic affinity ligand 22/8 using three different methods. The MNP_Dex support modified with the ligand synthesized directly on the solid support adsorbed around 130 mg of IgG/g of MNP and presented less nonspecific adsorption. Moreover, this support presented specificity and capability to adsorb IgG and its fragments from crude extracts expressed in yeast and mammalian cells.

Keywords: magnetic nanoparticles; biopolymers; enzyme cleavage; affinity ligands; purification.

Contents

Agradecimientos	i
Resumo	iii
Abstract.....	v
Contents.....	vii
Index of Figures	xi
Index of Tables.....	xvii
List of Abbreviations.....	xix
1 Literature Review	1
1.1 Nanotechnology as an emerging field	3
1.2 Magnetic Nanoparticles.....	4
1.2.1 Magnetic Nanoparticles and their Properties.....	4
1.2.2 Magnetic Nanoparticles and Their Applications	7
1.3 Magnetic Nanoparticles for Biocatalysis	9
1.3.1 Production and Purification of Recombinant Proteins by tag Protein Fusion .	9
1.3.2 Magnetic Nanoparticles for Enzyme Immobilization	11
1.4 Magnetic Nanoparticles for Bioseparation	13
1.4.1 Production of Antibodies.....	13
1.4.2 Purification of Antibodies through Affinity-Based Strategies	14
1.4.3 Magnetic Nanoparticles for Bioseparation Processes.....	16
1.5 Aim of the Work.....	17
2 Materials and methods	19
2.1 Materials	21
2.1.1 Chemical Compounds.....	21

2.1.2	Biochemical Reagents.....	22
2.1.3	Equipment	22
2.1.4	Kinetics and Screening Material	23
2.1.5	Software.....	23
2.2	Methods	24
2.2.1	Selection and Study of Magnetic Supports	24
2.2.2	Immobilization of Enterokinase onto Magnetic Supports.....	26
2.2.3	Immobilization and Study of 22/8 onto Magnetic Supports	32
2.2.4	Quantification Methods	37
3	Selection and Study of Magnetic Supports	41
3.1	Introduction	43
3.2	Results and Discussion.....	44
3.2.1	Synthesis and Modification of Magnetic Supports	44
3.2.2	Stability of Magnetic Supports	48
3.2.3	Characterization of Magnetic Supports	50
3.3	Conclusions.....	55
4	Magnetic Nanoparticles applied on Biocatalysis	57
4.1	Introduction	59
4.2	Results and Discussion.....	60
4.2.1	Molecular Structure Analysis and Covalent Immobilization of Enterokinase.....	60
4.2.2	Determination of Reaction Parameters to Monitor the Product Released	63
4.2.3	Activity Studies with Synthetic Substrate of Free and Immobilized Enterokinase.....	66
4.2.4	Optimization and Testing of the Best Supports Selected	72
4.2.5	Fusion protein cleavage by Immobilized EK.....	75
4.3	Conclusions.....	78

5	Magnetic Nanoparticles Applied on Bioseparation	79
5.1	Introduction.....	81
5.2	Results and Discussion	82
5.2.1	Binding Properties of Magnetic Supports to Pure Protein Solutions.....	82
5.2.2	Binding Properties of Magnetic Supports to Crude Extracts	91
5.3	Conclusions	96
6	Concluding Remarks and Future Directions	97
7	Bibliography	101

Index of Figures

Figure 1.1 Representation of Enterokinase: A) Schematic representation of the structure of enterokinase (based on Light and Janska, 1989) and B) EK catalytic subunit structure with the residues of the catalytic center represented in dark red, representation obtained by the program PyMOL (code of pdb: 1ekb).	11
Figure 1.2 Structure of an IgG molecule, where V represents the variable regions, C the constant regions and the domains of the light chain are represented by the L whereas for the heavy chain are represented by the H.	14
Figure 1.3 Schematic representation of a bioseparation process using MNPs as adsorbent.....	16
Figure 1.4 Schematic representation of the research strategy followed in this work. ..	18
Figure 2.1 Schematic representation of amination of magnetic nanoparticles with APTES.	25
Figure 2.2 Schematic representation of EK Immobilization onto MNPs coated with Biopolymers (Gum Arabic, Dextran and EPS) by two different chemistries: A) EDC Coupling and B) Sulfo Coupling.....	27
Figure 2.3 Schematic representation of the Synthetic Affinity Ligand 22/8 Immobilized onto MNPs coated with Biopolymers (Gum Arabic, Dextran and EPS) by three different methods: Method A, Method B and Method C.	33
Figure 2.4 Schematic representation of the chemistry of Kaiser Test	38
Figure 2.5 Schematic representation of the chemistry of Anthrone Method.	39
Figure 2.6 Schematic representation of the chemistry of the Magnetite Method.....	39
Figure 2.7 Schematic representation of the chemistry of the BCA Method to protein quantification.	40
Figure 3.1 Representation of the superparamagnetic properties of MNPs in the present of an external magnetic field.....	44

Figure 3.2 Binding profile of Dextran at the surface of bare iron magnetic nanoparticles: A) Binding profile of different solutions of dextran with different concentrations and B) Binding profile of low dextran concentration at the surface of bare iron magnetic nanoparticles. Representation of q (the amount of bound Dextran in equilibrium per mass of solid support) as function of C_{eq} (the concentration of Dextran in equilibrium). Experimental data was fitted with the expression $q = (Q_{max} \times C_{eq}) / (K_d + C_{eq})$ for the Lagmuir isotherm (using the OriginLab 6.1 software), where Q_{max} corresponds to the maximum concentration of the matrix sites available to the partitioning solute (which can also be defined as the binding capacity of the adsorbent), and K_d is the dissociation constant. 46

Figure 3.3 Storage stability of the synthesized supports along the time, values determined by the anthrone method. 48

Figure 3.4 Chemical modification stability of the synthesized supports, values determined by the anthrone method 49

Figure 3.5 Schematic representation of the synthesis of the carbon coating magnetic nanoparticles based on Sun and Li, 2004; Qi *et al.*, 2009..... 49

Figure 3.6 Quantity of iron released from bare MNPs and carbon coated MNPs at different pHs ($n = 2$). 50

Figure 3.7 Hydrodynamic diameter (nm) of the magnetic supports by dynamic light scattering analysis ($n = 2$).52

Figure 3.8 Zeta Potential values (mV) at pH 7 for magnetic supports by dynamic light scattering analysis ($n = 2$).52

Figure 4.1 Schematic representation of a biocatalysis process using iron oxide magnetic nanoparticles for the immobilization of enzymes and cleavage of tag protein fusion. 59

Figure 4.2 Structure analysis of the catalytic subunit of Enterokinase: Thiol groups available on the surface of EK, represented in red color. This image was produced with the program PyMOL by making use of the crystalline catalytic subunit structure of EK from pdb (accession code 1ekb)..... 61

Figure 4.3 Structure analysis of the catalytic subunit of Enterokinase: A) Carboxylic groups available on the surface of EK, where the orange sticks represent the glutamic acid groups and the blue groups represent the aspartic acid residues and B) Amine

groups available on the surface of EK, where the pink groups represent the lysine residues and the light blue represent the arginine groups. This image was produced with the program PyMOL by making use of the crystalline structure of EK from pdb (accession code 1ekb).	62
Figure 4.4 Adsorption spectra of 2-NA solutions at different concentrations.	63
Figure 4.5 Fluorescence intensity spectra of 2-NA solutions at different concentrations by making use of the excitation wavelength of 334 nm.	64
Figure 4.6 Comparasion of the absorption values between GD ₄ K-2NA and 2-NA at the same concentration (1 mM).....	64
Figure 4.7 Comparison of fluorescence intensity values between GD ₄ K-2NA and 2-NA at the same concentration values (0.001 mM) with an excitation wavelength of 340 nm.	65
Figure 4.8 Schematic representation of the action of EK immobilized on the substrate GD ₄ K-2NA and consequent release and quantification of the product 2-NA obtained.	65
Figure 4.9 Quantity of enterokinase immobilized on magnetic nanoparticles by two different chemistries (n = 2).....	66
Figure 4.10 Percentage of substrate converted by EK immobilized on different magnetic supports through EDC Coupling. The reaction solution was removed after 24 hours and new solution was added for a new cleavage reaction. The set reaction conditions involved 25 µl of 1 mM GD ₄ K-2NA in 50 mM Tris-HCl, pH 7.4 incubated with 1 mL of magnetic support containing EK immobilized.	69
Figure 4.11 Percentage of substrate converted by EK immobilized on different magnetic supports through Sulfo Coupling. The reaction solution was removed after 24 hours and new solution was added for a new cleavage reaction. The set reaction conditions involved 25 µl of 1 mM GD ₄ K-2NA in 50 mM Tris-HCl, pH 7.4 incubated with 1 mL of magnetic support containing EK immobilized.	70
Figure 4.12 Hydrodynamic diameter (nm) of the magnetic supports immobilized with EK by EDC Coupling by dynamic light scattering analysis (n = 2).	71
Figure 4.13 Zeta Potential values at pH 7 for magnetic supports immobilized with EK by Sulfo Coupling by dynamic light scattering analysis (n = 2).....	71

Figure 4.14 Comparison of the quantity of Enterokinase immobilized on MNP_Dex by the two different chemistries before and after optimizing the immobilization conditions (n = 2).....72

Figure 4.15 Percentage of substrate converted by EK immobilized on different MNP_Dex by the EDC and Sulfo Coupling. The reaction solution was removed after 24 hours and new solution was added for a new cleavage reaction. The set reaction conditions involved 25 µl of 1 mM GD4K-2NA in 50 mM Tris-HCl, pH 7.4 incubated with 1 mL of magnetic support containing EK immobilized. 74

Figure 4.16 Electrophoreses gel 12,5 % in denaturation conditions to verify the digestion of the Cleavage Control Protein: A) Digestion of Cleavage Control Protein by soluble Enterokinase and B) Digestion of Cleavage Control Protein by immobilized Enterokinase: LMW (Low Molecular Weight).77

Figure 4.17 Electrophoreses gel 12,5 % in denaturation conditions to verify the digestion of the Fusion Protein: A) Digestion of Fusion Protein by soluble Enterokinase and B) Digestion of Fusion Protein by immobilized Enterokinase: LMW (Low Molecular Weight).....77

Figure 5.1 Binding of Human IgG to different solid supports modified with synthetic affinity ligand 22/8 (artificial protein A) - Results normalized per gram of particles used in each assay (n = 2). 84

Figure 5.2 Binding of Human IgG to different solid supports modified with synthetic affinity ligand 22/8 (artificial protein A) – Results normalized per µmol of amine available in each support (n = 2). 85

Figure 5.3 Human IgG eluted from magnetic supports at 50 mM Glycine – NaOH, pH 11 (n = 2). 86

Figure 5.4 Binding of Albumine Serum Bovine and Human IgG to MNP_Dex modified with ligand 22/8 through the Method C (n = 2). 87

Figure 5.5 Binding of hIgG at the surface of MNP_Dex modified with ligand 22/8 by Method C. Representation of q (the amount of bound hIgG in equilibrium per mass of solid support) as function of C_{eq} (the concentration of hIgG in equilibrium). Experimental data was fitted with the expression $q = (Q_{max} \times C_{eq}) / (K_d + C_{eq})$ for the Lagmuir isotherm (using the OriginLab 6.1 software), where Q_{max} corresponds to the maximum concentration of the matrix sites available to the partitioning solute

(which can also be defined as the binding capacity of the adsorbent), and K_d is the dissociation constant.....88

Figure 5.6 Hydrodynamic diameter (nm) of the magnetic support modified with synthetic affinity ligand 22/8 through Method C by dynamic light scattering analysis ($n = 2$).89

Figure 5.7 Zeta Potential values (mV) at pH 7 of the magnetic support modified with synthetic affinity ligand 22/8 through Method C by dynamic light scattering analysis ($n = 2$).90

Figure 5.8 Electrophoreses gel 12,5 % in denaturation conditions to verify the binding capacity and the best elution conditions for ScFv from the MNP_Dex_22/8. LMW (Low Molecular Weight); Loading (Sample of the crude extract incubated with the adsorbent); FT (Flowthrough); W₁ (First Wash with Binding Buffer); W₂ (Second Wash with Binding Buffer); W₃ (Third Wash with Binding Buffer); E₁ (First Elution with 50 mM Glycine – HCl, pH 3); E₂ (Second Elution with 50 mM Glycine – HCl, pH 3); E₁* (First Elution with 50 mM Glycine – HCl, pH 11); E₂* (Second Elution with 50 mM Glycine – HCl, pH 11).93

Figure 5.9 Electrophoreses gel 12,5 % in desaturating conditions to verify the inertness of MNP_Dex for ScFv. LMW (Low Molecular Weight); Loading (Sample of the crude extract incubated with the adsorbent); FT (Flowthrough); W₁ (First Wash with Binding Buffer); W₂ (Second Wash with Binding Buffer); W₃ (Third Wash with Binding Buffer); E₁ (First Elution with 50 mM Glycine – HCl, pH 3); E₁* (First Elution with 50 mM Glycine – HCl, pH 11).93

Figure 5.10 Electrophoreses gel 12,5 % in denaturation conditions to verify the inertness of MNP_Dex for Mabs. LMW (Low Molecular Weight); Loading (Sample of the crude extract incubated with the adsorbent); FT (Flowthrough); W₁ (First Wash with Binding Buffer); W₂ (Second Wash with Binding Buffer); W₃ (Third Wash with Binding Buffer); E₁ (First Elution with 50 mM Glycine – HCl, pH 3); E₁* (First Elution with 50 mM Glycine – HCl, pH 11).94

Figure 5.11 Electrophoreses gel 12,5 % in denaturation conditions to verify the inertness of MNP_Dex for Mabs. LMW (Low Molecular Weight); Loading (Sample of the crude extract incubated with the adsorbent); FT (Flowthrough); W₁ (First Wash with Binding Buffer); W₂ (Second Wash with Binding Buffer); W₃ (Third Wash with

Binding Buffer); E1 (First Elution with 50 mM Glycine – HCl, pH 3); E1* (First Elution with 50 mM Glycine – HCl, pH 11).....	94
------------------------------------------------------------------------------------------------------------------------------	----

Index of Tables

Table 1.1 Summarized comparison of the different synthesis methods of Magnetic Nanoparticles (Adapted from Lu <i>et al.</i> , 2007).....	5
Table 1.2 Known methods of Enterokinase immobilization onto specific support materials.	12
Table 1.3 Purification of antibodies by affinity methodologies using biological and synthetic affinity ligands with purity percentage for each strategy.	15
Table 2.1 Strategies used to synthesize magnetic nanoparticles coated with different biopolymers.....	25
Table 2.2 Necessary volumes to prepare two gels 12.5% of Acrilamide/Bisacrilamide. .	31
Table 3.1 Parameters adjusted for the synthesis of MNP coated with Gum Arabic, Dextran and EPS by the co-precipitation method according to Roque <i>et al.</i> , 2009; Marcos, 2010.	45
Table 3.2 Degre of amination of the magnetic supports synthesized, values measured by the Kaiser test (n = 4).	48
Table 3.3 Hydrodynamic Diameter and Polydispersitivity values for magnetic nanoparticles (n = 2).	51
Table 4.1 Percentage of residues and total groups available on the surface of the catalytic subunit of Enterokinase. Note: These values were estimated taking into account only the residues on the surface and discarding the residues near the binding site.	62
Table 4.2 Immobilization methodologies for enterokinase to magnetic nanoparticles yielding the quantity of EK immobilized and activity retention.	67
Table 4.3 Immobilization methodologies for Enterokinase to magnetic nanoparticles yielding the quantity of EK immobilized and activity retention after optimizing immobilization conditions (n = 2).	73

Table 4.4 Characterization of the hydrodynamic diameter (nm) and Zeta Potential (mV) values by DLS of MNP_Dex with EK immobilized by two different chemistries (n = 2).	74
Table 5.1 Binding of hIgG to bare agarose and magnetic supports, being the agarose results from Batalha <i>et al.</i> , 2010 (n = 2).	84
Table 5.2 Comparison of binding isotherm of human IgG to immobilized protein A and ligand 22/8 onto agarose (Teng <i>et al.</i> , 2000) to ligand 22/8 immobilized on MNP_Dex through Method C.....	88
Table 5.3 Hydrodynamic Diameter and Polydispersity values for MNP_Dex modified with ligand 22/8 by Method C.	89

List of Abbreviations

2-Na - 2-naphtylamide

APTES - Aminopropyltriethoxysilane

BCA – Bicinchnonic Acid

Dex – Dextran

DLS – Dynamic Light Scattering

EDC - N-(3-dimethylaminopropyl)-N'-ethylcarbodiimide

EDTA - Ethylenediaminetetraacetic acid

EPS - Extracellular Polysaccharide

EK – Enterokinase

FDA - Food and Drugs Administration

Ga - Gum Arabic

GD₄K - 2NA - Gly-Asp-Asp-Asp-Lys-2-naphtylamide

HGMS - High Gradient Magnetic Separation

MNP_Dex - MNP coated with Dextran

MNP_Dex_EK_EDC – EK immobilized by EDC coupling onto MNP coated with Dextran

MNP_Dex_EK_Sulfo - EK immobilized by Sulfo coupling onto MNP coated with Dextran

MNP_Dex_22/8 – Synthetic affinity ligand 22/8 immobilized onto MNP coated with dextran

MNP_EPS - MNP coated with EPS

MNP_EPS_22/8 - Synthetic affinity ligand 22/8 immobilized onto MNP coated with EPS

MNP_Ga - MNP coated with Gum Arabic

MNP_Ga_22/8 - Synthetic affinity ligand 22/8 immobilized onto MNP coated with Gum Arabic

MNP(s) - Magnetic Nanoparticle(s)

MRI - Magnetic Resonance Imaging

Mabs - Monoclonal Antibodies

NHS ester - N-hydroxysuccinimide

NNI - National Nanotechnology Initiative

PSA - Ammonium Persulphate

scFv - Single-chain antibody Fragment

Sulfo-SMCC - 4-(N-Maleimidomethyl)cyclohexane-1-carboxylic acid 3-sulfo-N-hydroxysuccinimide ester sodium salt

TEMED - N,N,N,N - Tetramethylethylenediamine

1 LITERATURE REVIEW

This first chapter describes the unique properties and some applications of magnetic nanoparticles. In particular, the advantages of implementing these materials in the biocatalysis and bioseparation fields are discussed. Finally, the motivation for this work is presented.

1.1 Nanotechnology as an emerging field

In recent years, most of the technological revolutions have focused on the ability to create products with smaller dimensions, but with higher precision. This principle is particularly true at the level of nanotechnology (deMello and Woolley, 2010). Thus, nanotechnology refers to the creation and use of materials, devices and systems through control of matter at the nanoscale, to create new materials with different functional characteristics of the common materials. It is defined by the National Nanotechnology Initiative (NNI) as the understanding of matter at dimensions of roughly 1 to 100 nm as a unique phenomenon that enables new applications (Roco, 2004). Nanotechnology is a multidisciplinary field, combining different knowledge areas such as chemistry, physics, biology and engineering (Roco, 2004; Fatehi *et al.*, 2011).

In order to develop nanotechnology two approaches can be followed: the bottom - up strategy, which involves the assembly of smaller units to obtain a larger structures and the top - down strategy, which involves ultra-miniaturization from larger materials (Ramsden, 2005; Shoseyov and Levy, 2008). Through the bottom - up strategy appears the nanobiotechnology concept, which is defined as the incorporation of nanoscale devices into biological organisms in order to improve monitoring, regulation and characterization of the biological processes and systems (Shoseyov and Levy, 2008; Amin *et al.*, 2011).

Overall, nanotechnology is an interdisciplinary area with great potential to create new discoveries in main areas such as materials, nanoelectronics, medicine and healthcare, biotechnology and information technology, as well as, to bring together different fields of science (Bhushan, 2004; deMello and Woolley, 2010; Amin *et al.*, 2011).

1.2 Magnetic Nanoparticles

In the last decades the interest in the use of nanomaterials, in special nanoparticles, has increased markedly because these materials combine the fields of material science and biology with a view of numerous technological applications (De *et al.*, 2008). The growing interest in nanoparticles comes from the fact that these materials possess unique properties dependent on their size and also can be modified with different materials and biomolecules (Liu, 2006; De *et al.*, 2008). A considerable emphasis has been given to Magnetic Nanoparticles (MNPs) due to their properties, especially the superparamagnetic phenomena which have found remarkable applications in different areas (Safarik and Safarikova, 2009).

1.2.1 Magnetic Nanoparticles and their Properties

Iron oxide nanoparticles are an important class of inorganic nanomaterials being the most promising materials of this class the magnetite (Fe_3O_4) and maghemite ($\gamma - \text{Fe}_2\text{O}_3$) due to their biocompatibility (Gupta and Gupta, 2005; Wu *et al.*, 2008; Boyer *et al.*, 2010). The magnetite material presents a tetrahedrally - octahedrally coordinated structure with the iron atoms coordinated with oxygen atoms (Grillo *et al.*, 2008). These particles act as Lewis acids because the iron atoms can coordinate with molecules that donate lone-pair electrons (Laurent *et al.*, 2008; Dias *et al.*, 2011). So, depending on the medium in which the MNPs are dissolved the surface charge varies, considering an isoelectric point around pH 6.8. Consequently, below isoelectric point occurs protonation of the particles and H^+ coordinate to the oxygen atoms and the surface became positively charged. On the other hand above the isoelectric point desprotonation occurs and leads to the formation of a negatively charged surface. At neutral solutions Fe-OH groups are formed and the charge of the surface of the particles slightly decreases (JianHan *et al.*, 2007; Dias *et al.*, 2011).

MNPs attract attention due to their distinguished features such as superparamagnetism, no coercitivity, and high magnetic susceptibility. These superparamagnetic properties correspond to an intermediate state between paramagnetic and ferromagnetic, which means that these materials are magnetized when exposed to a magnetic field but they lose the magnetic properties once the magnetic field is removed. These materials are well-known by not having the so-called magnetic memory (Gupta and Gupta, 2005; Huber, 2005; Boyer *et al.*, 2010; Dias *et al.*, 2011). Apart from its magnetic proprieties, MNPs are also biocompatible, easy to

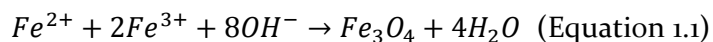
synthesize and subsequently coat and functionalize. They also present unique versatility provided by the high surface area to volume ratio, which translates in high loading, and minimum diffusion limitations due to the fact of these materials being non-porous which reduces mass transfer limitations (Fang and Zhang, 2009; Boyer *et al.*, 2010; Won *et al.*, 2010; Dias *et al.*, 2011).

MNPs can be synthesized through several methods, such as co-precipitation, thermal decomposition, microemulsion and hydrothermal synthesis, as summarized in Table 1.1 (Lu *et al.*, 2007; Laurent *et al.*, 2008).

Table 1.1 Summarized comparison of the different synthesis methods of Magnetic Nanoparticles (Adapted from Lu *et al.*, 2007).

Synthesis Method	Reaction Temperature	Size distribution	Shape control	Yield
Co-precipitation	20 – 90 °C	Relatively narrow	Not good	High / scalable
Thermal decomposition	100 – 320 °C	Very narrow	Very good	High / scalable
Microemulsion	20 – 50 °C	Relatively narrow	Good	Low
Hydrothermal Synthesis	220 °C	Very narrow	Very good	Medium

The most common, efficient and easy method to synthesize magnetite is the co-precipitation method which is based in the reaction between ferric and ferrous ions (in a molar ratio of 1:2) under basic conditions and oxygen-free environment (Equation 1.1). The formation of the particles is firstly based in the formation of the crystalline nuclei (called as nucleation) when the medium is supersaturated, followed by crystal growth by diffusion of the solutes to the surface of the crystal (Gupta and Gupta, 2005; Laurent *et al.*, 2008).



The main advantage of this method is the high quantity of particles that can be synthesized. The size distribution of MNPs is difficult to control as it only depends of kinetic factors. In order to control size, shape, properties and dispersibility of the MNPs several parameters (type of salt used, temperature, pH range, concentration, stirring rate) can be adjusted (Laurent *et al.*, 2008; Wu *et al.*, 2008). It has already been studied that the Fe^{2+}/Fe^{3+} ratio and iron concentration are determinant factors in size, morphology and magnetic properties of MNPs in the co-precipitation method. A homogeneous core formation is obtained in presence of Fe^{2+}/Fe^{3+} molar ratio close to

0.5, because the decrease of this ratio induces the appearance of an initial deposit and for values of this ratio above 0.6 the average particle size increases. The iron concentration is the second most relevant parameter with an optimum value between 39 and 78 mM and an explanation similar to that of the $\text{Fe}^{2+}/\text{Fe}^{3+}$ ratio. These parameters combined with high pH, ionic strength and nitrogen bubbling contributes for the decrease of the size of the particles (Babes *et al.*, 1999; Laurent *et al.*, 2008).

Despite the work that has been made to synthesize MNPs with higher quality, stability and dispersibility, it still continues to be one of the major problems (Gupta and Gupta, 2005; Lu *et al.*, 2007; Laurent *et al.*, 2008; Dias *et al.*, 2011). This low colloidal stability is associated with the highly active surface and with the high surface area to volume that creates a high energy on the surface of the particles and in order to diminish this energy, the particles tend to agglomerate. Both phenomena influence the size, shape and stability of the particles when in solution (Ditsch *et al.*, 2005; Kuchibhatla *et al.*, 2005; Lu *et al.*, 2007). Since the loss of stability has some drawbacks for the application of MNPs in certain areas, particularly those where MNPs are required in aqueous media, it is essential to develop strategies of stabilizing these particles. Different materials have been investigated to coat these particles and improve their properties (Gupta and Gupta, 2005; Lu *et al.*, 2007; Dias *et al.*, 2011).

The coating of MNPs consists in the protection of the core structure with a layer through encapsulation or hydrophobic interactions, in order to isolate the core against harsh conditions, which improve biocompatibility of the particles and increase functionalization for further modifications (Lu *et al.*, 2007; Fang and Zhang, 2009; Dias *et al.*, 2011). The coatings most commonly used include: organic coatings such as surfactants and polymers or inorganic coatings as silica, carbon and precious metals (Lu *et al.*, 2007). For the surface coating of MNPs different strategies can be applied, since in-situ coatings to post-synthesis coatings. In the last years the coating of MNPs with polymers, particularly biopolymers such as polysaccharides, attracted attention of researchers to be known to increasing biocompatibility, chemical functionality and colloidal stability of different materials, such as carbon nanotubes and silver and gold nanoparticles. However, these materials were also chosen because they are renewable, non-toxic and biodegradable which make them an environmental and sustainable choice (Dias *et al.*, 2011).

Polysaccharides are structures formed of repeating units (either mono- or disaccharides) interconnected by glycosidic bonds. These structures are often linear or branched (Dias *et al.*, 2011). Some of the polysaccharides used for covering MNPs,

include agarose (Nixon *et al.*, 1992), alginate (Ma *et al.*, 2007), chitosan (Kievit *et al.*, 2009), starch (Kim *et al.*, 2003), dextran (Hradil *et al.*, 2007) and gum arabic (Roque *et al.*, 2009). The biopolymers chosen to use in this work were Gum Arabic (Ga), Dextran (Dex) and Extracellular Polysaccharide (EPS).

Gum Arabic is a natural gum taken from acacia tree steams. It is a negatively charged polysaccharide being mainly composed by 44% of galactose, 27% arabinose, 16% glucuronic acid, 13% rhamnose and 2-3% of peptide moieties. It finds applications in the food and pharmaceutical industries due to its excellent emulsifying properties and for the controlled release of actives and flavor compounds (Dias *et al.*, 2011).

Dextran a neutral polysaccharide is known for its several applications in the biomedical areas and to be the oldest polymer for coating MNPs. It is produced by certain lactic acid bacteria and it is mainly constituted of glucose molecules of several chain lengths and molecular weights (Dias *et al.*, 2011).

Finally, EPS which is also a negatively charged polysaccharide was used. This is a high molecular weight biopolymer mainly constituted by several neutral sugars as galactose, which is the most abundant monosaccharide, mannose, glucose and rhamnose and a small portion of acyl groups as pyruvil, succynil and aceyl. EPS is produced by a culture of gram-negative bacteria (*Pseudomononas oleovorans*) using glycerol as carbon source. But since this is a byproduct of biodiesel production it is available in high quantity and reduces the cost of production of this biopolymer making this polysaccharide a profitable choice for MNPs coating (Freitas *et al.*, 2009).

Biopolymers can also be used for increasing surface functionalization with promising active groups. Various biological molecules such as antibodies, targeting ligands and catalytically active species can modify the surface of these particles creating multifunctional supports with an enormous range of applicability, as explained below (Gupta and Gupta, 2005; Lu *et al.*, 2007; Dias *et al.*, 2011).

1.2.2 Magnetic Nanoparticles and Their Applications

The superparamagnetic properties of MNPs find interesting applications in the biomedical and biotechnological areas (Safarik and Safarikova, 2009; Dias *et al.*, 2011). In the biomedical area, MNPs have tremendous potential in cancer treatment by hyperthermia, magnetic resonance imaging (MRI), cellular therapy and labeling, tissue engineering, gene and drug delivery (Dias *et al.*, 2011). This preference is due to the superparamagnetic behavior that allows MNPs to be distal controlled or thermal

activated. It is also emphasized the relationship between the size of the particles and their movement in living organisms (Corchero and Villaverde, 2009; Dias *et al.*, 2011). In terms of biotechnological applications, MNPs are applied in bioseparation processes, biosensing, biocatalysis, bioremediation and magnetofection (Dias *et al.*, 2011). The major benefits of using these particles in the biotechnological and bioengineering areas are the low-cost, speed, scalability and compatibility with complex biological suspensions (Batalha *et al.*, 2010).

Despite the several applications listed for MNPs the present work focus on MNPs applied to the biocatalysis and bioseparation fields.

1.3 Magnetic Nanoparticles for Biocatalysis

Enzymes are extremely used in several industrial applications due to their unique properties, such as specificity, mild reaction conditions, biodegradability which translates into higher chemical precision and less side reactions. However, they have some problems associated to their use, such as short lifetimes, deactivation under harsh conditions and cost. The immobilization of enzymes, specifically in MNPs, brings a lot of advantages in the biocatalysts field. One of the main benefits is the potential for reusability and the easy recovery due to the magnetic proprieties of the solid support used (Kim *et al.*, 2006).

1.3.1 Production and Purification of Recombinant Proteins by tag Protein Fusion

The market of recombinant proteins for biopharmaceutical applications has grown immensely and these proteins produced need to be highly purified and well characterized but at the same time economically profitable. Consequently, tag protein fusion became an essential tool to achieve the high standards required to implement these products and to reduce costs.

A tag protein fusion system is a system based in the expression of a peptide fused with a protein of interest. Afterwards the tag protein fusion is purified in a chromatographic system against a specific affinity ligand for the tag (Waugh, 2005). Examples of tags commonly used are hexahistidine, maltose-binding protein, streptavidin, glutathione-S-transferase (Jenny *et al.*, 2003). The major advantage of this system is the facile detection and purification of recombinant proteins by reducing the chromatographic steps needed to purify a protein, which becomes economically viable. Also, the insertion of a tag at the N-terminal position in an expression system is known to have influence in the production of the recombinant protein by improving protein yield, solubility and enhancing the correct folding of the protein (Hu *et al.*, 2001; Terpe, 2003; Waugh, 2005; Arnau *et al.*, 2006; Gasparian *et al.*, 2011).

However, after the affinity-purification step it is crucial to remove the affinity tag. This step is essential according to the application for the purified product because the affinity tag might interfere with the structure or biological activity of the target protein. For the cleavage of the tag, a chemical treatment can be employed. In this method the reagents used are inexpensive, accessible and easily to scale-up. However,

denaturation of the proteins may occur due to the harsh conditions applied. Enzymatic cleavage is often preferred because of the higher selectivity and milder reaction conditions, which do not affect the structure of the protein. However soluble enzymes are costly and unstable. The most used protease enzymes are factor Xa, thrombin, tobacco etch virus (TEV) and enterokinase (EK) (Hu *et al.*, 2001; Jonasson *et al.*, 2002; Terpe, 2003; Waugh, 2005).

EK is a very popular enzyme used for proteolytic cleavage, because it cleaves with high specificity after the sequence (Asp)₄Lys, which allows the fusion protein to preserve its native amino-acid terminus without any additional unwanted cleavage amino-acid residues from the recognition sequence (Terpe, 2003; Bosse-Doenecke *et al.*, 2008; Gasparian *et al.*, 2011).

Enterokinase is a membrane-bound protease of the intestine which controls an enzymatic cascade responsible by the intestinal digestion. This activation occurs through the recognition, cleavage and activation of trypsinogen by EK to yield active trypsin responsible for activation of pancreatic zymogens important in the digestion of food. This is a heterodimeric enzyme constituted by a heavy chain of 82-140 kDa that is disulfide linked to a C-terminal light chain of 35-62 kDa. The EK heavy chain is responsible to associate the enzyme to the membrane, whereas the light chain consists on the catalytic subunit (Light and Janska, 1989; Kitamoto *et al.*, 1994; Lu *et al.*, 1997; Lu *et al.*, 1999). The binding site of this subunit consists of three main structural residues, Histidine 57, Asparagine 102 and Serine 195 and the catalytic activity of this enzyme is promoted by a divalent charge (Figure 1.1) (Lu *et al.*, 1999). However, for the cleavage of fusion proteins, the recombinant catalytic subunit of EK alone has superior ability to cleave an artificial fusion protein containing the D₄K recognition sequence (Lu *et al.*, 1997; Gasparian *et al.*, 2011).

So far Enterokinase is known for the cleavage of fusion proteins mainly with therapeutic interest for cancer treatment including, mucin (Bäckström *et al.*, 2003; Ditsch *et al.*, 2005; Dziadek *et al.*, 2005), deacetylases (Li *et al.*, 2004), human growth hormones (Sturmfels *et al.*, 2001) and cytokines (Wagner *et al.*, 2005).

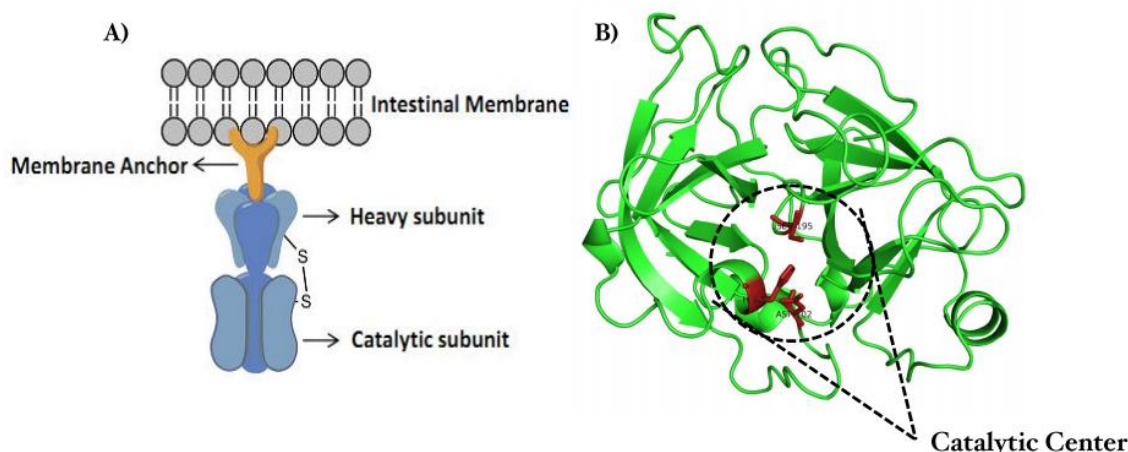


Figure 1.1 Representation of Enterokinase: A) Schematic representation of the structure of enterokinase (based on Light and Janska, 1989) and B) EK catalytic subunit structure with the residues of the catalytic center represented in dark red, representation obtained by the program PyMOL (code of pdb: 1ekb).

1.3.2 Magnetic Nanoparticles for Enzyme Immobilization

The challenging demand for highly stable enzymes to be applied in several processes and products triggered the development of immobilized enzymes (Kim *et al.*, 2006; Kubitzki *et al.*, 2009). Through enzyme immobilization it is possible to reutilize the enzyme, which reduces the costs associated, and allows working in continuous mode. The environment of the enzyme is also more controlled which increases stability (Suh *et al.*, 2005; Kubitzki *et al.*, 2009). However, the immobilization process also leads to changes in the physical and chemical properties of the enzyme with consequent change in the activity of the immobilized enzyme. The main disadvantages of enzyme immobilization are related to the stereochemical and conformational effects, partition effects and the internal and external limitations to mass transfer (Buchholz *et al.*, 2005). Enzyme immobilization consists in the attachment of an enzyme into or onto modified surfaces through adsorption, covalent attachment or encapsulation. Depending on the support used the biocatalyst can have more or less efficiency (Kim *et al.*, 2006).

MNPs appear as an interesting alternative support for enzyme immobilization. These supports present a lot of advantages related to its properties and already proved to be efficient for the immobilization of some enzymes, as for the case of glucose oxidase used in blood glucose sensors (Rossi *et al.*, 2004).

For EK very few methods were developed for its immobilization (Table 1.2). EK has been immobilized on phospholipid vesicles and porous materials and some preliminary studies were also done in the immobilization of this enzyme in

commercial paramagnetic microspheres. Due to the applications of this enzyme in recombinant protein production, it is important to continue developing better immobilization methods.

Table 1.2 Known methods of Enterokinase immobilization onto specific support materials.

Enzyme	Support	References
Catalytic subunit EK	Paramagnetic microspheres	(Kubitzki <i>et al.</i> , 2008)
Catalytic subunit EK	Hexamethylamino Sepabeads	(Kubitzki <i>et al.</i> , 2008)
Catalytic subunit Recombinant EK	Hexamethylamino Sepabeads	(Kubitzki <i>et al.</i> , 2009)
Native EK	Glyoxyl agarose	(Suh <i>et al.</i> , 2005)
Purified bovine EK from duodenal mucosal cells	Reconstituted Soybean phospholipid vesicles	(Fonseca and Light, 1982; Fonseca and Light, 1983)

1.4 Magnetic Nanoparticles for Bioseparation

The demand for high quality of therapeutic proteins but at the same time low cost associated therapies brought the need for exploring different types of separation techniques, in order to improve downstream processing known to be responsible for a significant percentage of the total manufacturing costs. MNPs appear as a viable choice for biotechnological industries, especially for the bioseparation processes since this option can overcome many problems, specifically cost reduction and process integration (Roque *et al.*, 2004; Birch and Racher, 2006; Roque *et al.*, 2007).

1.4.1 Production of Antibodies

Immunoglobulins, also known as antibodies, constitute approximately 20% of the plasma human proteins. These proteins are responsible for the response to foreign molecules or agents in the body to protect the organism against external aggressions and are produced by plasma B-cells as a response of the immune system (Roque *et al.*, 2004).

Antibodies are conventionally represented as a Y-shaped structure, which is distinguished by two identical locations, the antigen-binding regions at the end of the Fab regions (fragment antigen binding) and one Fc (fragment crystallizable) region involved in effector functions. They are constituted by two identical heavy (H) chains of 50 kDa each, carrying covalently attached oligosaccharide groups; and two identical, non-glycosylated light (L) chains of 25 kDa each. The heavy chain and the light chain are linked together by a disulfide bond as well as the heavy chains. All the polypeptide chains contain constant regions (C) found at the carboxyl amino terminal, whereas at the amino terminal portions variable (V) regions are found and these regions are responsible for the affinity and specificity to the target molecules. The antibody structure is represented in Figure 1.2 (Roque *et al.*, 2004).

The success of antibodies as important therapeutic and diagnostic agents is related to the fact that they can bind to a diversity of antigens with high specificity, they present ability to conjugate antibodies with other therapeutic for efficient delivery of these agents to a specific target and also the reduction of side effects (Wang *et al.*, 2007).

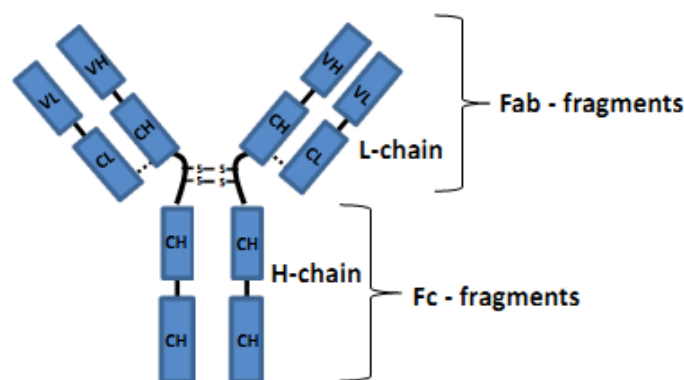


Figure 1.2 Structure of an IgG molecule, where V represents the variable regions, C the constant regions and the domains of the light chain are represented by the L whereas for the heavy chain are represented by the H.

Protein engineering tools allowed the production of immunoglobulin fragments. One of the advantages of using antibodies fragments (Fab, Fc, Single-chain antibody Fragment (scFv)) are the capacity of entering more rapidly in certain targets and also to be cleared from the circulation more rapidly than full size antibodies which increases the applications in certain therapies such as tumor therapy (Marty *et al.*, 2001; Cunha *et al.*, 2004; Wang *et al.*, 2007).

1.4.2 Purification of Antibodies through Affinity-Based Strategies

For the in-vivo administration of the several forms of antibodies a very demanding production and purification is required by FDA (Food and Drugs Administration) in order to avoid contaminations of the therapeutic products and produce safe, pure and consistent products. However, besides the demand for more effective and robust strategies of production and purification, the industries have the challenge to reduce total manufacturing costs. The total costs of antibody production are incurred in the downstream processing which account for 50-80% of the total cost. So, in order to overcome these situations, purification strategies have to be designed to target high purity and yield product and minimum costs associated (Lowe *et al.*, 2001; Roque *et al.*, 2007).

The traditional antibody purification processes involved several steps such as an initial enrichment where water and main contaminants are eliminated by precipitation and filtration techniques, followed by the intermediary purification where chromatographic steps, such as ionic exchange separations, are mainly utilized. Finally, a polishing step to obtain high purity percentage (greater than 95%) are conducted frequently using gel filtration techniques (Roque *et al.*, 2007). This

conventional purification process was substituted by affinity based methodologies (Lowe *et al.*, 2001; Roque *et al.*, 2007).

Affinity based methodologies, are a suitable strategy to purify antibodies because they are based in a selective recognition strategy where the antibody molecule recognizes a specific complementary ligand. Since this binding is highly specific, the nonspecific interactions are reduced with increased yield and also there is elimination of several contaminants without requiring several steps to remove impurities. In the affinity based chromatography a ligand is covalently immobilized onto a solid support, commonly agarose or derivatives. Despite the advantages presented by the affinity methodologies the choice of the affinity ligand it is also important for the purification process. The affinity ligands mostly used to capture antibodies are biospecific ligands which are natural immunoglobulin binding ligands (Protein A, Protein L). However, these ligands are costly, labile and can leach under certain conditions. An alternative and promising choice is the use of synthetic affinity ligands, mimicking the biological ligands, which can be designed based in combination of molecular modeling tools and combinatorial synthesis. These synthetic ligands normally present lower affinity for antibodies but it is still possible to obtain high purity percentage of the products. These ligands are inexpensive, scalable, durable and present extraordinary stability under harsh conditions which improves purification processes of antibodies based on affinity methodologies. Examples of purification of antibodies by affinity methodologies using biological and synthetic affinity ligands are summarized in Table 1.3 (Lowe *et al.*, 2001; Labrou, 2003; Roco, 2004; Roque *et al.*, 2007).

Table 1.3 Purification of antibodies by affinity methodologies using biological and synthetic affinity ligands with purity percentage for each strategy.

Type of Ligand	Target Protein	Ligand	Purity	Reference
Biological Ligands	Mab (mouse IgG _{2b})	Protein A	98%	(González <i>et al.</i> , 2003)
	Bispecific diabody	Protein L	-	(Kriangkum <i>et al.</i> , 2000)
	scFv – Fc fusion protein	Protein G	-	(Powers <i>et al.</i> , 2001)
Biomimetic Ligand	IgG, IgA, IgM	Ligand 22/8	97 – 99 %	(Teng <i>et al.</i> , 2000)
	IgG, Fab	Ligand 8/7	90 – 95%	(Roque <i>et al.</i> , 2005a; Roque <i>et al.</i> , 2005b)

1.4.3 Magnetic Nanoparticles for Bioseparation Processes

Affinity chromatography is the most widely used technique for antibody purification, but presents some limitations when using crude feeds related to the column operation and clogging of the packed bed adsorbents. This requires a clarification step before introduction of the sample in the column, which translates into increased costs and process complexity. One option that has been used to overcome these problems is the bed expanded system. However, this system also suffers limitations of low capacities due to the diffusion limitations and the short contact times for capture protein between the adsorbent beads and the proteins (Bucak *et al.*, 2003; Roque *et al.*, 2004; Ditsch *et al.*, 2006; Roque *et al.*, 2007). MNPs appear as a promising support for magnetic-based separations, since they present minimum diffusion limitations and permit rapid and easy removal of the functionalized MNPs from complex heterogeneous reaction mixtures, without being necessary previously filtration or centrifugation. In addition these supports are of easy manipulation which makes them a good choice for a downstream process (Figure 1.3) (Bucak *et al.*, 2003; Roque *et al.*, 2004; Ditsch *et al.*, 2006; Horák *et al.*, 2007; Roque *et al.*, 2007).

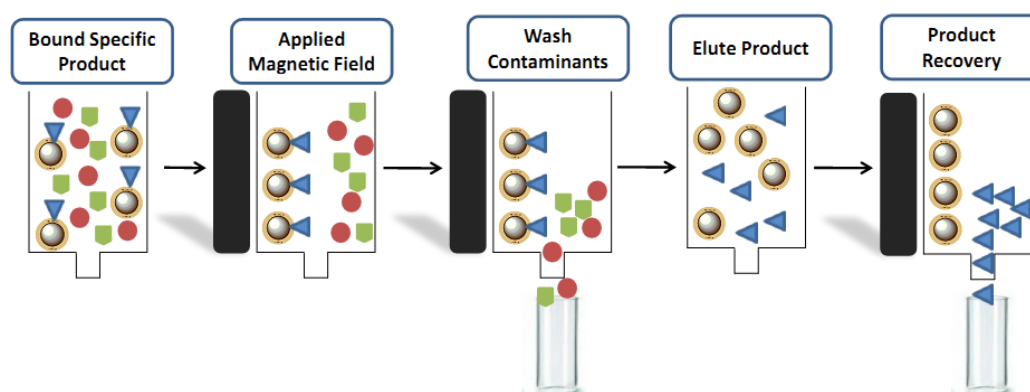


Figure 1.3 Schematic representation of a bioseparation process using MNPs as adsorbent.

In High Gradient Magnetic Separation (HGMS) once the product of interest is bound to MNPs, they are pumped into a separated column controlled by a magnetic field containing a filter. The first step of the separation process is based in switching on the magnetic field to retain the adsorbent, with the product of interest, while contaminants are eliminated. Subsequently fresh solutions of washing buffer enter the column and through cycles of switch on and off of the magnetic field the particles are resuspended and recollected from the washing buffer to eliminate unbound proteins. After washing the particles, the product recovery occurs through passing elution buffer with the magnetic field off to resuspending the particles. Finally, through action of the magnetic field the particles are recovered and the eluted product is purified (Hubbuch *et al.*, 2001; Bucak *et al.*, 2003; Ditsch *et al.*, 2006; Franzreb *et al.*, 2006).

1.5 Aim of the Work

In this thesis, magnetic nanoparticles were explored as solid supports for biocatalysis and bioseparation. MNPs were synthesized with the purpose of producing controlled, stable and biocompatible particles by coating with three different biopolymers, Gum Arabic, Dextran and EPS (Figure 1.4).

Specifically, when magnetic nanoparticles were applied for biocatalysis the enzyme Enterokinase was immobilized by two different chemistries, one based on the carboxylic groups available on the surface of the enzyme and other in the cysteine group available. For both immobilizations strategies the stability and activity of the immobilized enzyme was studied with a synthetic substrate and two fusions proteins.

For the bioseparation field this work focus on modifying magnetic supports with a synthetic affinity ligand which mimics protein A, for the purification of antibodies from purified and unpurified mixtures.

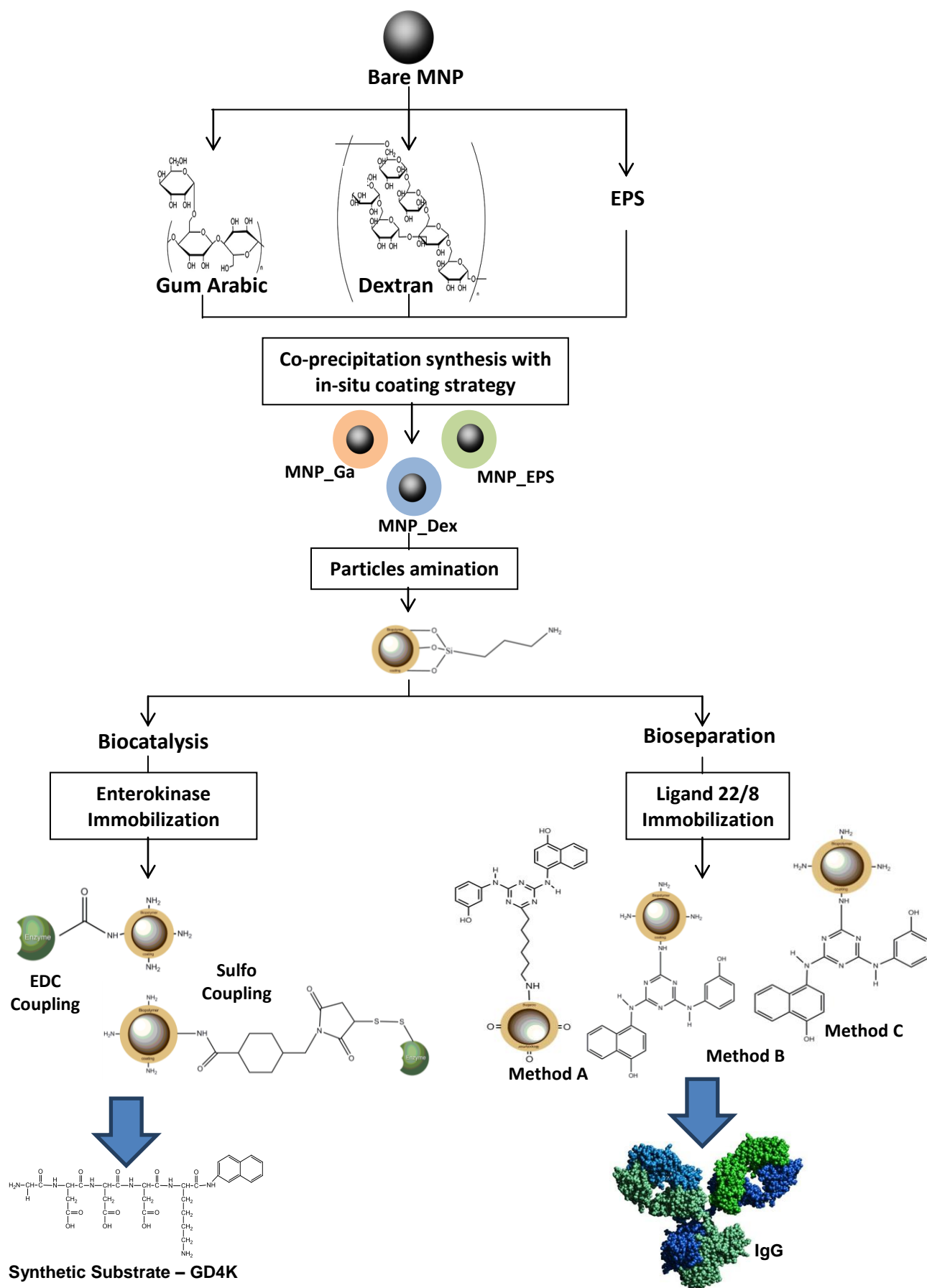


Figure 1.4 Schematic representation of the research strategy followed in this work.

2 MATERIALS AND METHODS

This chapter presents the materials and methods utilized to achieve the intended objectives. In the first section all the chemical compounds, biochemical reagents, equipment and software used are described. In the second section the protocols performed to select and study the magnetic supports, immobilize the selected enzyme and the synthetic affinity ligand are described and schematically represented.

2.1 Materials

2.1.1 Chemical Compounds

The reagents utilized were of the highest grade available.

Glycine 98% (120072500), Hydroxylamine Hydrochloride 97% (17036100) were purchased from Acros. (3-Aminopropyl)triethoxysilane 99% (APTES) (44,014-0), 3-hydroxyanilin (100242), 4-amino-1-naphtol hydrochloride 90% (133485), Cyanuric chloride 99% (S32029-066), N-(3-dimethylaminopropyl)-N'-ethylcarbodiimide (EDC) (39391), N-Hydroxysuccinimide (NHS) (S33678-046), Sodium Citrate Dihydrate $\geq 99\%$ (W302600), Tris(Hydroxymethyl)amino methane (154563) were acquired from Aldrich. Glucose Monohydrate (5996-10-1) was from Fagron. Ammonium hydroxide (25%) (986030501), Ninhydrin $> 99\%$ (33437) were purchased from Fluka. 1,10-phenanthroline 1-hydrate (131321), Ethanol Absolute PA (121086.1212 PA), Hydrochloric acid 37% (1310201211), Sodium Chloride (1316591211), Sodium-di-hydrogen Phosphate 1-hydrate (1319651211), (Di) Sodium-hydrogen Phosphate 2-hydrate (12507.1211), Sodium Hydroxide (1316871211) were from Panreac. Calcium chloride dehydrate (31307) was from Ridel-de Haën. 2-propanol (9866.5), Acetone $\geq 99.5\%$ (5025.5), Hydrochloric acid 1 mol/L (K025.1), L-Cystein (1693.1) were purchased from Roth. 2-Naphtylamide (N8381), Dextran from *Leuconostoc mesenteroides* (D4876), Glutaric dialdehyde 50 wt% sol in water (340855), Gly-Asp-Asp-Asp-Asp-Lys- β -naphtylamide (G5261), Gum arabic from acacia tree (G9752), HEPES (H3375), Iron (III) chloride hexahydrate (307718), Iron (II) chloride tetrahydrate (44939), Phenol (185450), Potassium Cyanide (60178), Pyridine $> 99\%$ (P57506), N,N-Dimethylformamide (319937) were acquired from Sigma. 4-(N-Maleimidomethyl)cyclohexane-1-carboxylic acid 3-sulfo-N-hydroxysuccinimide ester sodium salt (Sulfo-SMCC) (M6035), Anthrone (319899), Ethylenediaminetetraacetic acid (ED) (EDTA), Sodium Bicarbonate (S6014), Sulfuric Acid (258105) were from Sigma – Aldrich. Nitrogen was provided by Air Liquide. The extracellular polysaccharide (EPS) was kindly provided by Prof.^a M.^a Reis from DQ, FCT-UNL.

The protein quantification assay used was Bichinchoninic Acid (BCA) kit from Sigma.

For the SDS-PAGE Gels the reagents used were: 30% Acrylamide /Bis Solution 37.5:1 (161-0158), Sodium dodecyl sulphate Solution 10% (161-0416) purchased from BIO-RAD. Ammonium Persulphate (PSA) (9592.2), N,N,N,N – Tetramethylethylenediamine (TEMED) (2367.3), Bromphenol blue sodium salt (A5212.1) acquired from Roth.

Glycerol (G9012) purchased from Sigma – Aldrich. SDS Micropellets (Sodium dodecyl sulphate) (MBo1501), Tris Base ultra-pure for Molecular Biology (MBo1601), Glycine ultra-pure for Molecular biology (MBo1401) were purchased from NzyTech. 2-Mercaptoethanol (M6250) purchased from Aldrich. Hydrochloric acid 37% (concentrated) (1310201211) acquired from Panreac.

To stain polyacrylamide gels the Silver Stain Plus Kit (161-0449) was used, which includes fixative enhancer concentrate (161-0461), silver complex solution (161-0462), reduction moderator solution (161-0463), image development reagent (161-0464) and development accelerator reagent (161-0448), from BIO-RAD. It was also necessary to use Methanol $\geq 99\%$ (8388.5) acquired from Roth and Acetic Acid Glacial (CAS 64-19-7) purchased from Pronalab.

2.1.2 Biochemical Reagents

For the biocatalysis studies the Enterokinase and Cleavage Control Protein purchased from Novagen (69066-3) and a fusion protein expressed at the Biomolecular Engineering Group, FCT-UNL, were used. For the bioseparation studies the proteins tested were Human Normal Immunoglobulin (Gammanorm) from Octapharma (5044011), Albumin from bovine serum (A7906), from Sigma, and two different crude extracts kindly provided by Prof. Rui Oliveira from REQUIMTE, Portugal, and Dr. Paula Alves from ITQB, Portugal.

The protein marker used in the SDS-PAGE was the Low Molecular Weight SDS Kit (NZYTECH) and Low Molecular Weight Precision Plus Protein Dual Xtra Standards (BIO-RAD).

2.1.3 Equipment

For the MNPs synthesis and chemical modification a mechanic stirrer from IKA, a water-bath SHC 2000 from Scanvac, a Sonicator SilverCrest and a centrifuge Scanspeed mini from Scanlav were utilized, whereas for the carbon coated MNP a GC 6000 vega series 2 from Carlo ERBA instruments was used for the hydrothermal reaction at high temperature.

Hydrodynamic diameter and Zeta Potential measurements of MNPs samples were performed in a Dynamic Light Scattering Zetasizer Nano ZS from Malvern (ITQB, UNL).

The enzymatic kinetic assays were performed in the incubator KS 4000 ic control from IKA, whereas the immobilization of the ligand 22/8 onto the magnetic supports was undertaken in the hybridization oven Boekel Big Shot IIITM from Bockel Scientific. For the adsorption isotherms of Dextran and hIgG onto MNPs a Digital Thermo Mixer Vortemp 56, S2056-A, from Labnet, was utilized.

For the Anthrone and BCA Assays the reactions were incubated in the hybridization oven Boekel Big Shot IIITM from Bockel Scientific, while for the magnetite assay the pH of the reactions were adjusted in a microprocessor based Bench pH/ mV / °C meters from Hanna Instruments.

All the spectrophotometric and spectrofluorometric measurements were taken with the Microplate Reader – Tecan Infinite F200 from Tecan. For the study of the GD4K-2NA and 2-NA fluorimetric spectra a spectrophotometer PerkinElmer Lambda 35 UV/Vis Spectrometer and a spectrofluorimeter PerkinElmer LS 45 Luminescence Spectrometer, were used.

The Mini-Protean Tetra System from BIO-RAD was utilized for the electrophoresis SDS-PAGE gels.

2.1.4 Kinetics and Screening Material

The samples were analyzed in different types of microplates: for UV measurements, UV Star Plate 96 well Flat Bottom Half Area Greiner Bio-one were used; for colorimetric assays the Microplate 96 well Flat bottom Transparent Polystyrene (Starstedt) were utilized and in the fluorescence studies, BRAND Plates - Immunograde Tech Scientific were used.

2.1.5 Software

For the *in silico* analysis of enterokinase structural properties, it was utilized the PyMol 2009 DeLano Scientific LL. The illustrations were made using Marvin Sketch 4.1.6 Pre1, from ChemAxon and ChemBioDraw Ultra 12.0, from CambridgeSoft.

2.2 Methods

2.2.1 Selection and Study of Magnetic Supports

In this work, the coating and modification of MNPs with three different biopolymers (Ga, Dex, EPS) has been studied. Therefore three different types of supports were produced: MNP coated with Gum Arabic (MNP_Ga); MNP coated with Dextran (MNP_Dex) and MNP coated with EPS (MNP_EPS), the protocols followed were identical for all supports.

2.2.1.i *Synthesis of Bare MNP and MNP coated with Biopolymers*

Bare MNP and MNP coated with biopolymers were synthesized by co-precipitation of FeCl_3 and FeCl_2 salts, using a $\text{Fe}^{2+}/\text{Fe}^{3+}$ molar ratio of 0.5, through the addition of a base under inert atmosphere. The syntheses were performed at room temperature for the bare MNP and at different temperatures, depending on the biopolymer used for coating.

A solution of 0.7 M ammonium hydroxide in deionized water was purged with N_2 gas for 30 minutes in a closed reactor with mechanical stirring (1200 rpm). Then, a freshly prepared iron solution (5.4 g of $\text{FeCl}_3 \cdot 6\text{H}_2\text{O}$ and 2.0 g of $\text{FeCl}_2 \cdot 4\text{H}_2\text{O}$ in 25 ml of deionized water) was added dropwise to the ammonium hydroxide solution. For the coated magnetic nanoparticles an aqueous solution of the biopolymer selected was added dropwise to cover the bare MNP, the amount of biopolymer used and the temperature of reaction are described in Table 2.1. The reaction proceeded for two hours under an inert atmosphere. All the steps of the procedure were performed with agitation at approximately 1200 rpm and the pH was monitored and maintained at 10 by addition of ammonium hydroxide solution. Finally, to eliminate the excess of ammonium hydroxide, the synthesized MNPs were washed several times with distilled water using a magnet for separation.

Finally, in order to determine the concentration of the magnetic supports synthesized MNPs samples were dried overnight in the oven at 60°C . To quantify the amount of biopolymer bound onto the magnetic nanoparticles the amount of biopolymer in the washes, after in-situ coating strategy, were analyzed by anthrone method as described in section 2.2.4.ii.

Table 2.1 Strategies used to synthesize magnetic nanoparticles coated with different biopolymers.

Biopolymer	Quantity of Biopolymer used	Biopolymer Solubility	Temperature
Gum Arabic	2.0 g	40 mg/mL	25°C
Dextran	2.0 g	50 mg/mL	60°C
EPS	0.3 g	10 mg/mL	25°C

2.2.1.ii Stability to storage

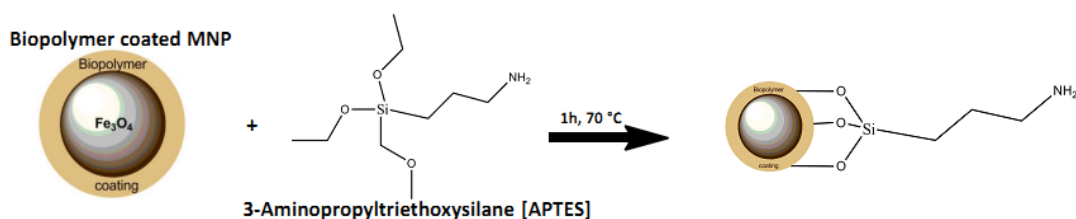
To determine the stability of the MNPs coated solutions to storage over time at 4°C, five washes with distilled water were performed at certain times. The supernatants of the washes were analyzed by the anthrone method (2.2.4.ii) in order to determine the quantity of biopolymer released.

2.2.1.iii Adsorption isotherm of Dextran onto Magnetic Nanoparticles

Solutions of bare MNPs (1 ml at 10 mg/mL) were washed six times with distilled water. Then, 1 mL of standard solutions of Dextran with concentrations between 0 and 85 mg/mL were added. The mixtures were incubated 1 h at 60°C under orbital shaking. After incubation, the supernatants were collected and the amount of dextran released was quantified by the anthrone method as described in section 2.2.4.ii.

2.2.1.iv Amination of the Magnetic Supports

The different MNPs supports (10 mg/mL) were washed five times with deionized water. Afterwards an equal volume of deionized water was added and the suspension was sonicated for 30 minutes. After this step, a 3-aminopropyltriethoxy silane (APTES) solution was added dropwise to the suspensions to a final concentration of 10% (v/v), Figure 2.1. The samples were then incubated for 1 hour at 70°C in a water bath or oven. Finally, MNPs were washed 6 times, and sonicated again for 30 minutes. In order to quantify the amount of amines functionalized in each support a Kaiser Test was performed as described in section 2.2.4.i.

**Figure 2.1** Schematic representation of amination of magnetic nanoparticles with APTES.

2.2.1.v Stability of the Supports to Amination

In order to determine the stability of MNP coated with biopolymers to amination, all the washes done after the amination step were analyzed by anthrone method (2.2.4.ii) to determine the quantity of biopolymer released.

2.2.1.vi Synthesis of Carbon Coated Magnetic Nanoparticles

Carbon Coated Magnetic Nanoparticles were synthesized by redispersing 20 mL at 10 mg/mL of bare MNPs in a 0.5 M aqueous solution of glucose and sonicated for 10 minutes. Then the suspension was transferred to an autoclave vessel and kept at 180 °C for 6 hours. In the end the particles were washed with distilled water six times and the MNP concentration was determined.

2.2.1.vii Characterization of the Supports

For all supports the physical properties (hydrodynamic diameters and zeta potential) were determined by Dynamic Light Scattering (DLS), using a Zetasizer Nano ZS from Malvern. For these analysis samples with a final concentration of 0.05 mg/mL in milli-Q water were prepared.

2.2.2 Immobilization of Enterokinase onto Magnetic Supports

The magnetic nanoparticles previously coated by the three different biopolymers (Ga, Dex, EPS) were used as new carriers to immobilize an enzyme, Enterokinase, by two distinct chemistries as schematized in Figure 2.2.

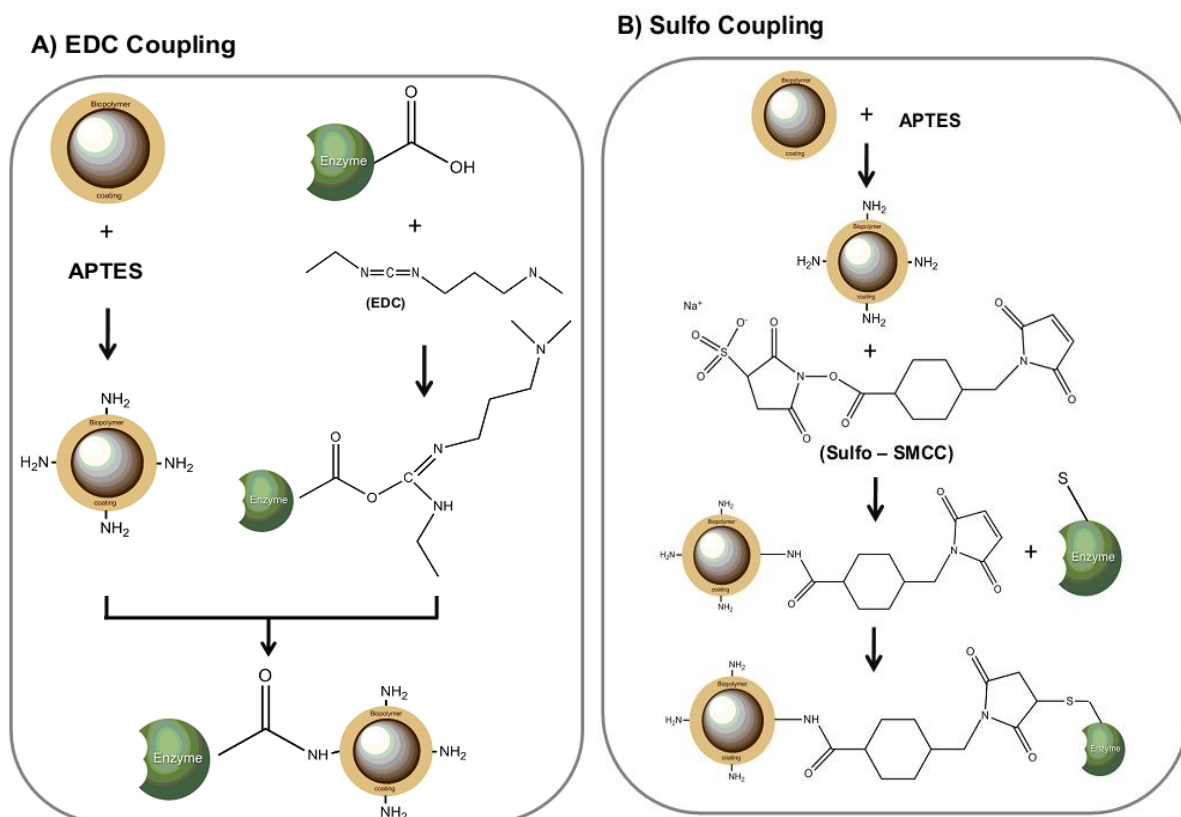


Figure 2.2 Schematic representation of EK Immobilization onto MNPs coated with Biopolymers (Gum Arabic, Dextran and EPS) by two different chemistries: A) EDC Coupling and B) Sulfo Coupling.

2.2.2.i Immobilization of Enterokinase by EDC Coupling

For the EDC coupling the enzyme was coupled on the surface of coated MNPs via carbodiimide activation by making use of the available carboxylic groups on the surface of the enzyme and the free amine groups at the surface of the particles. Each support (2 mL at 10 mg/mL with 5 μ mol of amines) was washed five times with PBS buffer (10 mM phosphate, 150 mM NaCl, pH 7.4) and in the end resuspended in 100 μ L of PBS buffer. The EK carboxylic groups were activated by adding 6 U EK (1 μ L), 5 μ mol EDC (0.885 μ L) and 1 mL PBS and this suspension was incubated for 15 minutes at room temperature with constant stirring. Afterwards the EK modified was added to 100 μ L of a magnetic support and the mixture was incubated overnight at 4 $^{\circ}$ C, with constant shaking. After that period the supernatant was collected and the supports were washed five times with 2 mL of PBS and finally resuspended in 2 mL of Tris-HCl buffer (50 mM NaCl, 20 mM Tris-HCl, 2 mM $\text{CaCl}_2 \cdot 2\text{H}_2\text{O}$, pH 7.4).

2.2.2.ii Immobilization of Enterokinase by Sulfo Coupling

Alternatively, in the Sulfo Coupling Method Sulfo-SMCC was used as crosslinker to create stable maleimide-activated supports that reacted with sulfhydryls available on

the enzyme. The aminated magnetic supports were activated by adding 10 μmol of Sulfo-SMCC in 2 mL of PBS to the magnetic support at 10 mg/mL (5 μmol amines). Then the mixture was incubated for 1 hour at room temperature with constant shaking. In the end the particles were washed five times with conjugation buffer (1 mM EDTA, 0.1 M phosphate, 0.15M NaCl, pH 7.2) and resuspended in 1 mL of the same buffer. Afterwards, to perform the biomolecule coupling, 6 U of EK (1 μL) were added to the maleimide-activated support and incubated overnight at 4 °C with constant stirring. Finally the supports were washed five times with PBS and in order to block the remaining functional groups, the support with EK immobilized was incubated 1 hour at 4 °C with constant shaking in the presence of a solution of 100 mM cysteine in PBS. To finish the immobilization process, the supports were washed five times with Tris-HCl buffer, pH 7.4 and resuspended in 2 mL of the same buffer for storage.

2.2.2.iii Study of the Synthetic Substrate (GD₄K – 2NA) and Product (2 - NA)

The EK activity was studied by using a microplate fluorimetry activity assay with the synthetic substrate Gly-Asp-Asp-Asp-Asp-Lys-2-naphtylamide (GD₄K – 2NA). The enzyme cleaved the substrate, releasing 2-naphtylamide (2-NA), a fluorophore that was monitored by spectrofluorimetry.

To monitor the product released over time, it was necessary to determine the excitation and emission wavelengths of the fluorophore. To determine the excitation wavelength, several solutions of 2-NA with concentrations between 0.0005 mM and 0.5 mM were prepared in Tris-HCl buffer, pH 7.4 (in order to dissolve the 2-NA 1% DMF was added) and absorbance was measured on a spectrophotometer PerkinElmer Lambda 35 UV/Vis Spectrometer. Consequently, for determining the emission wavelength solutions of 2-NA with concentration between 1×10^{-5} mM and 1×10^{-3} mM were also prepared in Tris-HCl buffer, pH 7.4 and analyzed in a spectrofluorimeter PerkinElmer LS 45 Luminescence Spectrometer by making use of the excitation wavelength determined before.

After determining the excitation and emission wavelengths a calibration curve of standard solutions of 2-NA was confirmed on the microplate reader. All the measurements were performed at room temperature in a microplate with 150 μL of sample.

To confirm if the method to quantify the 2-NA released is reliable a solution of 1 mM GD₄K – 2NA was prepared and measured at the same emission and excitation

wavelength determined previously to confirm if the substrate influence on the chosen method.

2.2.2.iv Quantification of EK immobilized on each support

To quantify the amount of EK immobilized on each support, the supernatants recovered after each immobilization step were analyzed by enzymatic activity. The amount of product formed by the free enzyme that remains in the supernatants was analyzed. A calibration curve was determined with known concentrations of free EK with a correlation between the mol of 2-NA released (y-axis) and the μg of Free EK (x-values) with typical values of $y = 3.0 \cdot 10^{-8} x - 1 \cdot 10^{-12}$.

The reaction mixture contained 62.5 μL of the supernatant of each support with EK immobilized, 62.5 μL of Tris-HCl buffer pH 7.4 and 25 μL of 1 mM GD4K-2NA. As controls 62.5 μL PBS-EDC or Conjugation Buffer, 62.5 μL Tris-HCl and 25 μL 1 mM GD4K-2NA were used, depending on the chemistry used to immobilize EK.

The reaction proceeded for 24 hours with constant stirring at 23 °C. The quantity of product released was measured in the microplate reader using an excitation filter of 340 nm and an emission wavelength of 430 nm and a gain of 37 (samples of 150 μL were used in each well).

2.2.2.v Kinetics assay of Free and Immobilized Enterokinase

Free and Immobilized Enterokinase activity was determined fluorometrically using the synthetic substrate Gly-Asp-Asp-Asp-Lys-2-naphthylamide. The released fluorophore 2-naphthylamine was determined using an excitation filter of 340 nm and an emission wavelength of 430 nm and a gain of 37 according to the calibration curve of the standard solution of 2-NA determined. The reaction mixture for Free EK contained 3U of Free EK, 500 μL of standard reaction buffer (Tris-HCl, pH 7.4) and 25 μL GD4K-2NA 1 mM. For the activity of the immobilized EK was used 1 ml of the 2 mL of MNPs modified with EK resuspended with 500 μL of Tris-HCl, pH 7.4 and 25 μL of 1 mM GD4K-2NA.

Reactions proceeded for 24 hours with constant shaking at 23 °C covered with aluminum foil. At particular reaction times samples were taken and analyzed. Kinetics assays were repeated ten times for the immobilized EK, after each cycle the supports with immobilized EK were recovered and washed several times (5x times) with the standard reaction buffer (Tris-HCl, pH 7.4).

The controls were standard reaction buffer (Tris-HCl, pH 7.4) and each of the magnetic nanoparticles coated with each of the biopolymers resuspended in Tris-HCl, pH 7.4. Each of the controls were incubated with 25 μ L of 1 mM GD4K-2NA and the reaction proceeded during 24 hours in the same conditions as the samples.

2.2.2.vi Optimization of EK Immobilization

After performing the kinetic assays with a synthetic substrate the best support of each chemistry (MNP_Dex) was selected to proceed with the studies. For the EDC Coupling the procedure in section 2.2.2.i was repeated but the particles were washed with, 1 M HEPES, 0.5 M NaCl, pH 8, and 5 μ mol NHS (0.0006 g) was added to the enzyme preparation. All the following steps were performed in the same conditions. For the Sulfo Coupling the protocol followed was performed as described on section 2.2.2.ii.

After optimization of the EK immobilization on MNP_Dex, new five kinetic cycles were performed by making use of the synthetic substrate (GD4K-2NA) as previously described (2.2.2.v). This time after each cycle the supports with immobilized EK were recovered and washed ten times with the standard reaction buffer (Tris-HCl, pH 7.4). The MNP_Dex_EK by EDC Coupling has been selected as the best support, and tested with two different proteins containing a cleavage site recognized by Enterokinase. It is known that one unit is defined as the amount of enzyme that will cleave 50 μ g of fusion protein in 16 hours at 23 °C, in a buffer containing 20 mM Tris-HCl pH 7.4, 50 mM NaCl, 2 mM CaCl₂ (supplier instructions).

For Cleavage Control Protein from Novagen the reaction mixture contained 3 U of soluble EK and 10 μ g of Cleavage Control Protein (Novagen) resuspended in 200 μ L of standard reaction buffer (Tris-HCl, pH 7.4). For the activity of the immobilized EK, 1 ml of MNP modified with EK was incubated with 10 μ g of Cleavage Control Protein (Novagen) resuspended in 200 μ L of Tris-HCl, pH 7.4 buffer. The reaction proceeded for 16 hours at 23 °C with constant shaking.

For the fusion protein 180 μ L of the protein (0.027 mg/ml) was reacted with 3 U of the soluble EK at Tris-HCl, pH 7.4 for 16 h at 23 °C. The immobilized EK was reacted at the same conditions as for Cleavage Control Protein from Novagen.

For both cases the cleavage yield was determined by reading the SDS-PAGE gel.

2.2.2.vii SDS-PAGE of the Protein Samples Tests

After testing real protein with the soluble and immobilized enzyme the samples collected (Loading, Samples after digestion with Free EK and Immobilized EK) were

analyzed by gel electrophoresis 12.5 % Acrylamide/Bisacrilamide in denaturing conditions. The respective gels were prepared according to a standardized protocol, as presented in Table 2.2.

Table 2.2 Necessary volumes to prepare two gels 12.5% of Acrilamide/Bisacrilamide.

Reagents	12.5% Polyacrylamide Gel	
	Running Gel Volume (mL)	Stacking Gel Volume (mL)
Solution I (3 M Tris-HCl, pH 8.8)	—	1.5
Solution II (0.5 M Tris-HCl, pH 6.8)	0.9	—
Solution III (Acrilamide – Bisacrilamide) (30:0.8)	0.6	4.16
10% SDS	0.036	0.1
Distilled H ₂ O	1.88	4.2
PSA 10%	0.027	0.076
TEMED	0.004	0.005

The Low Molecular Weight Marker and the samples were prepared by adding 2.5 and 20 μ L of each sample, respectively, and 5 μ L of sample buffer (prepared with Solution II, 10 % SDS, β – mercaptoetanol, Glycerol and Bromphenol blue sodium salt) and were boiled for two minutes immediately before applying on the gel. The gels ran for 80 minutes at 150 V and 250 mA by adding an electrophoresis Tris – Glicine Buffer (SDS-PAGE) diluted 10 times, prepared with 0.25 M Tris – Base, 1.92 M Glycine, 10 g SDS for 1000 mL of distilled water and pH adjusted at 8.3 with concentrated HCl. For detection of the protein bands, the gel was stained with Silver Stain Coloration kit. For this procedure, the two gels are placed for 20 minutes in a Fixative Enhancer Solution, prepared with 100 mL of Methanol, 20 mL of Acetic Acid, 20 mL of Fixative Enhancer Concentrate and 60 mL of Distilled Water, under gentle agitation. The Fixative Enhancer Solutions is removed, and the gels were rinsed in 200 mL of distilled water for 10 minutes with gentle agitation. After 10 minutes the water was decanted and replaced with fresh distilled water for an additional 10 minutes. For the Staining and Developing Step, a solution with 35 mL of distilled water and 5.0 mL Silver Complex Solution, 5.0 mL Reduction Moderator Solution and 5.0 mL Image development Reagent were mixed, immediately before use, with 50 mL of the Development Accelerator Solution (25 g Development Accelerator Reagent in 500 mL of high purity water) and quickly added to the gels. In this third step the gels were stained for 20

minutes with gentle agitation. Finally the gels were placed in a stop solution (5 % acetic acid solution) for 15 minutes. After stopping the reaction rinse the gels in high purity water for 5 minutes. The gels are then ready to be photographed.

2.2.2.viii Characterization of the Supports

Dynamic light scattering was used to determine the hydrodynamic diameter and the zeta potential of the various supports with EK immobilized. All the solutions were prepared as described on section 2.2.1.vii.

2.2.3 Immobilization and Study of 22/8 onto Magnetic Supports

The same supports of MNPs coated with Gum Arabic, Dextran and EPS were used to immobilize synthetic affinity ligands by three different methods as represented in Figure 2.3. These magnetic supports were then evaluated for protein purification.

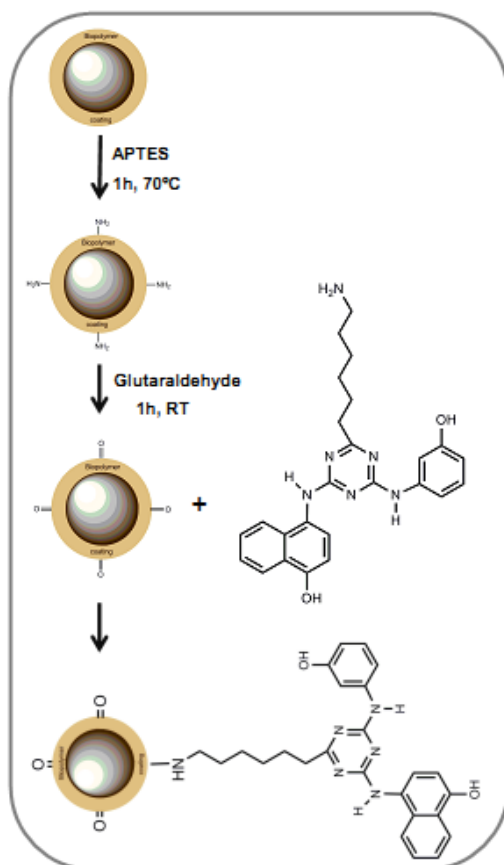
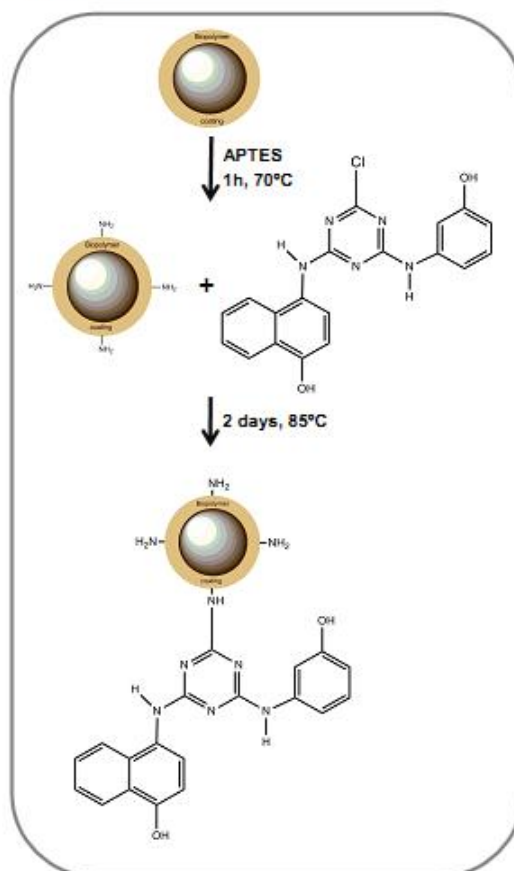
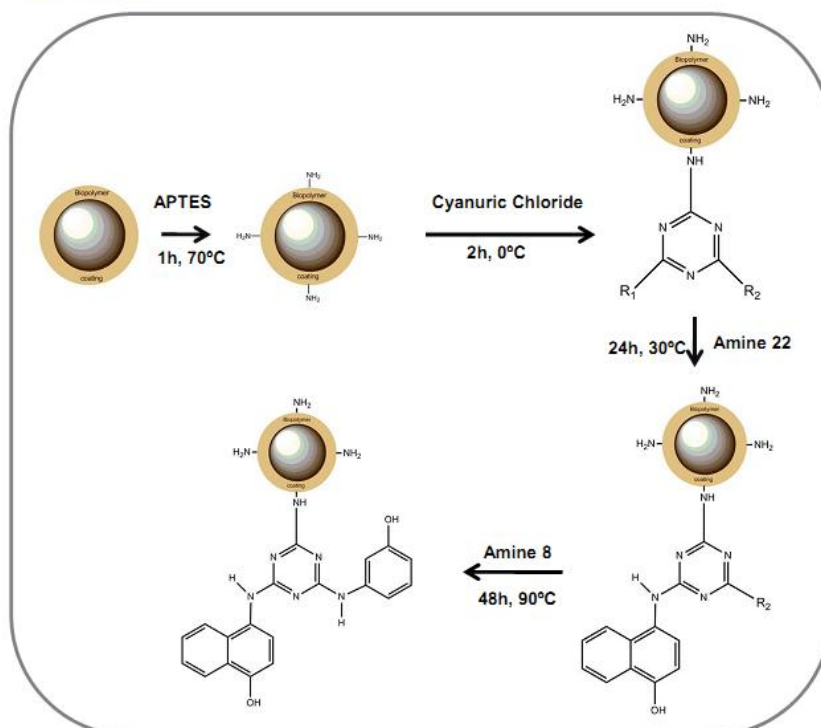
Method A**Method B****Method C**

Figure 2.3 Schematic representation of the Synthetic Affinity Ligand 22/8 Immobilized onto MNPs coated with Biopolymers (Gum Arabic, Dextran and EPS) by three different methods: Method A, Method B and Method C.

2.2.3.i Method A

The ligand 22/8 with a six carbon space arm was previously synthesized in solution phase and purified, based on Teng *et al.*, 2000. This compound was kindly prepared by Dr. Abid Hussain.

The aminated particles (10 mg/mL) were washed five times with distilled water and finally resuspended in a solution of glutaraldehyde with a final concentration of 5% (v/v). Then the suspensions were first sonicated for 10 minutes and subsequently incubated for 1 hour at room temperature with constant shaking. After incubation the particles were washed five times with Milli-Q water.

For the immobilization procedure (Figure 2.3 – Method A), magnetic nanoparticles modified with aldehyde groups (at 10 mg/mL) and respective controls (MNP_Ga, MNP_Dex and MNP_EPS), without any modification, were firstly washed five times with Milli-Q water. Then, the supports were incubated in a 1:1 stoichiometry (taking into account the number of amines of the support available) with the ligand 22/8 previously dissolved in DMF:H₂O (50:50) and centrifuged for 5 minutes at 13000 rpm to make sure the insoluble part was discarded. The incubation proceeded for 1 hour at room temperature at 300 rpm in an orbital shaker. Finally the particles were washed two times with DMF:H₂O (50:50) and more five times with PBS and resuspended in PBS. The washes were collected in order to quantify the amount of ligand bound to the particles (by measurement of absorbance at 280 nm). However, it was not possible to quantify the amount of ligand bound due to problems with the solubilization step.

Finally, in order to block the remaining functional groups the supports modified with ligand 22/8 by Method A were washed five times with distilled water and were incubated 1 hour at room temperature with constant shaking in the presence of a solution of 100 mM glycine in distilled water.

2.2.3.ii Method B

Ligand 22/8 was synthesized in solid phase and purified, according to Teng *et al.*, 2000, but this time it was synthesized without the six carbon spacer arm. This compound was kindly prepared by Telma Barroso.

For this immobilization (Figure 2.3 – Method B), aminated magnetic nanoparticles at 10 mg/mL, and respective controls (MNP_Ga, MNP_Dex and MNP_EPS), were initially washed five times with distilled water. Then were incubated with 5 molar equivalent (taking into account the number of amines available on the support) of ligand 22/8

dissolved in DMF:H₂O (1:12) and with 1 equivalent of sodium bicarbonate. Incubation then proceeded for 2 days at 85 °C with constant shaking. Finally, the particles were washed two times with DMF:H₂O (50:50) and more five times with distilled water and resuspended in water. The washes collected were measured spectrophotometrically at 280 nm to quantify the amount of ligand bound to the particles. It was not also possible to quantify the amount of ligand bound to the particles.

2.2.3.iii Method C

Ligand 22/8 was synthesized directly on the particles based on the synthesis of triazine-based ligands (Figure 2.3 – Method C). The aminated supports were resuspended in 50% (v/v) Acetone/Water (MNP_Ga, MNP_Dex and MNP_EPS) and reacted with 5 molar equivalents (according to the amount of amines available on the support) of Cyanuric chloride, dissolved in acetone, during 2 hours at 0°C at 300 rpm. In the end of this reaction the magnetic nanoparticles were washed one time with acetone, one time with 50% (v/v) acetone/water and finally five times with water. The first nucleophilic substitution on triazine ring was performed by adding 2 equivalents (relative to the amount of amines on the supports) of 3-hydroxyaniline in water. This reaction proceeded 24 hours with stirring at 30°C and after the reaction the particles were washed five times with water. Finally, for the second nucleophilic substitution, 5 molar equivalents of 4 – amino – 1 – naphthol – hydrochloride, in the presence of 5 equivalents of sodium hydroxide, dissolved in 50% (v/v) DMF/water, were added to the reaction and it was left to incubate for 48 hours with stirring at 90°C. The particles were then washed one time with 50% (v/v) DMF/water and more five times with water. Finally, the particles modified with ligand 22/8 were resuspended in water. All the washing procedures were based on the magnetic fishing properties of the supports.

2.2.3.iv Assessment of hIgG and BSA binding to magnetic supports modified with affinity ligands

The different carriers of magnetic nanoparticles modified with affinity ligand 22/8 (250 µL at 6.0 mg/mL) were tested with a pure solution of hIgG, and with a pure solution of BSA for the best support chosen.

The nanoparticles suspensions were washed with regeneration buffer (0.1 M NaOH in 30% (v/v) isopropanol), followed by deionized water to neutralize the pH. These cycles of washes were repeated two times. Then the nanoparticles suspensions were equilibrated with binding buffer (50 mM phosphate, pH 8). After preparation of the supports the supernatants were removed and 250 µL of a hIgG or BSA solution in binding buffer (1 mg/mL) were added to the nanoparticles and incubated for 15

minutes at room temperature with constant stirring. The supernatant was then collected and the particles were washed five times with binding buffer (250 μ L). Bound protein was eluted with a 50 mM Glycine – NaOH, pH 11 buffer. All samples were analyzed by the BCA assay (microplate reader assay), as described on section 2.2.4.iv, in order to quantify the amount of protein bound and eluted from the supports. For both assessments the non-modified particles (MNP and MNP_biopolymer) were tested at the same time and in the same conditions of the magnetic supports modified with affinity ligand.

2.2.3.v Adsorption of hIgG binding to magnetic support

Partition equilibrium experiments were performed with solutions of human IgG (0-18 mg/mL; 250 μ L) in phosphate buffer (50 mM, pH 8) and 250 μ L at 6.1 mg/mL of MNP_Dex functionalized with ligand 22/8 by the Method C. The samples were incubated for 12 h at room temperature, after which the supernatants were collected and the amount of free protein quantified by the BCA protein assay as described on section 2.2.4.iv. The adsorption phenomenon followed Langmuir type isotherms (experimental data fitted with OriginLab 6.1) and was represented by

$$q = \frac{Q_{max} \cdot C_{eq}}{K_d + C_{eq}} \text{ (Equation 2.1)}$$

In which q is the amount of bound protein in equilibrium per volume of solid support, C_{eq} is the concentration of bound protein in equilibrium, Q_{max} corresponds to the maximum concentration of the matrix sites available to the partitioning solute (which can also be defined as the binding capacity of the adsorbent) and K_d the dissociation constant.

2.2.3.vi Testing crude extract with magnetic supports

After studying all the supports with a pure solution of hIgG, the best supports chosen were tested with two distinct crude extracts (kindly provided by Prof. Rui Oliveira, REQUIMTE, Portugal and Dr. Paula Alves, ITQB, Portugal) with the purpose of testing the specific and non-specific adsorption of contaminants on the magnetic supports. The functionalized (MNP_Dex_22/8 by the Method C) and non-functionalized supports (MNP_Dex) (500 μ L with 54 mg/mL) were tested with 500 μ L of each of the crude extracts, without any previously preparation, and incubated for 15 minutes at 4 $^{\circ}$ C. For preparing the supports the procedure applied was the same as described at section 2.2.3.iv. Supernatants were collected and the particles were washed five times with binding buffer (500 μ L). After washing, MNPs were divided and each 250 μ L were

tested with an elution buffer, a 50 mM Glycine – HCl, pH 3 solution and a 50 mM Glycine – NaOH, pH 11 solution, respectively, in order to study the best elution conditions.

All collected samples were analyzed by SDS-PAGE and stained with Silver Staining kit to confirm the bound and elution of the specific protein, but a BCA assay was also performed (microplate reader assay), as described on 2.2.4.iv, in order to quantify the amount of total protein in each of the samples collected.

2.2.3.vii SDS-PAGE of the Crude Extract Test Samples

After the Crude Extracts Tests the samples collected (Loading, Flowthrough, First three washes with Binding Buffer and First Two washes with each of the Elution Buffers) were analyzed by gel electrophoresis 12.5 % Acrylamide/Bisacrilamide in denaturing conditions. The respective gels were prepared according to a protocol standardized (2.2.2.vii section).

Then the Low Molecular Weight Marker and the samples were prepared by adding 2.5 and 10 µl of each sample, respectively, and 5 µl of sample buffer and boiled for two minutes immediately before applying on the gel. The gel ran for 80 minutes at 150 V and 250 mA by adding an electrophoresis Tris – Glycine Buffer (SDS-PAGE). For detection of the protein bands, the gel was stained with Silver Stain Coloration kit. All the buffers and gel preparations were performed as described on section 2.2.2.vii.

2.2.3.viii Characterization of best Method to modified Magnetic Supports with affinity ligands

Dynamic light scattering was used to determine the hydrodynamic diameter and the zeta potential of the various supports immobilized with the ligand 22/8 by the Method C. All the solutions were prepared as described on section 2.2.1.vii.

2.2.4 Quantification Methods

2.2.4.i Quantification of the Amine content by Kaiser Test

The quantity of amines functionalized in each support was determined by the Kaiser Test. This is a qualitative test based on the reaction of ninhydrin with primary amines, as schematized in Figure 2.4, which gives a characteristic dark blue colour. To the aminated magnetic nanoparticles support (10 mg of particles to a total volume of 1 ml) were added 50 µL of each of the following reagents: 80% crystalline phenol in ethanol (w/v), 2% 0.001 M aqueous solution of potassium cyanide in pyridine (v/v) and 5%

ninhydrin in ethanol (w/v). The samples were then incubated in a water-bath at 100°C for 5 min. The calibration curve was performed with standard solutions of glycine (0-5 $\mu\text{mol/mL}$) and the absorbance measurements of the samples (diluted 1:16) were performed at 560 nm. The calibration curve of the Kaiser test has typical values of $y = 4.057x - 0.1354$, with a correlation factor of $R^2 = 0.9961$, where the y-axis represented the absorbance at 560 nm and the x-axis the concentration of glycine in $\mu\text{mol/mL}$.

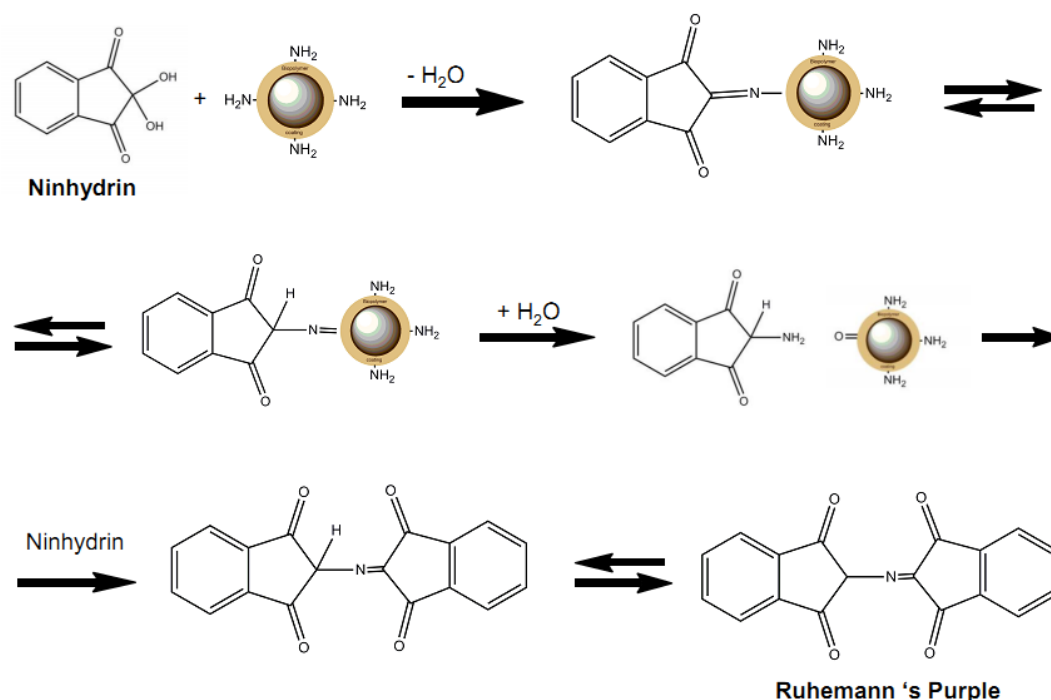


Figure 2.4 Schematic representation of the chemistry of Kaiser Test

2.2.4.ii Quantification of Saccharides by Anthrone Method

This is a colorimetric assay where the anthrone reagent in sulfuric acid allows determining saccharides, as demonstrated in Figure 2.5. To perform this assay 110 μL of sample were mixed with 220 μL of digestion reagent, which is prepared by adding 5 mL of 67% Sulfuric acid to 6.25 mg of anthrone. Then the reaction is incubated during 14 minutes at 100°C. Finally, the samples are left to cool and the product formed is read at the wavelength of 600 nm by using 200 μL of sample in each well of the microplate. The calibration curve was performed with standard solutions of the biopolymer under analyses (0 – 0.5 mg/mL). The values of the calibration curve obtained depend on the biopolymer used, for Gum Arabic the typical values were $y = 5.676x - 0.0044$ ($R^2 = 0.9987$), for the Dextran the typical values were $y = 5.4112x - 0.0229$ ($R^2 = 0.9918$) and finally for the EPS the typical values were $y = 3.8371x + 0.0011$ ($R^2 = 0.9983$).

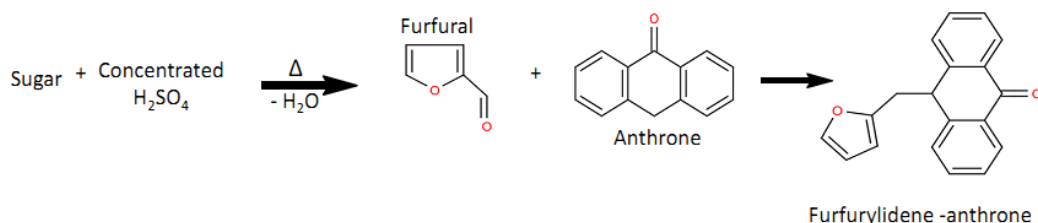


Figure 2.5 Schematic representation of the chemistry of Anthrone Method.

2.2.4.iii Quantification of Iron content by Magnetite Assay

The amount of iron released during the pH resistance assays were determined by the magnetite assay which is based on ferrous ion formed. The principle of this colorimetric assay relies on the formation of ferric ions by magnetite under acidic conditions. The ferric ions were reduced to ferrous ions by the presence of the hydroxylamine hydrochloride. Then, three molecules of 1,10 – phenanthroline react with Fe^{2+} ion, forming a characteristic orange-red colored complex that absorbs light at 509 nm. The intensity of the color formed is directly proportional to the amount of Fe^{2+} in the sample (Magnetite Assay schematized in Figure 2.6).

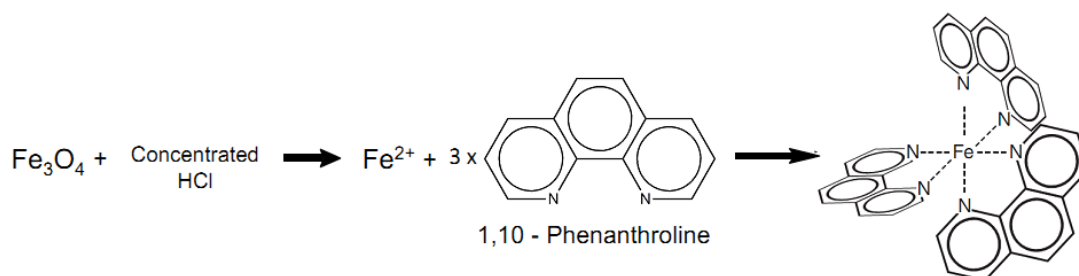


Figure 2.6 Schematic representation of the chemistry of the Magnetite Method.

During the magnetite assay to the 100 μL of each sample 0.5 ml of concentrated HCl followed of 0.5 ml of 1.44 M hydroxylamine hydrochloride solution were added. After 15 minutes, 1 ml of 0.0126 M o-phenanthroline solution was added, the mixture was then neutralized with 0.25 mL of 12 M NaOH. Finally, the pH was adjusted to about 4.0 through the addition of 0.5 M sodium citrate buffer. The absorbance was read at 492 nm in a microplate reader (by using 200 μL of sample in each well). To quantify the amount of iron released in the assay was used a calibration curve from 2.44×10^{-3} to 2.5 mg/ml of Bare MNP. The typical values of calibration curve obtained for this assay are $y = 0.5095x + 0.0072$ with a correlation factor of $R^2 = 0.9949$.

2.2.4.iv Quantification of Protein content by BCA Assay

In order to quantify the amount of total protein the BCA Method (Bicinchoninic acid - Figure 2.7) was employed. This colorimetric method has the advantage of being a more sensitive method and easy-to-use method when compared with Lowry Assay.

This method relies on the formation of a complex Cu^{2+} -Protein under alkaline conditions, followed by the reduction of copper ($\text{Cu}^{2+} \rightarrow \text{Cu}^+$). On a second step the monocation formed reacts with two molecules of bicinchoninic acid and forms a purple solution which absorbs light at any wavelength between 550 – 570 nm. The magnitude of absorbance is directly related to the amount of protein existent due to the proportionality between the degree of reduction of Cu^{2+} and the protein content.

To perform the BCA assay 25 μL of sample (samples collected in the loading, washes and elution obtained in the assessment of protein binding to magnetic supports) were added in each well of a 96-well microplate. The BCA reagent was prepared by adding 50 parts of reagent A (BCA Solution, sodium carbonate, sodium tartrate and sodium bicarbonate in 0.1 N NaOH at pH 11.25) and 1 part of reagent B (Copper (II) Sulfate Pentahydrate 4% Solution). Then, 200 μL of BCA working reagent was added in all the wells and the microplate was incubated in the dark at 37 °C for 30 minutes. Finally, the absorbance was measured at 560 nm in the microplate reader. To determine the amount of Total Protein in the different assays was used a calibration curve from 0 to 1 mg/mL of hIgG ($y = 1.4607x + 0.0438$, $R^2 = 0.9901$) or BSA protein ($y = 1.203x + 0.0346$, $R^2 = 0.9938$) depending on the assay performed.

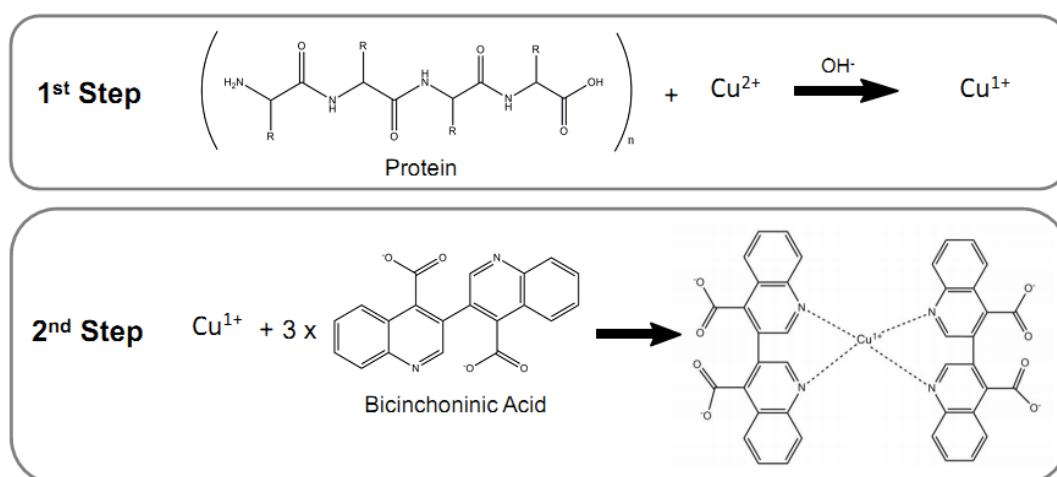


Figure 2.7 Schematic representation of the chemistry of the BCA Method to protein quantification.

3 SELECTION AND STUDY OF MAGNETIC SUPPORTS

This chapter presents the work developed towards the study and selection of magnetic supports for further applications in biocatalysis and bioseparation fields. The results of the synthesis, stability and characterization of magnetic nanoparticles coated with three different biopolymers – Gum Arabic, Dextran and Extracellular Polysaccharide are presented.

3.1 Introduction

The synthesis of materials at the nanoscale has experienced a tremendous growth in the last decade and it is possible to observe a huge interest in their use in technological and biomedical applications (West and Halas, 2000; Liu, 2006). The great interest in nanoparticles is related to the fact that these new materials have similar dimensions to biomolecules which enables a better integration with biological systems (West and Halas, 2000; De *et al.*, 2008).

Thus, nanoparticles became a highly attractive new platform for biotechnological applications mostly due to their new and unique physical and chemical properties obtained from the different materials and size. There has been an intense search for methods of synthesis with an extreme control on the size and morphology of the nanoparticles (West and Halas, 2000; Liu, 2006; De *et al.*, 2008). This growing interest lies in the fact that there is a strong dependence between the dimensions and properties of the nanomaterials.

Nanoparticles of several materials have been studied, however there has been given a considerable emphasis to MNPs because of the size, large surface area and superparamagnetic properties (Gupta and Gupta, 2005). However, these particles reveal several problems related to the colloidal stability, once they tend to form agglomerates associated to the high surface area to volume ratio. Besides that, the chemistry of the bare MNPs is highly active which makes them easily oxidized and subsequently susceptible of losing magnetism and dispersibility (Gupta and Gupta, 2005; Liu, 2006; Dias *et al.*, 2011).

Since the size, morphology and colloidal stability are the most important features for most of the applications (Gupta and Gupta, 2005; Laurent *et al.*, 2008), there is an indispensable need of developing strategies to fabricate and protect the MNPs in order to stabilize and obtain robust nanoparticles which can endure the necessary conditions to a certain application (Lu *et al.*, 2007).

3.2 Results and Discussion

3.2.1 Synthesis and Modification of Magnetic Supports

For the synthesis of the magnetic supports the method applied was the chemical co-precipitation technique of iron salts based on previous works (Batalha *et al.*, 2010). This method is simple and with well determined conditions the quality of the MNPs are entirely reproducible. Through this method it was possible to synthesize iron oxide particles with superparamagnetic properties, as shown in Figure 3.1.

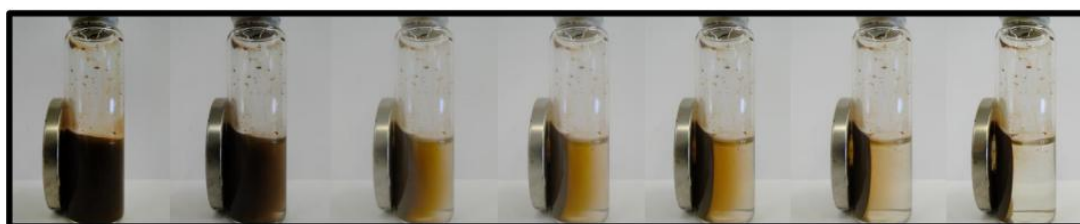


Figure 3.1 Representation of the superparamagnetic properties of MNPs in the presence of an external magnetic field.

Due to the inherent instability of these materials (Gupta and Gupta, 2005; Lu *et al.*, 2007; Dias *et al.*, 2011), the surface was coated with three different biopolymers, Gum Arabic, Dextran and Extracellular Polysaccharide by making use of the in-situ coating strategy. These polysaccharides were chosen as agents for the surface modification of these carriers since they were found to be colloidal stabilizers, mediators for increase biocompatibility and for introducing several functional groups on the support surface. Besides that, they are renewable materials, produced from other biological compounds and they are non-toxic and biodegradable (Dias *et al.*, 2011). For the production of these materials a diversity of parameters can be adjusted in the synthesis to control the characteristics and properties of the supports (Laurent *et al.*, 2008). For the specific case of the supports synthesized the conditions applied, Table 3.1, were suggested according to previous works already studied and to the binding profiles of the biopolymers at the surface of bare MNP (Hong *et al.*, 2008; Batalha *et al.*, 2010; Marcos, 2010).

Table 3.1 Parameters adjusted for the synthesis of MNP coated with Gum Arabic, Dextran and EPS by the co-precipitation method according to Roque *et al.*, 2009; Marcos, 2010.

Biopolymer Coating	Biopolymer used	Biopolymer Solubility	Temperature	Biopolymer Adsorbed (g) / MNP (g)	Q _{max} [Biop. Adsorbed (g) / MNP (g)]
Gum Arabic	2.0 g	40 mg/mL	25°C	0.80	1.04 ± 0.07
Dextran	2.0 g	50 mg/mL	60°C	0.88	1.3 ± 0.1
EPS	0.3 g	10 mg/mL	25°C	0.14	0.9

For the MNP coated with Gum Arabic, the synthesis was based on previous works (Batalha *et al.*, 2010) but the amount of Ga added to the reaction was adjusted according to the binding profiles of Ga previously studied (Roque *et al.*, 2009). According to Roque and co-workers the formation of the Gum Arabic monolayer onto bare MNP follows a Langmuir profile with an optimum value of 1.04 g Ga adsorbed/g MNP (Roque *et al.*, 2009). Considering this value, and taking into account that in each synthesis 2 g of MNP are produced, 2 g of Gum Arabic dissolved in water were added during MNPs synthesis, as described in section 2.2.1.i.

The quantity of Ga adsorbed onto bare magnetite by the in-situ co-precipitation strategy was then confirmed by the anthrone method, as described in section 2.2.4.ii. By this method it was estimated that 0.80 g Ga adsorbed/g MNP were adsorbed. This value is slightly lower than the maximum adsorption profile (1.04 g/g) but this difference is probably due to the sensitivity of the quantification method used, to the heterogeneity of the MNP or GA samples and also due to the difference between the synthesis performed and the conditions followed for the adsorption isotherm, where adsorption of Ga onto the MNPs is performed after the synthesis of the particles. It is believed that the carboxyl groups of Ga, mainly from the glucuronic acid, react with the surface hydroxyl-groups of the particles and the amine groups, mainly in the peptide moieties, interact with iron oxide surface to form hydrogen-bonds (JianHan *et al.*, 2007; Roque and Wilson Jr, 2008).

Regarding the synthesis of MNP coated with Dextran the protocol followed was based on the works of Hong *et al.*, 2008; Batalha *et al.*, 2010. For this protocol the temperature of the reaction was set to 60 °C, since according to some previous studies the reaction temperature increased the adsorption of dextran onto magnetite surface. This parameter is also responsible for decreasing the average diameter of the nanoparticles which has direct influence in reducing the problems related to agglomeration of the particles (Xu *et al.*, 2005; Hong *et al.*, 2008; Zhao *et al.*, 2008). In terms of the quantity of dextran used in the synthesis, this parameter was selected

according to the binding profile of Dextran at the bare MNPs surface as determined in Figure 3.2 – A and B.

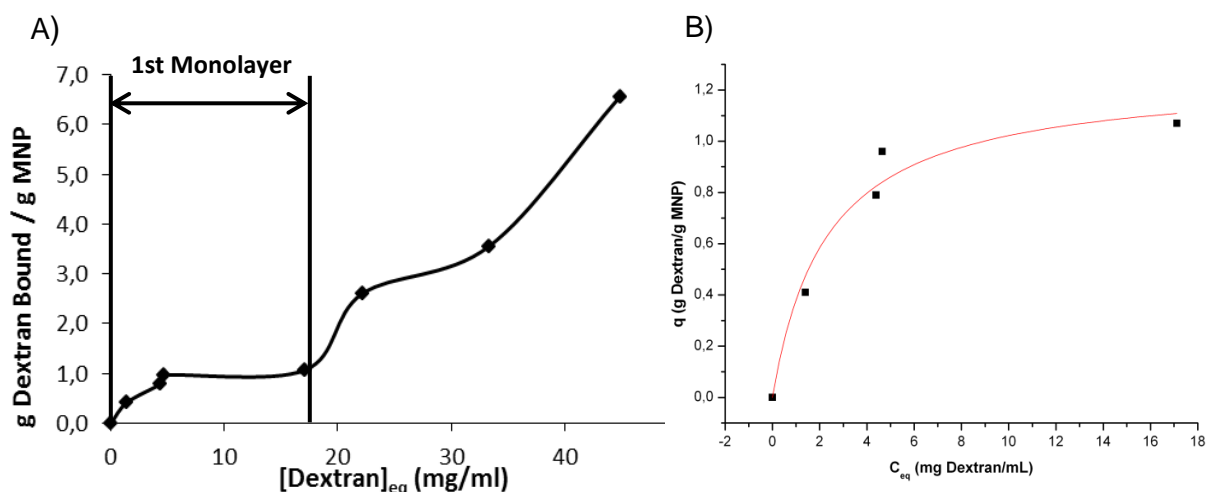


Figure 3.2 Binding profile of Dextran at the surface of bare iron magnetic nanoparticles: A) Binding profile of different solutions of dextran with different concentrations and B) Binding profile of low dextran concentration at the surface of bare iron magnetic nanoparticles. Representation of q (the amount of bound Dextran in equilibrium per mass of solid support) as function of C_{eq} (the concentration of Dextran in equilibrium). Experimental data was fitted with the expression $q = (Q_{max} \times C_{eq}) / (K_d + C_{eq})$ for the Langmuir isotherm (using the OriginLab 6.1 software), where Q_{max} corresponds to the maximum concentration of the matrix sites available to the partitioning solute (which can also be defined as the binding capacity of the adsorbent), and K_d is the dissociation constant.

By the results of the adsorption isotherm of Dextran, quantified by the anthrone method, it was possible to fit the results for low dextran concentration with a Langmuir model with a correlation factor of 0.97, a dissociation constant of 2.3 ± 0.8 mg Dex adsorbed/mL and with an estimated maximum of 1.3 ± 0.1 g Dex adsorbed/g MNP. This fitting gave the value at which the MNPs surface becomes saturated after the formation of a biopolymer monolayer. For this case, the adsorption mechanism is probably attributed to Van der Waals forces, electrostatic interactions and mostly to hydrogen bonds which have often been involved in the interaction between neutral polysaccharides and mineral surfaces (Li and Spencer, 1992; Hong *et al.*, 2008), because dextran is composed by glucose molecules of varying chain lengths being rich in hydroxyl groups.

The biopolymer seems to form multiple layers around MNPs. After the formation of the first monolayer, the amount of Dextran adsorbed increased for higher concentration of Dextran in solution (Figure 3.2 – A). An attempt was made to fit the total data points from Figure 3.2 – A using other adsorption isotherms models

available, but with no success. Probably there are not enough points that define the second or more adsorption layers. Assuming the formation of a first monolayer, these results were kept to define the amount of dextran to coat the MNPs.

Finally, for the MNP coated with EPS the amount of biopolymer added during the MNPs formation was 0.3 g due to the poor solubility in water (Table 2.1). Previous works indicate that the adsorption isotherm of EPS on MNPs do not follow a perfect Langmuir model but a maximum of EPS adsorbed per gram of MNPs was estimated around 0.9 g EPS adsorbed/g MNP (Marcos, 2010). Therefore the quantity of EPS added to the reaction fell far short from the optimal amount necessary for the formation of a biopolymer monolayer. Still, almost 47% of the biopolymer (0.14 g EPS adsorbed/g MNP), added in the beginning of the reaction, adsorbed to the surface of the MNPs. However, it is important to keep in mind that the adsorption isotherm is performed in conditions slightly different from the synthesis of the particles because the biopolymer is added after the MNPs formation. With these results it is possible to predict that 84% of the support is not properly coated with the biopolymer and part of the magnetite core is exposed making this support extremely reactive. The adsorption of EPS to MNPs is most likely mediated between the hydroxyl groups present on MNPs and on the polymer, mainly in the galactose groups which are the major constituent of this polymer. However, this biopolymer also establishes some bonds between the carboxyl groups, available in the small percentage of acyl groups of this polymer, and the hydroxyl groups present in the surface of the MNPs.

In conclusion, it was possible to coat magnetite particles with the three biopolymers selected to increase colloidal stability and reduce nonspecific adsorption effects. In the case of the MNPs coated with Ga and Dex were bound 80% and 90%, respectively, of each biopolymer to the surface of MNPs. For the case of the MNPs covered with EPS to improve the coating with this polymer, the synthesis strategy should be optimized in terms of the quantity of biopolymer added in the beginning of the synthesis of this support.

MNPs were successfully coated with the three different biopolymers, but the efficiency of a support in a certain area of application also depends on the binding specificity of the support (Gupta and Gupta, 2005; Laurent *et al.*, 2008; Dias *et al.*, 2011). This specificity is acquired through the introduction of biological molecules or specific receptors on the surface of the carriers (Gupta and Gupta, 2005; Dias *et al.*, 2011). One common step for the modification of magnetite particles is the amino-silanization, a method that produces covalently bound amino groups on the surface of the supports

through the use of the free hydroxyl groups at the particles surface, Figure 2.1 (Wu *et al.*, 2008). This step is also crucial since the introduction of the aminopropyltriethoxy silane groups can work as spacer arm between the immobilized biomolecules and the supports. In this work all, the biopolymer coated supports were modified with aminopropyltriethoxy silane, as described in section 2.2.1.iv (Table 3.2).

Table 3.2 Degree of amination of the magnetic supports synthesized, values measured by the Kaiser test (n = 4).

MNP Samples	$\mu\text{mol NH}_2$ / g MNP
Gum Arabic	189 ± 18
Dextran	214 ± 44
EPS	196 ± 8

3.2.2 Stability of Magnetic Supports

The preparation of a magnetic support should meet the conditions required for its application. It is important to assess the support's stability towards storage, chemical modification, pH and oxidation (Gupta and Gupta, 2005; Laurent *et al.*, 2008).

In the present work, the stability of the supports towards storage (Figure 3.3) and modification with amino-silane (Figure 3.4) was assessed. Also a preliminary study was performed to optimize the pH resistance of the supports.

Data indicates that the amount of biopolymer bound to MNPs is very stable to storage and chemical modification with APTES.

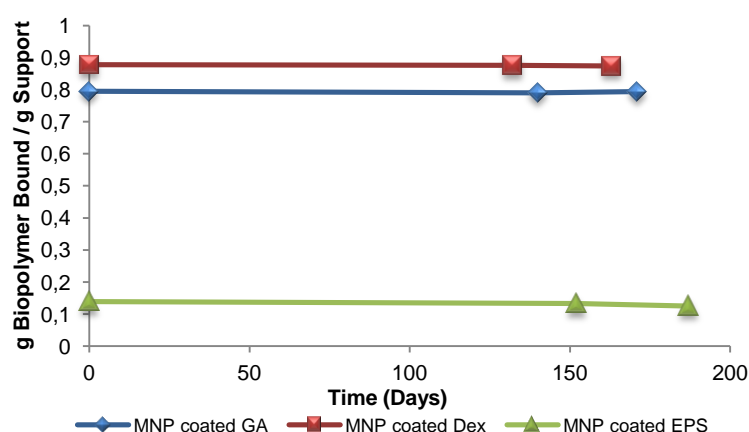


Figure 3.3 Storage stability of the synthesized supports along the time, values determined by the anthrone method.

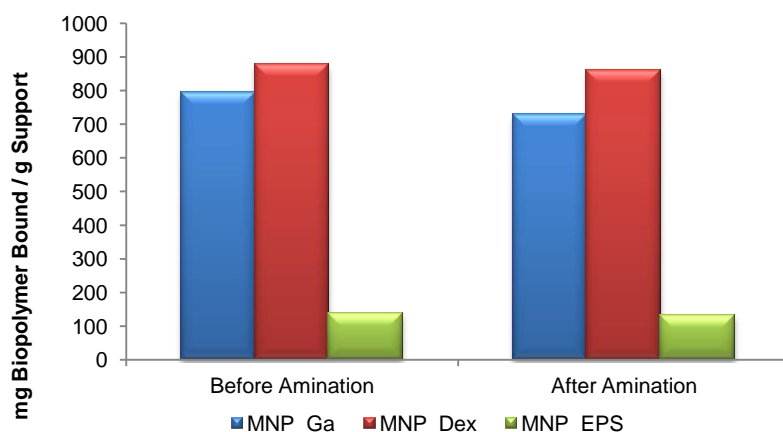


Figure 3.4 Chemical modification stability of the synthesized supports, values determined by the anthrone method

The magnetite particles tend to oxidize to maghemite at high temperatures (80 °C) and dissolve under acidic conditions (Batalha *et al.*, 2010). In particular the low resistance to acidic pH can decrease the range of applications of these MNPs. A preliminary study was conducted with a carbon coating of the magnetite particles. This coating method, schematized in Figure 3.5, consists on the formation of carbon nanospheres through the aromatization and carbonization of glucose under hydrothermal conditions, where iron oxide nanoparticles are the nuclei for the formation of the carbon composites (Sun and Li, 2004; Wang *et al.*, 2006; Qi *et al.*, 2009). Through this chemical modification of glucose a large number of functional groups as hydroxyl groups appear at the surface of the support. Previous reports indicate that this carbon-layer increases thermal stability, high stability against oxidation and acidic leaching, and also provide an active surface for covalent attachment of biomolecules (Sun and Li, 2004; Lu *et al.*, 2007).

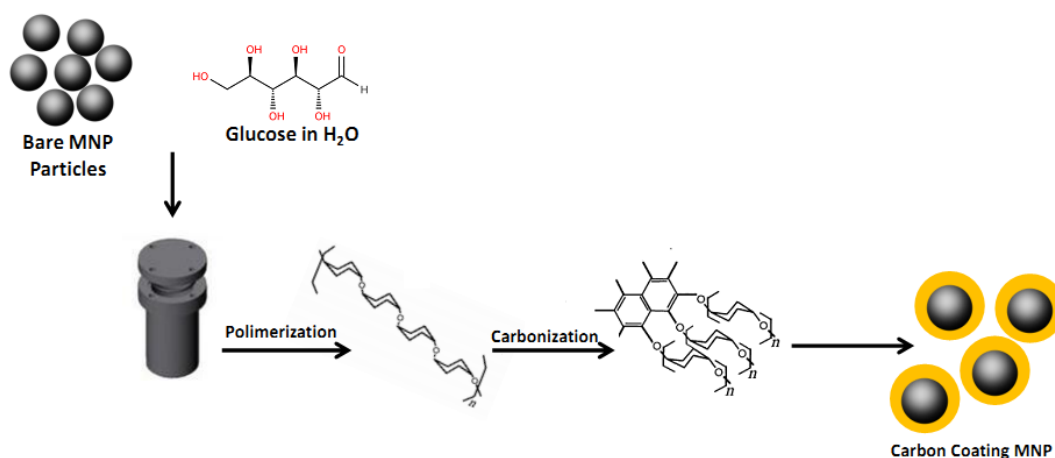


Figure 3.5 Schematic representation of the synthesis of the carbon coating magnetic nanoparticles based on Sun and Li, 2004; Qi *et al.*, 2009.

After the synthesis of the carbon coated nanoparticles, this support was tested with different pH solutions in order to quantify the amount of magnetite released to the solution, as described in section 2.2.4.iii (Figure 3.6). It is possible to observe that carbon coated particles are more resistant to pH 3 when compared with the bare MNPs, as described in literature (Sun and Li, 2004; Lu *et al.*, 2007). However, at neutral and basic pHs the carbon coated particles seem to lose stability which is confirmed by an increase in magnetite in solution. It was not possible to find literature to support these results. On the other hand the magnetite method utilized is less sensitive than ICP-AES, as shown in Batalha *et al.*, 2010 where at pH 11 magnetite was released from bare MNP.

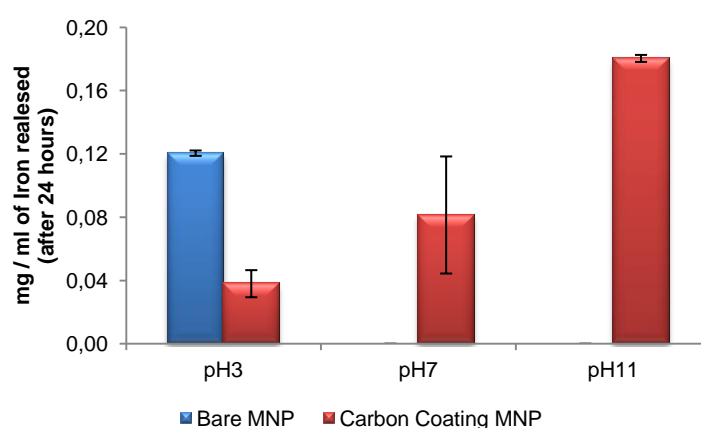


Figure 3.6 Quantity of iron released from bare MNPs and carbon coated MNPs at different pHs (n = 2).

3.2.3 Characterization of Magnetic Supports

The Dynamic Light Scattering Zetasizer Nano ZS from Malvern (DLS) measures the hydrodynamic diameter, analyzed in Figure 3.7 and Table 3.3 and the zeta potential, Figure 3.8, of the MNPs.

The coating of the particles with different biopolymers leads to an increase of the hydrodynamic diameter of the particles for values between 1500 – 3000 nm. The formation of larger agglomerates when the particles were coated has already been observed in other works (Williams *et al.*, 2006; Wilson Jr *et al.*, 2008; Batalha *et al.*, 2010). One should bear in mind that the diameter of each individual magnetic core is around 10-12 nm (Batalha *et al.*, 2010). This might be explained by the non-covalent interactions between the coating biopolymers of neighbor nanoparticles. It is also interesting to observe the slight decrease of the hydrodynamic diameter for the MNP_Ga and MNP_EPS and an increase of the hydrodynamic diameter for the MNP_Dex when the supports are aminated, however the errors associated are too

high. For the Carbon Coated MNPs, the hydrodynamic diameter is around 1000 nm and here it is also possible to conclude the presence of some agglomeration of the particles.

According to Table 3.3 it is possible to conclude that the supports synthesized are not uniform in size and present a high polydispersitivity with values between 0.6 and 1, which is corroborated by the higher error bars determined and through the aggregates that are big enough to be seen by naked eye, which means that this values are not reliable and a different method should be used to analyze this parameter. This can be explained by the fact that DLS is a good technique for measure particles with size smaller than 1 μm . Since the particles synthesized present sizes in the magnitude order of 1 to 2 μm the technique used has no sensibility to perform a good measurement hence present values of polydispersit so high. In order to determine the size of the particles synthesized should be chosen a different technique, such as Mastersizer also from Malvern. This is a technique with a higher measuring range (0.02 μm – 2000 μm) that is more appropriate for the particles that were synthesized.

Table 3.3 Hydrodynamic Diameter and Polydispersitivity values for magnetic nanoparticles (n = 2).

MNP Supports	Hydrodynamic Diameter (nm)	PDI
Bare MNP	568 \pm 37	1.0 \pm 0.0
MNP_Ga	1650 \pm 234	0.77 \pm 0.02
MNP_Dex	1526 \pm 638	0.76 \pm 0.04
MNP_EPS	2919 \pm 409	0.79 \pm 0.02
Carbon Coating MNP	1080 \pm 159	0.67 \pm 0.18
MNP_Ga_NH ₂	1093 \pm 64	0.61 \pm 0.06
MNP_Dex_NH ₂	3506 \pm 1078	0.80 \pm 0.38
MNP_EPS_NH ₂	2403 \pm 309	1.0 \pm 0.0

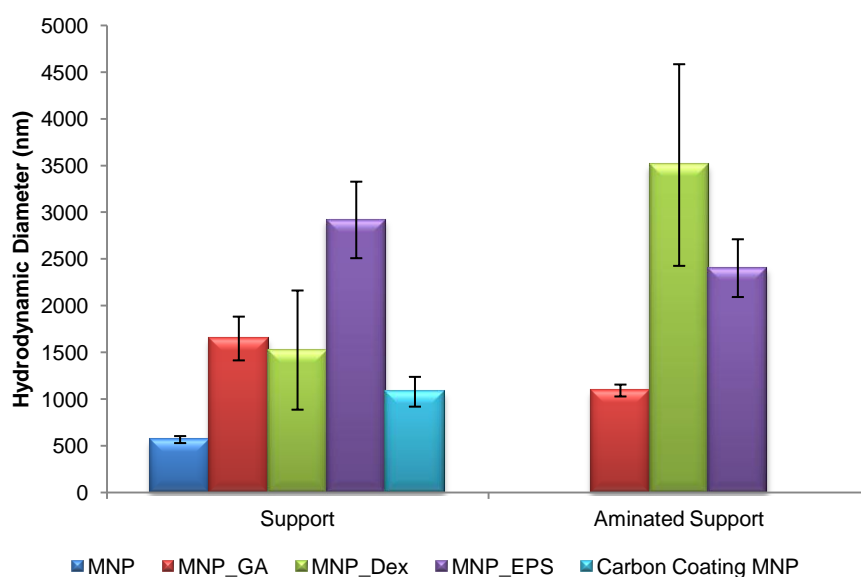


Figure 3.7 Hydrodynamic diameter (nm) of the magnetic supports by dynamic light scattering analysis (n = 2).

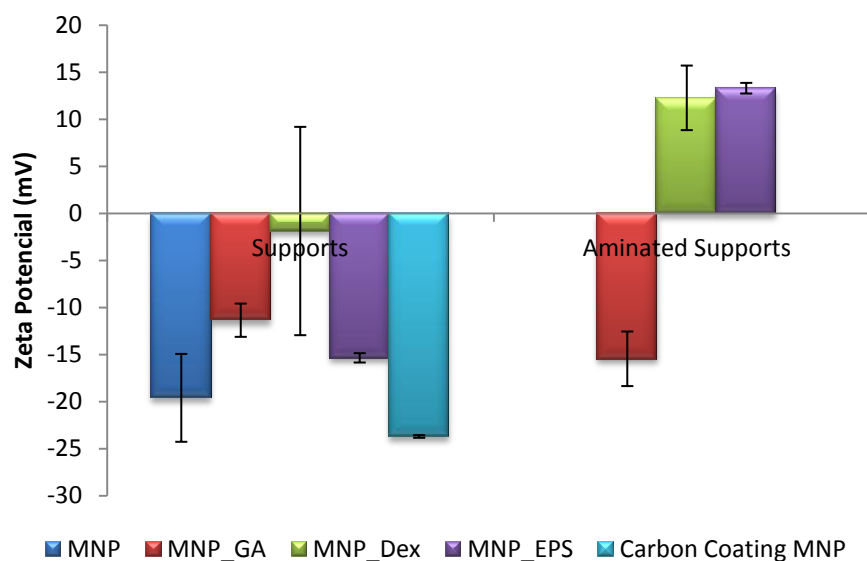


Figure 3.8 Zeta Potential values (mV) at pH 7 for magnetic supports by dynamic light scattering analysis (n = 2).

The majority of the particles dispersed in an aqueous solution will have a charged surface either by ionization of surface groups or adsorption of charged species. This will modify the distribution and will increase the concentration of the surrounding ions. The liquid layer surrounding the particle exists as two parts; an inner region (Stern layer) where the ions are strongly bound and an outer (Diffuse layer) region where they are less firmly connected. Within the diffuse layer there is a notional

boundary inside which the ions and particles form a stable entity. When a particle moves (e.g. due to the voltage that is applied), ions within the boundary move it. Those ions beyond the boundary stay with the bulk dispersant. This boundary is called slipping plane. The potential that exists at this boundary is called the zeta potential.

The magnitude of the zeta potential gives an indication of the potential stability of the colloidal system. Particles in suspension with a high zeta potential of the same charge tend to repel each other and resist aggregation. However, if the particles have low zeta potential values then there will be no force to prevent the particles coming together and flocculating. It is conventionally assumed that high zeta potential values are below -30 mV or above +30 mV. This means that particles with zeta potentials more positive than +30 mV or more negative than -30 mV are normally considered stable.

Through Figure 3.8 bare MNP have a zeta potential of -20 mV, this potential is attributed to the oxygen groups available in the tetrahedrally - octahedrally structure. When particles are coated with the different polymers the global charge is altered according to the type of biopolymer used. For the MNP coated with Gum Arabic, Batalha and co-workers concluded that the zeta potential value of Ga in suspension is -16.45 mV (Batalha *et al.*, 2010). For the particles synthesized in this work it is possible to conclude that the particles are well coated because the zeta potential of MNP_Ga is in the same order of magnitude of the Ga in suspension. The negative zeta potential of the Gum Arabic is mainly attributed to the carboxylic groups available on its structure.

For the case of MNP coated with Dextran, particles presented zeta potential of -1.88 mV which is corroborated with the values determine by Xu and co-workers (Xu *et al.*, 2005). Dextran is a neutral polysaccharide and when the bare MNP are well coated with this biopolymer the zeta potential became all most zero because of the neutral charge of the biopolymer.

MNPs coated with EPS became less negative when compared with the bare MNP particles. This also can be explained because of the zeta potential value of the EPS in suspension, determine in Marcos, 2010. EPS has a zeta potential of -10 mV and when the particles were covered with this biopolymer the zeta potential is -15 mV. This once again indicates that MNP were probably not completely covered with EPS.

When particles are aminated different behaviors are observed depending on the supports that are being analyzed and once again this behavior is dependent on the charge of the biopolymer used to cover the bare MNP. In the case of MNP_Ga the amination step does not seem to have a considerable effect on the zeta potential

values. This might be explained by the fact that the Ga has a negatively surface and the amount of amines functionalized by the amination step is not enough to change the charge of the surface. These results have already been demonstrated in other works (Batalha *et al.*, 2010).

For the case of the MNP_Dex and MNP_EPS the amination step increases the density of amines on the surface of the supports which alters the charge of the surface of the carriers from negative to positive. This probably can be explained by the fact that the dextran is a biopolymer with a neutral charge and the EPS has a low quantity of carboxylic groups on its surface which can be easily dominated by the positive charge of the amine groups. For bare MNP, according to the literature works when these particles are aminated they also became positively charged (9 mV) (Batalha *et al.*, 2010).

Finally, the zeta potential value for the carbon coated nanoparticles is in the same magnitude of order of the bare MNP considering the error associated to this value. Since through this coating method the majority of the groups added to the surface of the particles are hydroxyl groups, as previously discussed, it would be expected that these particles presented zeta potential values less negative. This might be indicative that the coating of the particles was not well done and the majority of the magnetite core is exposed. However, these were preliminary studies and more characterization methods and probably a quantification method to confirm if the particles were coated with glucose should be tested to understand better the phenomena involving this new support.

3.3 Conclusions

Iron oxide nanoparticles coated with three different biopolymers, Gum Arabic, Dextran and Extracellular Polysaccharide have been synthesized by the co-precipitation method with an in-situ surface coating strategy. By quantifying the amount of biopolymer bound to magnetite it was concluded that about 80%, 90% and 16% of the MNPs surface were coated with Ga, Dex and EPS, respectively. The synthesis of MNP_EPS must be improved in order to increase the quantity of biopolymer coating the surface of the particles and thus improve the stability of the support. Also, the characterization of these supports in terms of hydrodynamic diameter and zeta potential values confirmed the coating with the biopolymers and further chemical modifications.

In terms of stability to storage and chemical modification, all the supports revealed to be extremely stable. However, in future studies, it would be interesting to test the stability of these supports to different temperatures and solvents, in order to increase the range of applicability and to study in more detail each of these carriers.

Finally, a preliminary attempt for bare MNP become resistant to oxidation and to acid conditions was performed but further studies must be conducted in the future to optimize this procedure.

4 MAGNETIC NANOPARTICLES APPLIED ON BIOCATALYSIS

This chapter focuses on the application of magnetic nanoparticles in the biocatalysis field, specifically in Enterokinase immobilization onto MNPs. The results for the activity and stability of Enterokinase immobilized on three different magnetic supports through two different chemistries are discussed. Finally some conclusions about the best support for the immobilization of Enterokinase are presented.

4.1 Introduction

Recombinant proteins of therapeutic importance such as antibodies and growth hormones represent an important class of biopharmaceuticals (Kubitzki *et al.*, 2008). This implies that the quality, safety and efficacy of these products need to be extremely controlled (Clonis, 2006).

In order to obtain high-throughput purification of the products of interest, the use of affinity-tag systems bring a lot of advantages. Specifically, the purification of recombinant proteins can be done in one-step and on a simple and precise way (Terpe, 2003). However, due to the therapeutic applications of these products, the affinity tags need to be further removed after protein purification. This can be carried out by harsh chemical treatments (e.g. cyanogen bromide) or by enzymatic cleavage that is by far more specific and less detrimental for the target protein, due to the milder reaction conditions. Enzymes are highly efficient reagents, but usually costly and labile (Arnau *et al.*, 2006; Kubitzki *et al.*, 2008).

To improve stability, easy recovery and reutilization of the biocatalyst it is common to immobilize enzymes on solid supports. Recently magnetic nanoparticles attracted attention as possible solid supports for enzyme immobilization, as they provide minimum diffusion limitations, maximum surface area per unit mass, easy recovery and high enzyme loading (Kim *et al.*, 2006).

Kubitzki and co-workers performed studies with EK immobilized on commercial paramagnetic microspheres and hexamethylamino sepabeads for the cleavage of mucin fusion protein, which highlights the potential applications of EK systems for the production of biopharmaceuticals (Kubitzki *et al.*, 2008; Kubitzki *et al.*, 2009). In this work, EK was immobilized on MNPs with the intent of cleaving a fusion protein tag, as schematized in Figure 4.1.

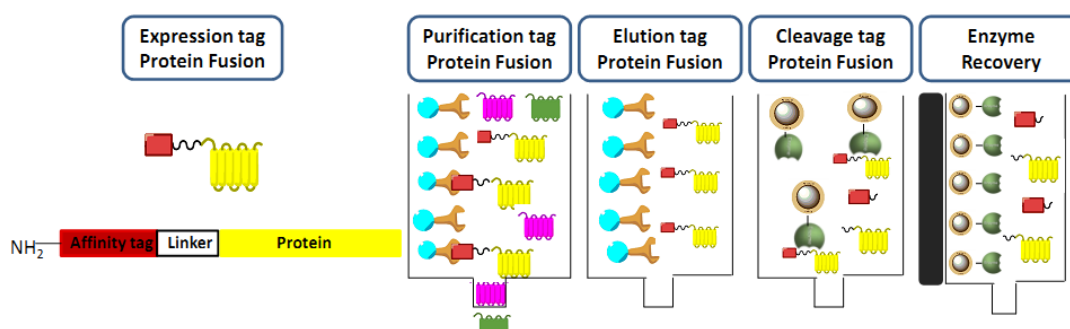


Figure 4.1 Schematic representation of a biocatalysis process using iron oxide magnetic nanoparticles for the immobilization of enzymes and cleavage of tag protein fusion.

4.2 Results and Discussion

In this work, three different magnetic supports, previously studied in chapter 3, were used for the covalent immobilization of EK, an endopeptidase that recognizes the DDDDK sequence and is commonly utilized for the cleavage of tags in recombinant fusion proteins (Kubitzki *et al.*, 2008). The enzyme immobilized on magnetic supports was tested with a synthetic substrate and two different model proteins in order to evaluate EK activity and stability when immobilized.

4.2.1 Molecular Structure Analysis and Covalent Immobilization of Enterokinase

The catalytic subunit of EK was analyzed by PyMOL to understand which would be the best methodologies to immobilize this enzyme.

By analyzing the existing cysteine groups on the surface of the catalytic subunit (Figure 4.2) it is possible to observe a total of nine cysteine groups available. All the cysteine residues establish disulfide bonds between them except residue 122 marked with a red circle. This residue is responsible to bind the heavy subunit to the catalytic subunit by a disulfide bond. In this work only the catalytic subunit of the enzyme will be used and therefore residue 122 is available to immobilize EK on MNPs. This method was called Sulfo Coupling. It consists on the immobilization of EK through the sulfhydryl group available, mimicking the flexibility of the enzyme in its native structure when it is bound to the heavy subunit. For the immobilization of this enzyme on magnetic nanoparticles through the Sulfo Coupling method the functional groups of the carrier were activated with 4-(N-Maleimidomethyl)cyclohexane-1-carboxylic acid 3-sulfo-N-hydroxysuccinimide ester sodium salt (Sulfo – SMCC). This is a water-soluble crosslinker which contains an amine-reactive N-hydroxysuccinimide (NHS ester) and a sulfhydryl-reactive maleimide group. The NHS esters react with the primary amines of MNPs to form stable amide bonds, while the maleimide react with sulfhydryl group of EK to form stable thioether bonds, as represented in Figure 2.2. After immobilizing the enzyme a post-treatment with cysteine is convenient to block the remaining thiol groups available on the surface of the supports.

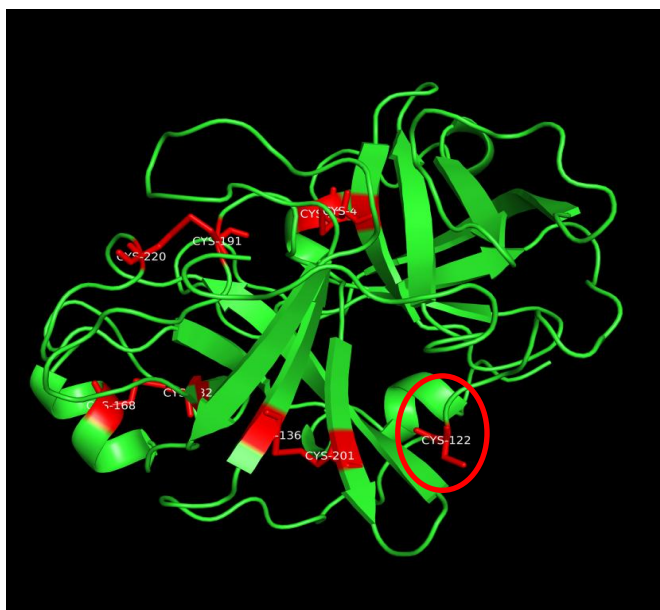


Figure 4.2 Structure analysis of the catalytic subunit of Enterokinase: Thiol groups available on the surface of EK, represented in red color. This image was produced with the program PyMOL by making use of the crystalline catalytic subunit structure of EK from pdb (accession code 1ekb).

For a second strategy to immobilize EK on the surface of magnetic nanoparticles the catalytic subunit of this enzyme was analyzed in terms of the percentage of carboxylic and amine groups available, as shown in Figure 4.3. There are a higher number of carboxylic groups (aspartic acid and glutamic acid residues), when compared with the amine groups available (lysine and arginine residues). However, since the intent is to immobilize the enzyme on a solid support, only the surface available residues will be considered. In addition, the residues close to the binding site were also discarded since these might be essential for the catalytic function of the enzyme. As summarized on Table 4.1, 58% of the carboxylic groups are available on the surface when compared with the 24% of the amine groups available. Taking into account the estimated values, the method applied to immobilize EK was based on the carboxylic groups available on the surface of the enzyme and was called EDC Coupling.

The EDC coupling method consists on the reaction of the crosslinker N-(3-dimethylaminopropyl)-N'-ethylcarbodiimide with the carboxylic groups available on the surface of EK to form a reactive o-acylisourea intermediate. This intermediate reacts with amines on the magnetic nanoparticles forming a stable amine bond between the enzyme and the MNPs. The schematic representation of the EDC coupling method to immobilize EK onto magnetic nanoparticles is represented in Figure 2.2.

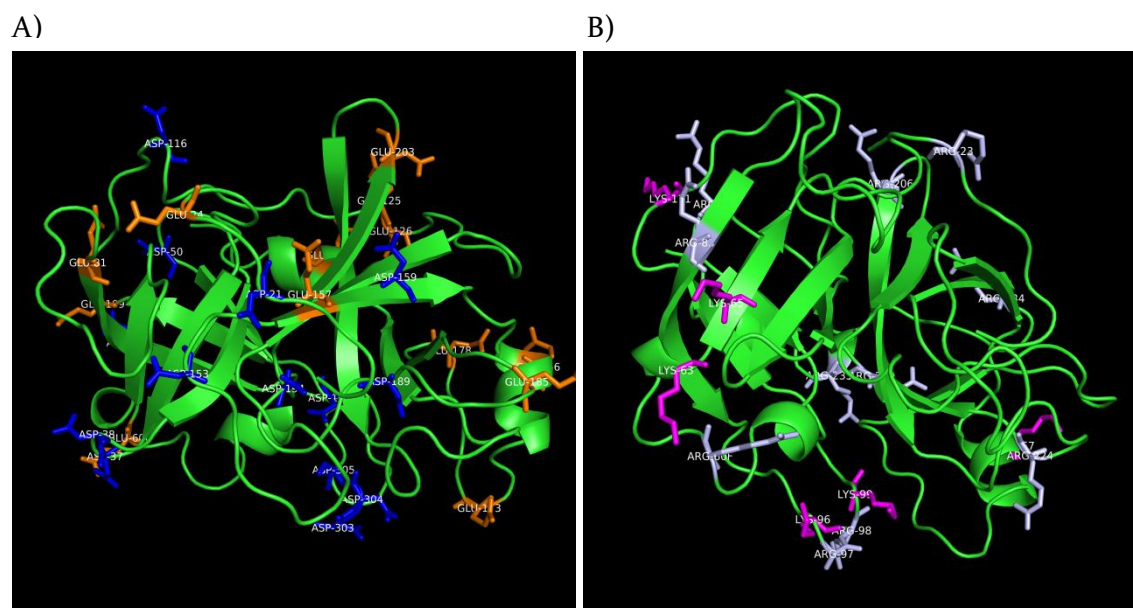


Figure 4.3 Structure analysis of the catalytic subunit of Enterokinase: A) Carboxylic groups available on the surface of EK, where the orange sticks represent the glutamic acid groups and the blue groups represent the aspartic acid residues and B) Amine groups available on the surface of EK, where the pink groups represent the lysine residues and the light blue represent the arginine groups. This image was produced with the program PyMOL by making use of the crystalline structure of EK from pdb (accession code 1ekb).

Table 4.1 Percentage of residues and total groups available on the surface of the catalytic subunit of Enterokinase. Note: These values were estimated taking into account only the residues on the surface and discarding the residues near the binding site.

Residues	Percentage of residues on the surface	Percentage of total groups available on the surface
Aspartic acid (COOH)	55 %	58 %
Glutamic Acid (COOH)	62 %	
Lysine (NH ₂)	50 %	24 %
Arginine (NH ₂)	9 %	

4.2.2 Determination of Reaction Parameters to Monitor the Product Released

The activity of EK immobilized onto magnetic nanoparticles was tested with a microplate fluorimetry activity assay using the synthetic substrate Gly-Asp-Asp-Asp-Asp-Lys-2-naphtylamide (GD₄K-2NA). The enzyme cleaved the substrate, releasing 2-naphtylamide (2-NA), a fluorophore that was monitored at several reaction times through a fluorescence assay. Before testing EK immobilized onto MNPs, the excitation and emission wavelengths of the reagents were determined. The calibration curve to quantify the product released was also studied.

In order to determine the emission spectrum of a particular fluorophore, the wavelength of maximum absorption, the same as the excitation maximum, is determined first. To determine the excitation wavelength, several solutions of the product 2-NA, with different concentrations, were prepared and the absorbance was measured as represented in Figure 4.4. Through analysis of this figure it is possible to conclude that the maximum adsorption wavelength of the fluorophore 2-naphtylamide is at 334 nm and at this wavelength the fluorophore is excited.

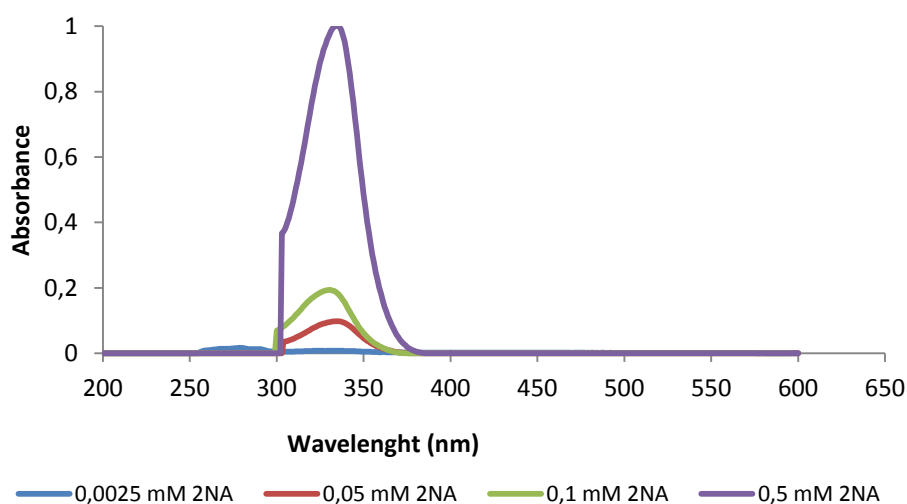


Figure 4.4 Adsorption spectra of 2-NA solutions at different concentrations.

After determining the excitation wavelength the emission spectra of several solutions of 2-NA, at different concentrations, was determined and represented in Figure 4.5. By analyzing the fluorescence intensity spectra of the product 2-NA it is possible to conclude that using 334 nm as excitation wavelength the maximum emission wavelength of this product is 410 nm.

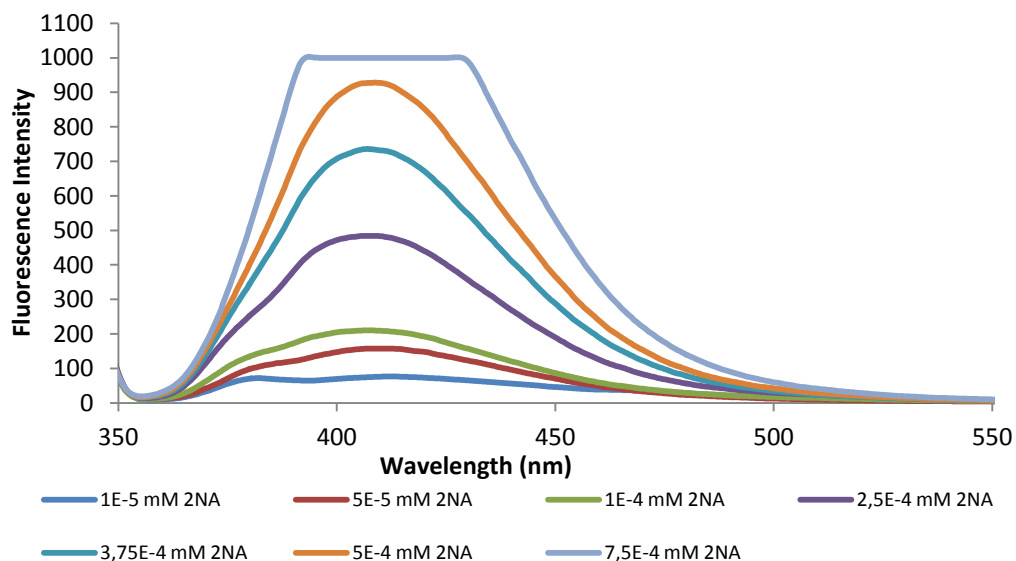


Figure 4.5 Fluorescence intensity spectra of 2-NA solutions at different concentrations by making use of the excitation wavelength of 334 nm.

To confirm if the substrate could interfere with the fluorescence of the product released, solutions of the substrate (GD₄K-2NA) with concentration of 1 and 0.001 mM were analyzed in terms of maximum absorption and maximum emission, respectively, for the same values determine for the 2-NA product. Through observation of Figure 4.6 and Figure 4.7 it is possible to confirm that the substrate GD₄K-2NA does not influence the absorbance and fluorescence values obtained for the product 2-NA.

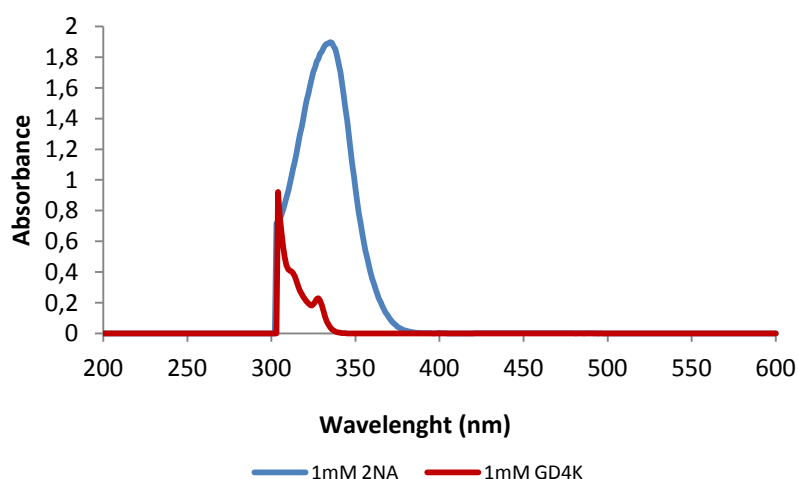


Figure 4.6 Comparison of the absorption values between GD₄K-2NA and 2-NA at the same concentration (1 mM).

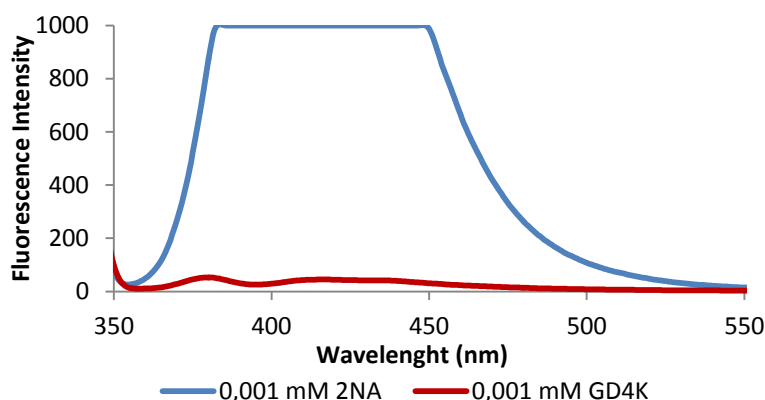


Figure 4.7 Comparison of fluorescence intensity values between GD₄K-2NA and 2-NA at the same concentration values (0.001 mM) with an excitation wavelength of 340 nm.

After determining the reaction parameters, the EK immobilized onto magnetic nanoparticles was tested for cleavage of the synthetic substrate GD₄K-2NA, and using the excitation wavelength of 340 nm and emission wavelength of 430 nm, it was possible to monitor the released fluorophore 2-naphtylamide. The product released was quantified through the calibration curve where fluorescence intensity of the 2-NA (y-axis) was represented in function of the concentration of 2-NA in mM (x-axis). This curve has typical values of $y = 7 \cdot 10^6 x$ with a correlation factor of 0.98 (Figure 4.8).

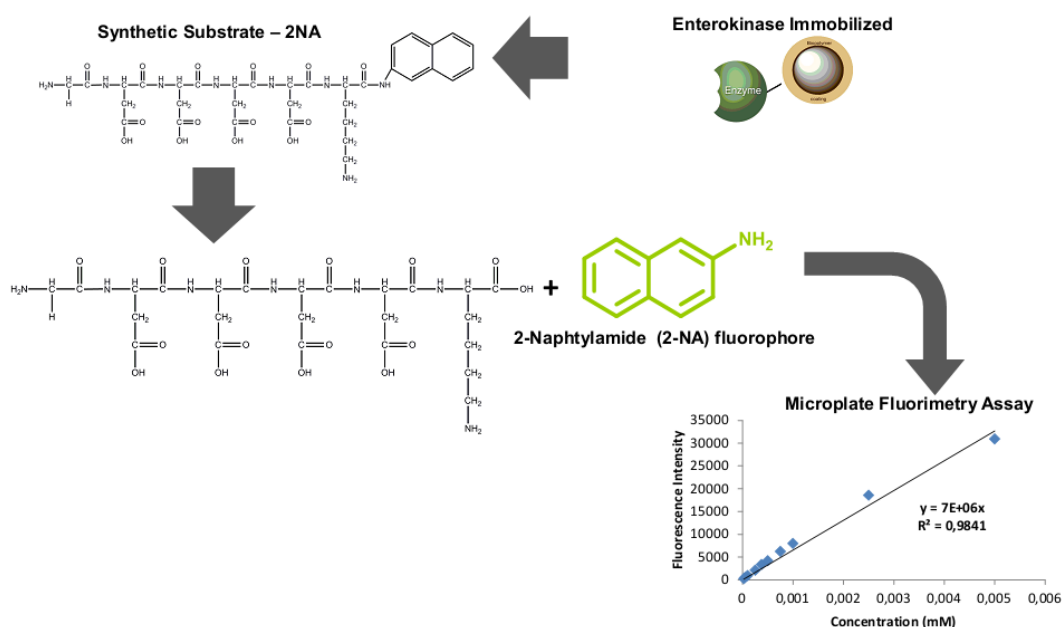


Figure 4.8 Schematic representation of the action of EK immobilized on the substrate GD₄K-2NA and consequent release and quantification of the product 2-NA obtained.

4.2.3 Activity Studies with Synthetic Substrate of Free and Immobilized Enterokinase

After immobilization of Enterokinase onto magnetic nanoparticles by two different chemistries, the supernatants were collected and analyzed to quantify the amount of unbound enzyme. To perform the quantification the synthetic substrate was added to the supernatants and the fluorescence was monitored along the time (this procedure is described in section 2.2.2.iv). After a cycle of 24 hours it was possible to estimate the amount of enzyme immobilized in each support as represented in Figure 4.9 and summarized in Table 4.2.

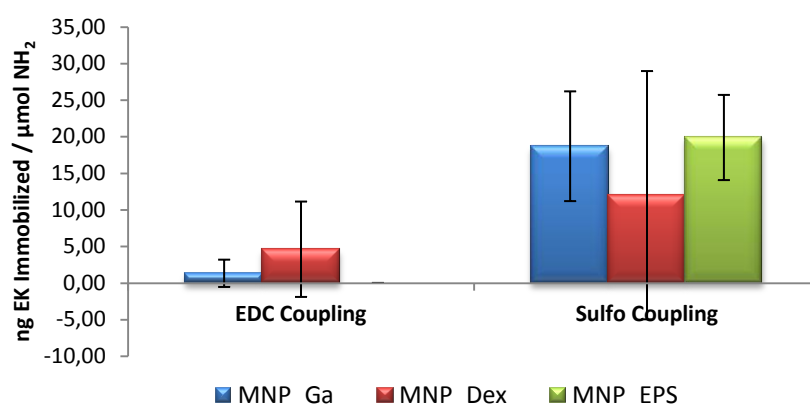


Figure 4.9 Quantity of enterokinase immobilized on magnetic nanoparticles by two different chemistries (n = 2).

It was possible to immobilize more enzyme by the Sulfo coupling method. This might be explained by the fact that the enzyme has available amines in its structure, and the intermediate compound formed during EDC activation instead of reacting with the available amines of the support, reacts with itself and some part of the enzyme remains in solution and is not immobilized on the support. In addition, the intermediate compound of this reaction is quite unstable. Although the EDC coupling method yields a lower amount of immobilized enzyme, retains more activity. This might be explained by the fact that when enzyme is immobilized by Sulfo coupling the EK might suffer some conformational effect.

Now analyzing each method in detail and starting by EDC Coupling it is possible to conclude that the support which immobilizes more quantity of enzyme is the MNP_Dex, followed by the MNP_Ga and MNP_EPS. For the case of the MNP_EPS the amount of EK immobilized is not measurable but the retention activity of this support is 28.5% (Table 4.2). This might be indicative that the method used to quantify enzyme is not sensitive enough to determine low quantity of enzyme immobilized. For

this immobilization method it is also observed that the MNP_EPS retains more enzymatic activity, despite being the method with less quantity of enzyme immobilized, followed by MNP_Dex and finally by MNP_Ga. Regarding the Sulfo coupling it is possible to conclude that the MNP_EPS immobilizes more quantity of EK followed by MNP_Ga and finally by MNP_Dex. Despite the MNP_Dex presented less quantity of EK immobilized it is the support that presents higher enzymatic activity retention.

Table 4.2 Immobilization methodologies for enterokinase to magnetic nanoparticles yielding the quantity of EK immobilized and activity retention.

Method	Support	ng EK immobilized / $\mu\text{mol NH}_2$	Activity Retention (%)
Free	Free EK	24 ^(Note 1)	-
EDC Coupling	MNP_Ga	1 \pm 2	1.4 %
	MNP_Dex	5 \pm 7	20.4 %
	MNP_EPS	0	28.5 %
Sulfo Coupling	MNP_Ga	19 \pm 8	0.5 %
	MNP_Dex	12 \pm 17	10.5 %
	MNP_EPS	20 \pm 6	1.0 %

Note 1: The quantity of Free EK “immobilized” per μmol of NH_2 available was estimated considering the maximum quantity of enzyme used in each immobilization (0.12 μg) and the maximum μmol of amines available in each support (5 $\mu\text{mol NH}_2$); **Note 2:** The activity retention was calculated by the ratio between the (Activity / $\mu\text{mol NH}_2$) of the immobilized EK and the (Activity / $\mu\text{mol NH}_2$) determined for the free EK and multiplied by 100 %, where activity is given by the mol of product released divided per the time of reaction. The activity retention was calculated only for the first cycle of use of the enzyme.

Overall and considering the quantity of enzyme used in each assay (values defined by the Free EK shown in the first row of Table 4.2) the MNP_EPS by Sulfo coupling immobilization was the support that was able to bind more enzyme. However, the MNP_Dex, for both immobilization methods, seems to be a better support because it has higher activity retention, which is preferable. Nevertheless some optimization studies in terms of immobilizing EK in magnetic supports should be performed because when compared with the literature studies, the EK immobilization on commercial paramagnetic microspheres and hexamethylamino sepabeads revealed an enzymatic activity retention of 42% and 60% (Kubitzki *et al.*, 2008), respectively, which is considerably higher when compared to the values obtained for EK immobilized on the magnetic nanoparticles synthesized in this work.

EK supports were then tested in single batch reactions for 24 hours with the synthetic substrate GD₄K-2NA. To compare and analyze the conversion of substrate, these assays were performed for immobilized and soluble EK. In these assays 25 µl of a solution 1 mM GD₄K-2NA, which corresponds to 2.5×10^{-8} mol of substrate, was used. Since the stoichiometry of this reaction is 1:1, if there is a conversion of 100%, in the end of each reaction must be quantified 2.5×10^{-8} mol of product (2-NA). These results were compared with the results of literature for EK immobilized on commercial paramagnetic microspheres and hexamethylamino sepabeads (Kubitzki *et al.*, 2008; Kubitzki *et al.*, 2009).

When an enzyme is immobilized usually there is a reduction of the activity which might be compensated by an increase in stability and the potential for re-utilization. Through analysis of Figure 4.10 and Figure 4.11, when immobilized EK is compared with soluble EK¹, it is possible to conclude that in the first batch there is a slight decrease in enzymatic activity, in both chemistries used. This might be explained by the immobilization effects caused on the enzyme. Due to the covalent immobilization of the enzyme the interaction between the support and the enzyme can modify the enzyme structure, which influences its activity and some denaturation might also occur. Also some steric hindrance effects might occur due to blocking of the active site of EK by adjacent functional groups or unsuitable immobilization position. Another effect caused by immobilization is internal mass transfer limitations that can happen due to some “porous” structure that the biopolymer net might create around the particles causing some encapsulation of the enzyme which hinders the accessibility of the substrate. Finally, some external diffusional limitations, despite being decreased by the surface area of the support used, might occur due to the difficult diffusion of substrate within the liquid phase to the surface of the support (Sun and Li, 2004; Buchholz *et al.*, 2005; Kubitzki *et al.*, 2008).

It is also possible to observe that the conversion percentage increases with the number of batches. This situation stands out more for the sulfo coupling but it is also notorious for the support MNP_EPS with EK immobilized by the EDC coupling. To explain this situation it is possible to predict that there is some adsorption of the substrate and/or product that is converted and desorb, over the number of reactions that occurred, this situation was already observed in other studies using EK immobilized due to the fact that enzyme – supports can act as a reservoir due to presence of a biopolymer net surrounding the MNPs (Kubitzki *et al.*, 2009). Despite

¹ In the free EK assays was used 3 U of EK in each reaction, that it is, theoretically, the maximum quantity of enzyme immobilized per ml of magnetic nanoparticles used.

this situation, EK immobilized on magnetic nanoparticles, independently of the chemistry used, was re-used 10 times in repeated batch reactions, which is slightly less when compared with the 18 times of re-utilization of EK described in the literature (Kubitzki *et al.*, 2009).

Now looking only for the conversion of EK immobilized by the EDC coupling it is possible to conclude that the MNP_Ga is the support where the enzyme is less active, followed by the MNP_Dex. Finally, the MNP_EPS it is the support where EK has higher percentage of conversion of the substrate. However, the MNP_EPS is also the support that presents higher nonspecific adsorption due to the reasons previously explained. For the EDC coupling method, based on the conversion percentage obtained, the support MNP_Dex seems to be the best support because presents a higher but stable conversion without an abnormal increase along the different batches performed.

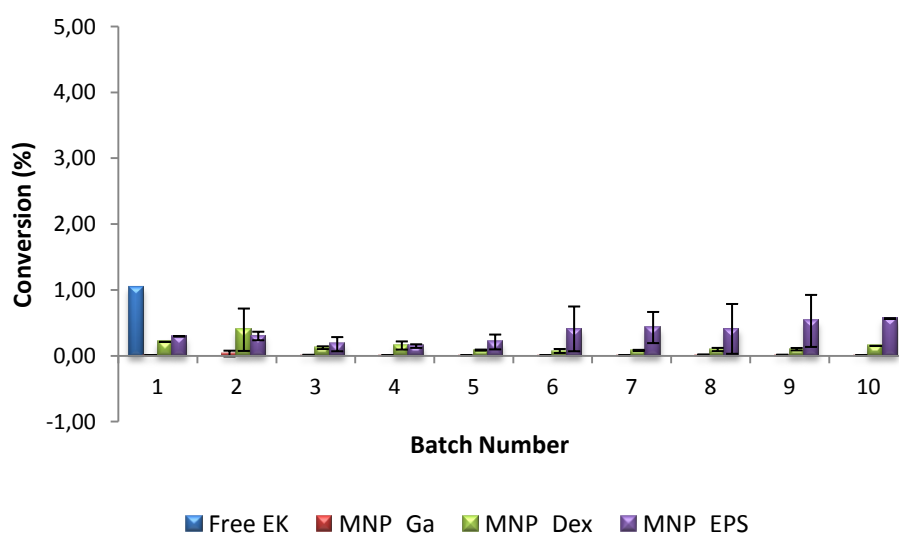


Figure 4.10 Percentage of substrate converted by EK immobilized on different magnetic supports through EDC Coupling. The reaction solution was removed after 24 hours and new solution was added for a new cleavage reaction. The set reaction conditions involved 25 μ l of 1 mM GD4K-2NA in 50 mM Tris-HCl, pH 7.4 incubated with 1 mL of magnetic support containing EK immobilized.

For the case of the Sulfo coupling method, once again MNP_Ga is the support where EK had less conversion of the substrate, while the MNP_EPS is the support where EK had higher conversion. However, for this method for both MNP_Ga and MNP_EPS is observed an abnormal increase of the conversion with the number of batches that could be indicative of some nonspecific adsorption by these carriers. Again MNP_Dex revealed to be the best support for the Sulfo coupling, since it is preferable a support with less conversion but without nonspecific adsorption.

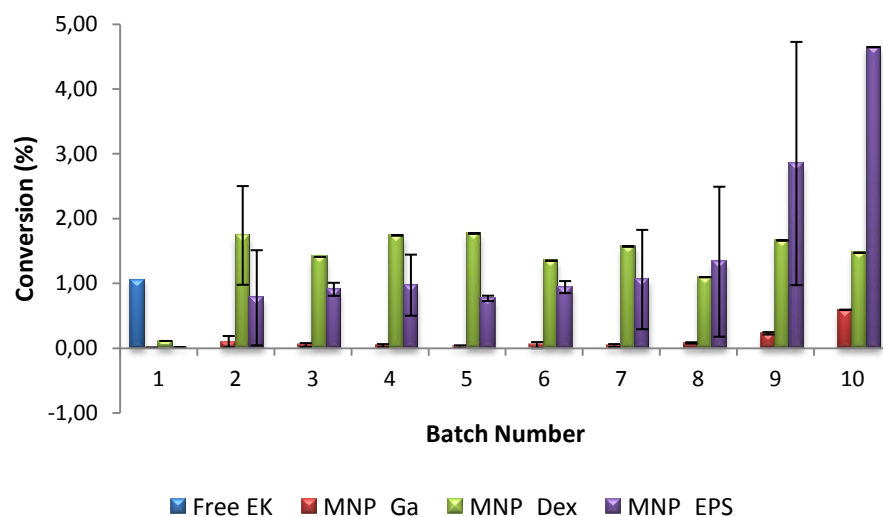


Figure 4.11 Percentage of substrate converted by EK immobilized on different magnetic supports through Sulfo Coupling. The reaction solution was removed after 24 hours and new solution was added for a new cleavage reaction. The set reaction conditions involved 25 μ l of 1 mM GD4K-2NA in 50 mM Tris-HCl, pH 7.4 incubated with 1 mL of magnetic support containing EK immobilized.

The modified supports with EK were characterized through DLS. The functionalization of EK seems to have different effects on the hydrodynamic diameters (Figure 4.12) depending on the different chemistry used to immobilize the enzyme. When EK is immobilized through EDC coupling the hydrodynamic diameter of these particles decreased. Whereas, when EK is immobilized by Sulfo coupling method the opposite happened, the hydrodynamic diameter slightly increased. These results are indicative that all the supports were functionalized with Enterokinase for both methodologies applied. About the zeta potential values obtained (Figure 4.13) it is also possible to conclude about the modification of the particles with the enzyme. The enzyme has an isoelectric point around 4 and at pH 7 becomes deprotonated (Faust *et al.*, 1974). After amination the particles become more positive, but these amines groups are used to bind to EK, therefore, upon EK immobilization the particles became more negatively charged. Regarding these considerations, when more enzyme is immobilized on the supports the more the negative these support became when compared with the zeta potential of the aminated support in Figure 3.8. This is confirmed in Figure 4.13 where the supports modified by the EDC coupling present less quantity of enzyme immobilized and consequently more positive values for zeta potential and the opposite happens for the supports modified by the sulfo coupling.

Taking into account all the presented results the MNP_Dex with EK immobilized by both chemistries were chosen to be the best supports and further studies with these two supports were performed.

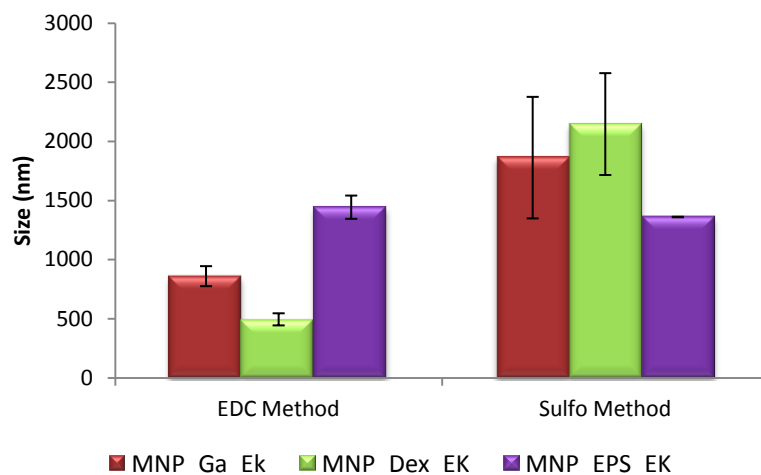


Figure 4.12 Hydrodynamic diameter (nm) of the magnetic supports immobilized with EK by EDC Coupling by dynamic light scattering analysis (n = 2).

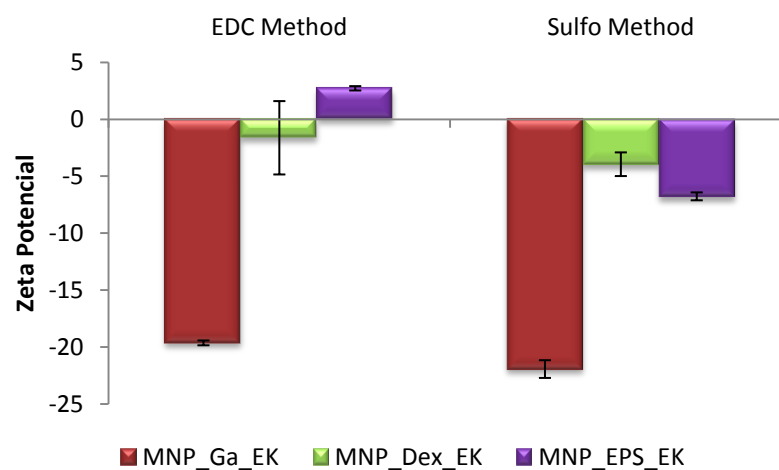


Figure 4.13 Zeta Potential values at pH 7 for magnetic supports immobilized with EK by Sulfo Coupling by dynamic light scattering analysis (n = 2).

4.2.4 Optimization and Testing of the Best Supports Selected

The immobilization of Enterokinase on MNP_Dex was repeated in order to optimize the amount and the activity of immobilized enzyme. For the case of the sulfo coupling no changes were made to the protocol previously followed (section 2.2.2.ii). On the other hand for the case of EDC coupling a different buffer was used during the immobilization method. A MES buffer (4-morpholinoethanesulfonic acid) was chosen because it is more suitable for carbodiimide reactions. Also a new reagent, *N*-hydroxysuccinimide (NHS), was added in the reaction in order to improve stability of the intermediate compound and to enhance the conjugation to the primary amines.

After repeating and optimizing the immobilization conditions for EK in the MNP_Dex supports, the quantity of EK immobilized and the activity retention were again calculated and discussed.

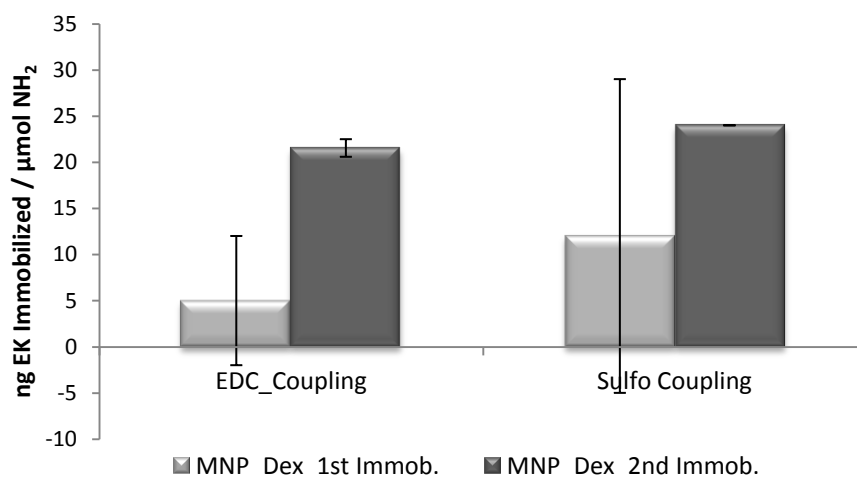


Figure 4.14 Comparison of the quantity of Enterokinase immobilized on MNP_Dex by the two different chemistries before and after optimizing the immobilization conditions (n = 2).

Through analysis of Figure 4.14 and Table 4.3 it is possible to conclude that after optimizing the immobilization conditions of EK to MNP_Dex supports there is an increase in the quantity of enzyme immobilized and this increase is reflected in the increase of the percentage of enzymatic activity retention. However, the sulfo coupling method continues to yield higher quantity of enzyme immobilized but less activity retention which is once again indicative that the chemistry used to immobilize EK might change the enzyme structure. For the EDC coupling these optimization bring an activity retention more comparable to the 42% activity retention of EK on the commercial paramagnetic microspheres described on literature (Kubitzki *et al.*, 2008).

Table 4.3 Immobilization methodologies for Enterokinase to magnetic nanoparticles yielding the quantity of EK immobilized and activity retention after optimizing immobilization conditions (n = 2).

Method	Support	ng EK immobilized / $\mu\text{mol NH}_2$	Activity Retention (%)
Free	Free EK	24	-
EDC Coupling	MNP_Dex	21 ± 1	35 %
Sulfo Coupling	MNP_Dex	24 ± 0	19 %

Note 1: The quantity of Free EK “immobilized” per μmol of NH_2 available was estimated considering the maximum quantity of enzyme used in each immobilization (0.12 μg) and the maximum μmol of amines available in each support (5 $\mu\text{mol NH}_2$); **Note 2:** The activity retention was calculated by the ratio between the (Activity / $\mu\text{mol NH}_2$) of the immobilized EK and the (Activity / $\mu\text{mol NH}_2$) determined for the free EK and multiplied by 100 %, where activity is given by the mol of product released divided per the time of reaction. The activity retention was calculated only for the first cycle of use of the enzyme.

To proceed with the studies, each of the supports was tested with the synthetic substrate. After each reaction the support was washed 10 times with Tris-HCl, pH 7.4 buffer and the fluorescence of the washes was monitored in order to improve the recovery of the supports and ensure that there is no product adsorbed to the supports. By analyzing Figure 4.15, the EDC coupling has two times more percentage of conversion when compared with the Sulfo coupling in the first batch. Then a decrease of the percentage of conversion is observed for both supports on the second and third batch. From the third batch onwards the conversion percentage stabilizes and it seems that this time there is no substrate and/or product adsorbed on the supports. Only five batches were tested in order confirm the conversion of the substrate by the enzyme and to conclude about what is the best support to proceed with further studies.

In terms of characterization (Table 4.4), for the MNP_Dex modified by the EDC coupling the hydrodynamic diameter increases while for the sulfo coupling slightly decreases, when compared with the first immobilization method performed. In terms of zeta potential values in both cases the values became more negative after enzyme immobilization, when compared with the first immobilized method performed, what is suggestive that more quantity of enzyme was functionalized on the supports.

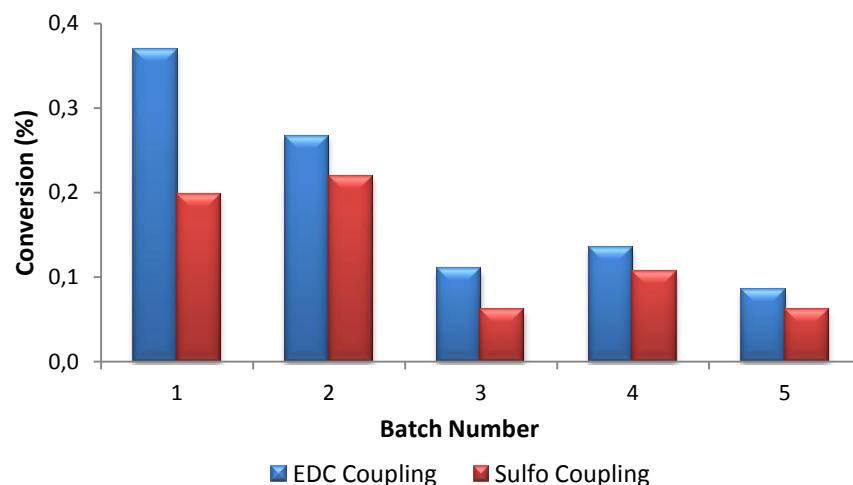


Figure 4.15 Percentage of substrate converted by EK immobilized on different MNP_Dex by the EDC and Sulfo Coupling. The reaction solution was removed after 24 hours and new solution was added for a new cleavage reaction. The set reaction conditions involved 25 μ l of 1 mM GD4K-2NA in 50 mM Tris-HCl, pH 7.4 incubated with 1 mL of magnetic

Overall the support that best suits higher activity retention of the enzyme and higher conversion, but lower nonspecific adsorption is MNP_Dex with EK immobilized by the EDC coupling and this support was used for further studies.

Table 4.4 Characterization of the hydrodynamic diameter (nm) and Zeta Potential (mV) values by DLS of MNP_Dex with EK immobilized by two different chemistries (n = 2).

Method	Support	Hydrodynamic diameter (nm)	Zeta Potential (mV)
EDC Coupling	MNP_Dex	1531 \pm 17	-15 \pm 7
Sulfo Coupling	MNP_Dex	1235 \pm 84	-13 \pm 3

4.2.5 Fusion protein cleavage by Immobilized EK

After choosing MNP_Dex with Enterokinase immobilized by EDC coupling, a preliminary study with two protein models, containing the EK recognition sequence, was performed in order to evaluate the capacity of this support to cleave a fusion protein.

One of the fusion proteins used was a Cleavage Control Protein from Novagen with a total molecular weight of 48 kDa. When cleaved it forms two proteolytic fragments of 32 kDa and 16 kDa. The second protein used was a crude extract of a fusion protein expressed at the Biomolecular Engineering Group, FCT-UNL. This fusion protein has a total molecular weight of 31 kDa and when is cleaved it forms two proteolytic fragments, 29 kDa for the protein and 2 kDa for the tag.

By analyzing Figure 4.16, that presents the results for the Cleavage Control Protein from Novagen, it is possible to observe that in the initial sample there is a band with a molecular weight of 48 kDa (total protein). However, the concentration of the protein used seems to be higher for the case of the soluble EK when compared with the immobilized EK. For the digestion with soluble EK (Figure 4.16– A), after 16 hours, is observed a band between 26 kDa and 32 kDa that corresponds to the first proteolytic fragment and the soluble enzyme. However, it is not possible to distinguish between the proteolytic fragment (32 kDa) and the enzyme (26.3 kDa), because they have similar molecular weights. It is also possible to observe a second band with molecular weight around 16 kDa that corresponds to the second fragment of the Cleavage Control Protein. For the case of immobilized EK (Figure 4.16– B) after digestion of the protein there might exist a low intense band at 32 kDa and no band at 16 kDa. This might be explained by different reasons. The enzyme might did not cleave the protein or the steric hindrance effect of the enzyme prevented the large protein to reach the small binding site of the enzyme, as already has been observed in literature (Kubitzki *et al.*, 2008). Therefore, a band at 48 kDa should be observed after digestion and in this case the low intense band at 32 kDa does not correspond to a real protein band. There is also the possibility of not having enough concentration of Cleavage Control Protein and when cleaved there is not enough concentration of which fragment to appear in the gel. Another reason to explain this situation is the adsorption of the substrate to the carrier, in this case the reaction time should be increased so there is enough time for the reaction product formed to desorb from the support (Kubitzki *et al.*, 2009). In this both case the low intense band at 32 kDa might correspond to the first proteolytic fragment.

For the case of the digestion of the second fusion protein, through analysis of Figure 4.17, it is possible to observe that in the initial sample there are some contaminant proteins. However, is notorious a more intense band slightly above 25 kDa marker which corresponds to the molecular weight of the fusion protein used. When this protein is digested with the soluble or the immobilized EK (Figure 4.17 A and B) two bands with different intensities, depending on the digestion used, appear around the molecular weight of 25 kDa that might correspond to the fusion protein not cleaved (31 kDa), to the fragment of 29 kDa of the fusion protein or to the soluble Enterokinase that presents a molecular weight of 26.3 kDa (in the case of the soluble EK if was used). Since the cleaved fragment with 2 kDa did not appear in any of the gels it is not possible to conclude about the cleavage capacity of the soluble and immobilized EK on MNP_Dex by EDC coupling.

Overall it was not possible to conclude about the cleavage capacity of fusion proteins by EK immobilized onto MNP_Dex. For the case of the Cleavage Control Protein it might be necessary to increase the concentration of this protein in the reaction mixture. Other viable option that was followed in the literature for the cleavage of mucin fusion protein would be to increase the reaction time to guarantee a total cleavage and/or desorption of the product (Kubitzki *et al.*, 2008; Kubitzki *et al.*, 2009). Whereas, for the case of the crude extract of fusion protein these tests should be performed with a different gel in order to confirm the presence of the second band at 2 kDa to evaluate the cleavage capacity of EK. One viable option would be testing this sample in a Tris-Tricine gel which presents higher resolution for low molecular weight proteins and peptides.

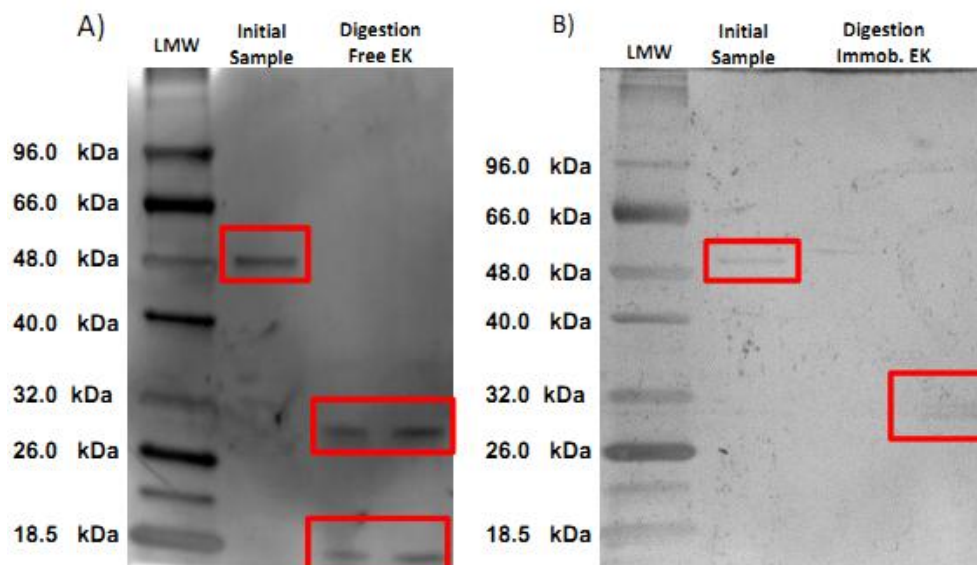


Figure 4.16 Electrophoreses gel 12,5 % in denaturation conditions to verify the digestion of the Cleavage Control Protein: A) Digestion of Cleavage Control Protein by soluble Enterokinase and B) Digestion of Cleavage Control Protein by immobilized Enterokinase; LMW (Low Molecular Weight).

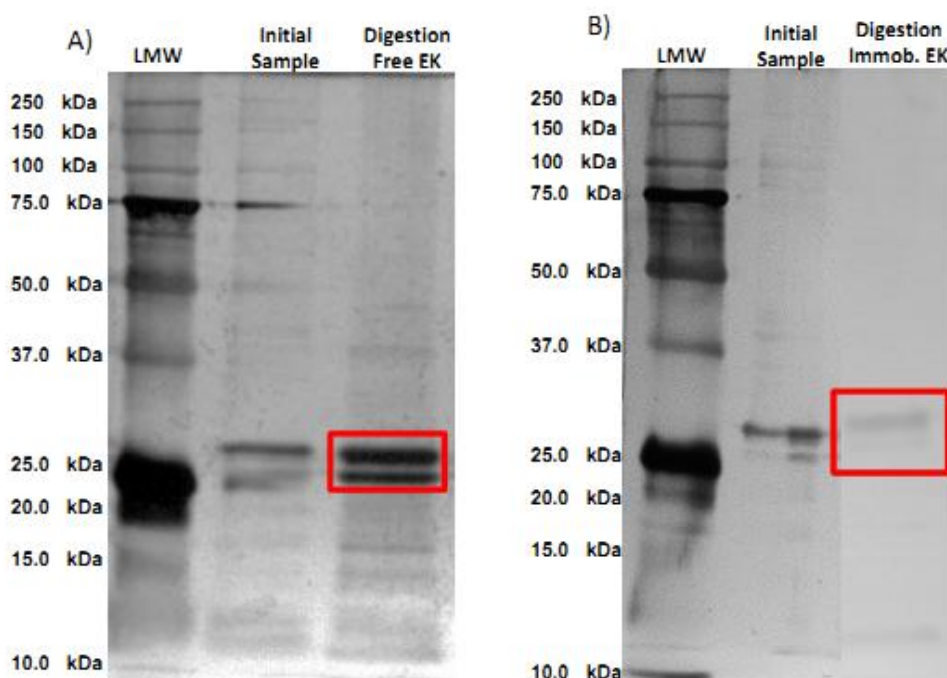


Figure 4.17 Electrophoreses gel 12,5 % in denaturation conditions to verify the digestion of the Fusion Protein: A) Digestion of Fusion Protein by soluble Enterokinase and B) Digestion of Fusion Protein by immobilized Enterokinase; LMW (Low Molecular Weight).

4.3 Conclusions

In this chapter, the immobilization of Enterokinase by two different chemistries in different magnetic supports has been studied. All the supports were tested with a synthetic substrate and re-utilized 10 times in single batch reactions. This support also proved to be able to simplify the product purification since it can easily be removed from the reaction mixture due to its superparamagnetic properties. The EDC coupling retained higher activity of the immobilized enzyme and seemed to have less nonspecific adsorption. The best support revealed to be the MNP_Dex and some immobilization conditions were optimized in order to repeat the immobilization of Enterokinase. After this optimization, the MNP_Dex with EK immobilized by EDC coupling revealed to be the best support with activity retention of 35% comparable to the 42% of EK immobilized on commercial paramagnetic supports. A percentage of conversion of 0.4% when compared with the 1% of conversion of the soluble enzyme was obtained. These low conversion results for soluble EK reveal the instability of this enzyme, which makes the process of EK immobilization extremely complicated to achieve. The EK immobilized in magnetic supports still has some drawbacks related to the fact that the cleavage of large fusion proteins can become more difficult and some optimization is needed.

Still, these preliminary studies using MNPs as solid supports for enzyme immobilization revealed to be highly attractive and promising.

5 MAGNETIC NANOPARTICLES APPLIED ON BIOSEPARATION

This chapter focuses on the application of Magnetic Nanoparticles for bioseparation processes, particularly for antibody purification. Three different immobilization methods of ligand 22/8, known to bind antibodies, on the three supports studied in chapter 3 have been explored. These supports have been initially tested for binding to pure human IgG solutions. Upon selection of the most promising magnetic support, studies with crude extracts containing antibodies and antibody fragments have been performed.

5.1 Introduction

The purification of antibodies from complex biological mixtures usually accounts for a large proportion of the total costs of production. In general the traditional processes involve several steps. Affinity chromatography appears as a useful technique due to its highly binding specificity, reduction of the nonspecific interactions, increased yield and better elimination of the unwanted contaminants (Roco, 2004; Roque and Lowe, 2006; Roque *et al.*, 2007).

In order to improve this technique there have been progresses in finding and generating affinity ligands of variable complexity and selectivity for the purification of different biomolecules (Roque *et al.*, 2007).

Synthetic affinity ligands were developed for the purpose of avoiding the disadvantages associated to the natural biological ligands, namely, high cost associated to the production, problems associated with reusability and harsh conditions to be applied in the elution steps which can contribute to ligand leaching and contaminate the final product (Roque *et al.*, 2004; Roque *et al.*, 2007).

Teng and co-workers designed, synthesized, characterized and immobilized a synthetic affinity ligand (22/8) which mimics the natural affinity receptor Protein A. This ligand possesses a triazine scaffold substituted with 3 - aminophenol and 4 - amino - 1 - naphthol and was chosen because it shows affinity for both Fab and Fc fragments of hIgG (Teng *et al.*, 2000).

The choice of the support where the ligand is immobilized is also a key step for binding the target molecule (Lowe *et al.*, 2001). The immobilization of ligand 22/8 on agarose beads is extensively studied on literature (Teng *et al.*, 1999; Teng *et al.*, 2000; Roque and Lowe, 2006; Roque *et al.*, 2007). However, as packed bed chromatography can face problems associated to column plugging, there is usually the need for the pre-treatment of the samples, such as centrifugation, filtration and membrane separation, in order to eliminate cell debris or other colloidal contaminants (Bucak *et al.*, 2003).

Regarding these considerations, Batalha and co-workers immobilized ligand 22/8 onto Gum Arabic coated iron oxide MNPs. This support revealed to be an alternative that can be applied on high gradient magnetic fishing processes (Batalha *et al.*, 2010).

5.2 Results and Discussion

Three different magnetic supports selected and studied in chapter 3 were tested for the bioseparation processes.

For separation applications a solid support must possess stability to the conditions of the synthesis and screening, reduced nonspecific interactions and possess chemical functionality for modifications (Guillier *et al.*, 2000; Batalha *et al.*, 2010).

After the synthesis of the solid supports (MNP_Ga; MNP_Dex and MNP_EPS) all the supports were modified with amine groups as already explained in chapter 3. Some supports were further modified with aldehyde groups. These steps were crucial for the functionalization with the synthetic affinity ligand 22/8, where three different methods of immobilization were tested (Figure 2.3). The synthetic ligand was synthesized based on triazine chemistry using cyanuric chloride as the scaffold structure and the two chloride atoms were shifted by the amines depending on its reactivity (Teng *et al.*, 1999).

In Method A, ligand 22/8 was synthesized in solution-phase with a six carbon spacer. The free amine groups on the spacer served as the handle to conjugate the ligand on the magnetic supports (Guillier *et al.*, 2000).

In Method B, the ligand 22/8 was also synthesized in solution-phase but without a six carbon spacer. In this case, the spacer was only introduced through the amino-silanization step. By removing the arm spacer of the ligand its solubility improved.

Finally, for Method C ligand 22/8 is synthesized directly on the solid support.

5.2.1 Binding Properties of Magnetic Supports to Pure Protein Solutions

After modification of the different magnetic supports with the affinity ligand 22/8 these were tested for binding to pure solutions of human IgG. The buffer conditions used for binding human IgG on the magnetic supports were selected according to previous studies using agarose as the solid support (Li *et al.*, 1998). Li and co-workers concluded that the best binding buffer was 50 mM phosphate, pH 8 because the interactions of IgG with immobilized ligand are stronger near neutral pH and promoted at higher salt concentration due to the hydrophobic interactions (Li *et al.*,

1998). In terms of the elution conditions, Teng and co-workers concluded that the buffer that has an optimum combination of yield and purity of the eluted hIgG in agarose was 0.1 M glycine – HCl, pH 3 (Teng *et al.*, 2000). However, due to the leaching problems at acidic pH of the iron oxide MNPs, Batalha and co-workers studied several elution conditions for hIgG and concluded that the best alternative would be to elute with 50 mM glycine-NaOH, pH 11 (Batalha *et al.*, 2010). During this work, the elution at basic pH was selected. During the assessment for binding human IgG the bound and eluted antibody was monitored by BCA method.

Through the results in Table 5.1, bare MNP and MNP coated with the different biopolymers were compared with the traditional support for bioseparation processes, agarose.

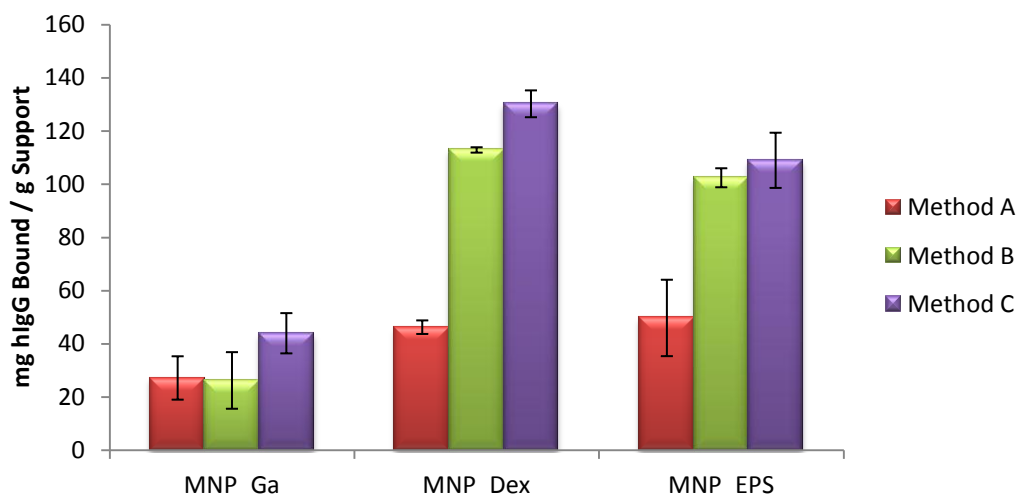
When compared with all the magnetic supports, bare agarose presented the lowest nonspecific interactions. In terms of the magnetic supports, bare MNPs are the supports with a less inert surface, binding 24 mg hIgG per gram of dried MNP. Most of the nonspecific interactions between bare iron oxide MNPs and hIgG are probably electrostatic.

Through these results once again is possible to conclude that the coating of the iron oxide particles with biopolymers it is a crucial step, because reduces the nonspecific interactions when compared with bare MNPs. This reduction can be explained through the creation of a more hydrophilic layer around the iron oxides particles which makes the magnetic supports more inert. In terms of the best coating, MNP_Dex presented the lowest values of binding to human hIgG, followed by MNP_EPS and finally by MNP_Ga. This might be explained by the way the coating of the surface of the supports was performed. As presented on chapter 3 MNP_Dex were successfully coated with Dextran, which is a neutral polysaccharide so its charge is practically zero, which makes of this support less reactive. Whereas the MNP_Ga despite having a good coating its biopolymer is negatively charged so they tend to have available groups that can create more easily interactions, which makes of this support the most reactive. For the MNP_EPS this support presents most of core unprotected which might be responsible for most of the nonspecific interactions of this carrier. However, it is important to keep in mind that even when there is a successfully coating it is not uniform and homogeneous which creates a net with “porous” structures that leave the reactive iron oxide of the particles partly exposed to create interactions and might have some contribution in the nonspecific adsorption of the supports.

Table 5.1 Binding of hIgG to bare agarose and magnetic supports, being the agarose results from Batalha *et al.*, 2010 ($n = 2$).

MNP Supports	mg hIgG Bound/g MNP
Agarose	0
Bare MNP	24 ± 2
MNP_Ga	16 ± 1
MNP_Dex	4 ± 4
MNP_EPS	11 ± 2

Afterwards, the different magnetic supports were immobilized with ligand 22/8 through different methods they were evaluated in terms of binding hIgG from a pure solution, as presented in Figure 5.1 and Figure 5.2. Different coating strategies yielded distinct behaviors for binding to hIgG.

**Figure 5.1** Binding of Human IgG to different solid supports modified with synthetic affinity ligand 22/8 (artificial protein A) - Results normalized per gram of particles used in each assay ($n = 2$).

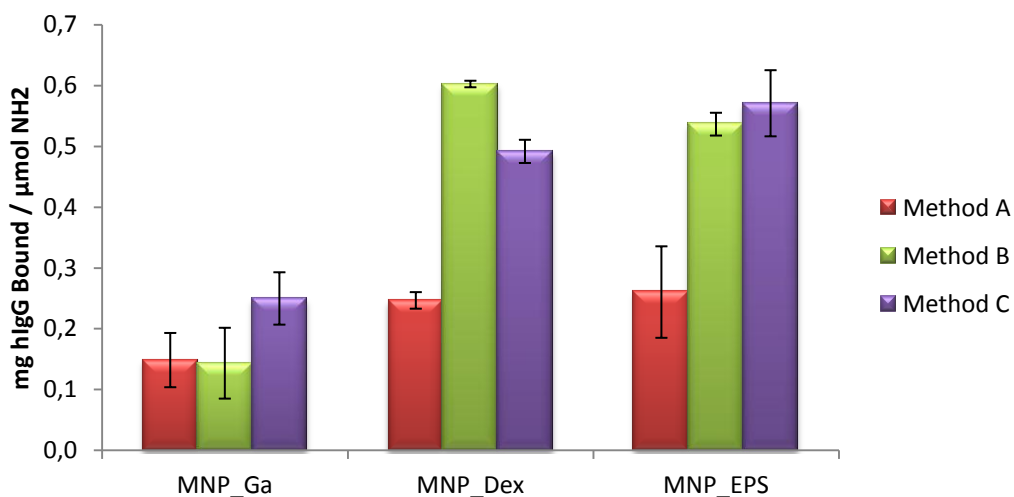


Figure 5.2 Binding of Human IgG to different solid supports modified with synthetic affinity ligand 22/8 (artificial protein A) – Results normalized per μmol of amine available in each support ($n = 2$).

For all ligand immobilization methods, MNP_Dex and MNP_EPS supports presented the best results of binding hIgG, when compared with MNP_Ga. The later revealed less capacity of binding hIgG, which might indicate that this support has less amount of ligand immobilized. In general MNP_Dex presented the best results for any of the immobilization methods performed.

These differences are correlated with the amount of amine groups available on the surface of the supports. As already presented in Table 3.2, MNP_Dex presented the highest percentage of amination, followed by MNP_EPS and finally by MNP_Ga. In principle, a support with less amines has less quantity of ligand 22/8 immobilized on the surface of the support, which can have a direct implication on the quantity of hIgG bound to the support. The amount of hIgG bound on each support was normalized in terms of the quantity of amines available (Figure 5.2). MNP_Dex and MNP_EPS presented similar results, and MNP_Ga still bound less hIgG.

In general, Method A revealed to be the less suitable method for immobilizing the synthetic affinity ligand, followed by Method B and method C.

In Method A, there is the need to use a strong crosslinker (glutaraldehyde) which can react also with amine groups from neighboring particles, therefore reducing the aldehyde groups available to react with the amine groups from the ligand. In addition, the solubility of the ligand is very poor. For Method B, this procedure is performed at high temperature (80-90 °C) at which the less reactive chloride of the ligand is substituted. Consequently the quantity of ligand that is immobilized on the support

may be compromised. In the case of Method C, this is a multistep reaction where the coupling of the triazine ring is done at 0°C through the most reactive chloride, therefore less likely to result in low reaction yields.

According to what was discussed in the chapter 5.2.1 about the elution conditions, after performing binding hIgG to the support modified with the ligand 22/8 the protein recovery was studied (Figure 5.3).

For MNP_Ga supports modified it is not possible to quantify eluted protein. This might indicate that the method used to quantify the amount of protein eluted is not sensitive enough for the small amount of protein that is recovered. The same conclusions are observed for the MNP_Dex and MNP_EPS with ligand 22/8 immobilized through Method A where less amount of hIgG bound to the supports.

For MNP_Dex, when ligand 22/8 was immobilized by method B it is possible to elute 42 ± 1 mg hIgG eluted/g MNP which corresponds to 37%² of the bound protein, while for the ligand immobilized through method C, 46% of bound protein (60.1 ± 0.7 mg hIgG eluted/g MNP) was eluted.

For MNP_EPS modified with ligand 22/8, these supports eluted 60% and 40% of protein bound from the ligand immobilized by method B and method C, respectively.

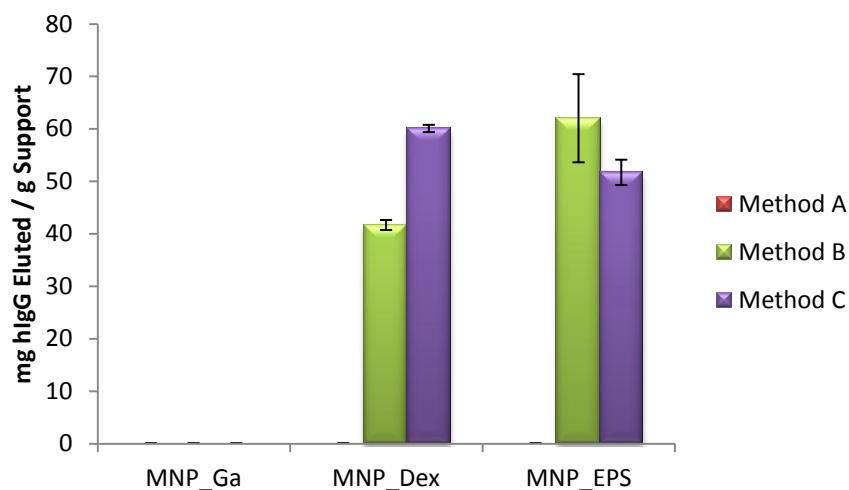


Figure 5.3 Human IgG eluted from magnetic supports at 50 mM Glycine - NaOH, pH 11 (n = 2).

² In all situations mentioned the % of eluted protein is calculated through the follow equation, (mg eluted*100)/mg bound

As a result of these studies, MNP_Dex appears as the most promising magnetic supports for binding IgG through ligand 22/8. When MNP_Dex is modified with ligand 22/8 immobilized through Method C, this support binds 130 ± 5 mg hIgG bound/g MNP, and elute 60.1 ± 0.7 mg hIgG eluted/g MNP and presents less nonspecific adsorption.

The magnetic support MNP_Dex modified with ligand 22/8 through Method C was utilized for further studies. The magnetic support was tested for binding to a model contaminant protein, Bovine Serum Albumin (BSA), for which the support should not present affinity.

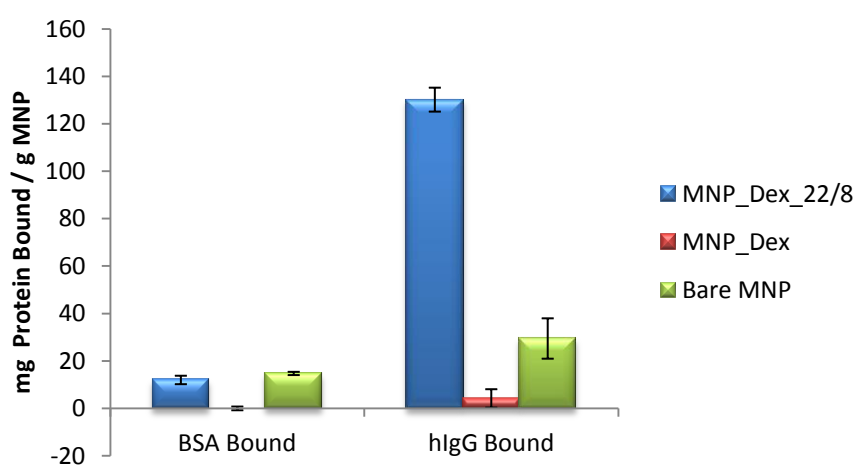


Figure 5.4 Binding of Albumine Serum Bovine and Human IgG to MNP_Dex modified with ligand 22/8 through the Method C (n = 2).

The magnetic support bound 12 ± 2 mg BSA bound/g MNP, a ten fold lower value when compared to the quantity of hIgG bound (130 ± 5 mg hIgG bound/g MNP) (Figure 5.4). Even when the naked supports (Bare MNP and MNP_Dex) are tested with BSA, these also present less nonspecific adsorption for BSA than for hIgG.

Other study performed with MNP_Dex modified with ligand 22/8 by Method C was the adsorption isotherm of human IgG on this support (Figure 5.5) which was fitted in a Langmuir type isotherm.

Through the fitting of the adsorption curve of hIgG, an affinity constant of $3.06 \times 10^5 \text{ M}^{-1}$ (K_a) and a theoretical maximum capacity of 512 ± 19 mg hIgG adsorbed/g MNP (Q_{\max}) were obtained with a correlation factor of 0.99 (Table 5.2). The affinity constant value is similar to the Protein A immobilized in agarose and higher than the value for ligand 22/8 immobilized in agarose. In terms of Q_{\max} value, the MNP_Dex modified with ligand 22/8 has a value nearly four times higher than the same ligand immobilized in

agarose and thirty times higher than the natural Protein A immobilized in agarose. These results suggest that the adsorbent studied in this work seems to be a potential option to be applied in bioseparation processes.

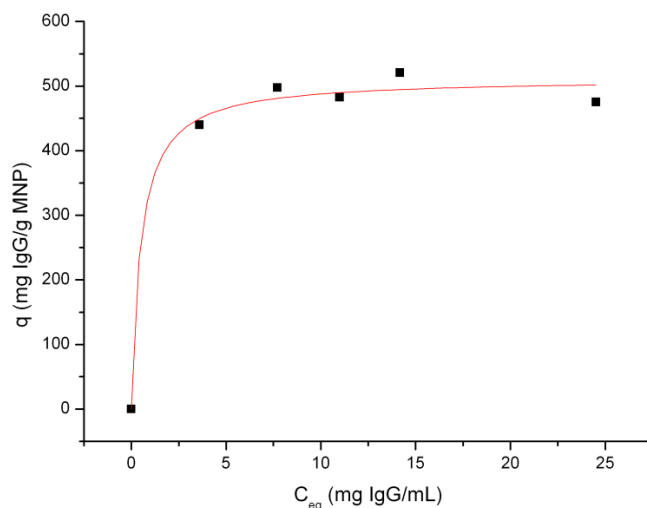


Figure 5.5 Binding of hIgG at the surface of MNP_Dex modified with ligand 22/8 by Method C. Representation of q (the amount of bound hIgG in equilibrium per mass of solid support) as function of C_{eq} (the concentration of hIgG in equilibrium). Experimental data was fitted with the expression $q = (Q_{max} \times C_{eq}) / (K_d + C_{eq})$ for the Langmuir isotherm (using the OriginLab 6.1 software), where Q_{max} corresponds to the maximum concentration of the matrix sites available to the partitioning solute (which can also be defined as the binding capacity of the adsorbent), and K_d is the dissociation constant.

Table 5.2 Comparison of binding isotherm of human IgG to immobilized protein A and ligand 22/8 onto agarose (Teng *et al.*, 2000) to ligand 22/8 immobilized on MNP_Dex through Method C.

Parameters	Protein A in agarose	Ligand 22/8 in agarose	Ligand 22/8 in MNP_Dex
K_a (M^{-1})	3.65×10^5	1.4×10^5	3.06×10^5
Q_{max} (hIgG adsorbed (mg) / Support (g))	17.0	151.9	512

The supports modified with ligand 22/8 through Method C were characterized by DLS, the results obtained are summarized in Figure 5.6, Table 5.3 and Figure 5.7.

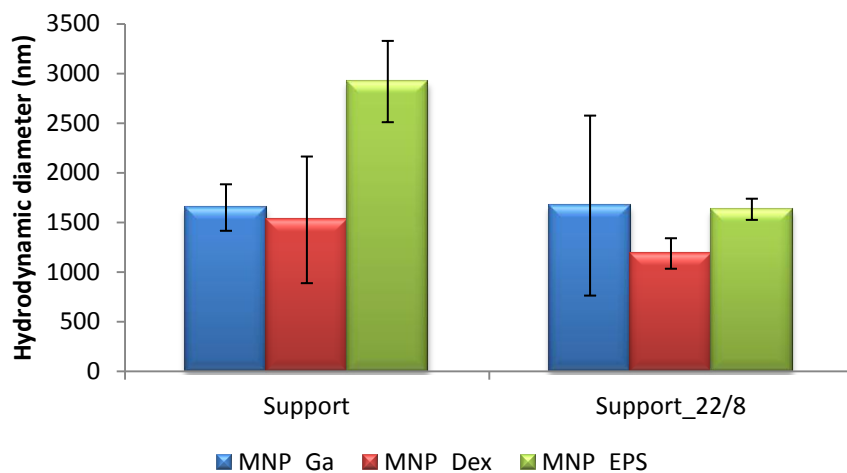


Figure 5.6 Hydrodynamic diameter (nm) of the magnetic support modified with synthetic affinity ligand 22/8 through Method C by dynamic light scattering analysis ($n = 2$).

Table 5.3 Hydrodynamic Diameter and Polydispersity values for MNP_Dex modified with ligand 22/8 by Method C.

MNP Supports	Hydrodynamic Diameter (nm)	PDI
MNP_Ga_22/8	1669 ± 906	0.6 ± 0.2
MNP_Dex_22/8	1187 ± 154	0.4 ± 0.3
MNP_EPS_22/8	1632 ± 107	0.97 ± 0.03

The hydrodynamic diameter for MNP_Ga before and after being modified does not change considerably which might corroborate the low quantity of ligand functionalized in this support. For MNP_Dex and MNP_EPS, the hydrodynamic diameter decreases slightly upon modification with ligand 22/8. The functionalization with ligand 22/8 can create steric restrictions, (Batalha *et al.*, 2010) alteration of surface charge or hydrophobicity which reduces the hydrodynamic diameter of the agglomerates. In terms of the polydispersity index this parameter continue to present high values, although more acceptable for MNP_Dex (0.4) which is indicative that the modification of the particles with the ligand 22/8 is not enough to create uniform particles.

As already mentioned in chapter 3, since the coating with biopolymers creates agglomerates and the functionalization with ligand 22/8 is not enough to reduce the size of these agglomerates, other technique should be tested to determine the hydrodynamic size of the particles such as Mastersize 2000 from Malvern as previously referred.

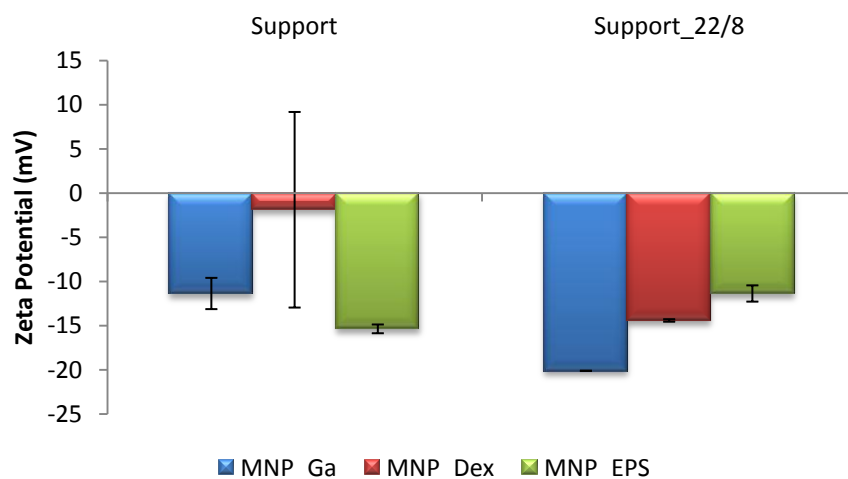


Figure 5.7 Zeta Potential values (mV) at pH 7 of the magnetic support modified with synthetic affinity ligand 22/8 through Method C by dynamic light scattering analysis (n = 2)

Finally in terms of zeta potential (Figure 5.7) the MNP_Ga and MNP_Dex when modified with ligand 22/8 became more negative and the MNP_EPS became slightly less negative. These changes in the zeta potential values are indicative of modifications in the supports because the charges in the surface rearrange due to the presence of new functionalization groups on the surface of the support, as already observed in literature (Batalha *et al.*, 2010).

In the future it might be useful to improve amination of the supports as an attempt to improve the amount of ligand immobilized which is directly related with the binding toward IgG. It would be also interesting to test other conditions of binding and elution in order to improve the quantity of antibody that is bound and recovered from the support.

5.2.2 Binding Properties of Magnetic Supports to Crude Extracts

After studying the supports with pure solutions of hIgG and BSA, the MNP_Dex particles were tested with two different crude extracts containing antibody related proteins. With these tests it was supposed to evaluate the binding specificity of the support in the presence of a mixture of different yeast and mammalian proteins, depending on the crude extracts used.

The yeast crude extract contains a Single-chain antibody Fragment (scFv) extracellularly expressed by *Pichia pastoris*, kindly provided by Professor Rui Oliveira (Requimte, DQ, FCT-UNL). A scFv is an engineered antibody consisting of a heavy and a light chain variable regions connected by a peptide linker. The supernatant of this extract is constituted by three different forms of scFv antibody: covalent homodimer, associative homodimer and monomer. The monomer form of the scFv is between 25 – 30 kDa, while the homodimer forms are around 50 kDa, although they became monomers with the same size under reducing conditions (Marty *et al.*, 2001; Cunha *et al.*, 2004).

The mammalian crude extract is rich in monoclonal antibody (Mab) expressed by Chinese hamster ovary cells (CHO cells), kindly provided by Doutora Paula Alves (ITQB/IBET). These antibodies are glycoproteins with a total molecular weight of 150 kDa. Under reducing conditions, antibody yield structures with several molecular weights (100 kDa; 50 kDa and 25 kDa).

The MNP_Dex modified with ligand 22/8 by Method C was tested with 500 μ L of each crude extract in the same conditions described for the pure solutions of hIgG. After the binding of the antibody to the support, this was washed five times to guarantee that all proteins adsorbed nonspecifically are removed. Subsequently, the total volume of adsorbent used in each case was divided in two vessels and two elution conditions were tested. The first elution condition tested was with a 50 mM Glycine – HCl, pH 3 based on the studies of Teng and co-workers (Teng *et al.*, 2000). The other elution condition was maintained according to what was explained in chapter 5.2.1 for the elution of pure solutions of hIgG in magnetic supports. All the samples collected, for both cases, were analyzed through SDS-PAGE and stained with Silver Staining because it is a more sensitive technique for staining proteins with capability of detecting bands containing less than 0.1 ng / mm² of protein.

Through observation of Figure 5.8 it is possible to conclude that the MNP_Dex modified with ligand 22/8 by Method C is able to bind and elute scFv from the crude

extract. The binding capacity is confirmed by the decrease in intensity of the flowthrough, when compared with the loading, of the bands around 25 kDa and 50 kDa, corresponding respectively for the monomer and homodimer scFv. It was possible to elute the scFv at pH 11, once again confirmed by the presence of the same bands at 25 kDa and 50 kDa. However at pH 3 it was not possible to elute scFv because there are no visible bands. For the MNP_Dex, through the analysis of Figure 5.9 it is possible to conclude that the support is inert because in the flowthrough is observed that most of the scFv is collected and neither at pH 3 or 11 is observed any band at 25 kDa and 50 kDa.

For the case of the purification of Mabs (Figure 5.10), it is possible to conclude that the chosen support is also capable of binding and eluting Mabs. These conclusions are confirmed by the presence of two distinct bands of IgG at 25 kDa and 50 kDa in the lanes of the elution. For this case it was possible to elute the Mabs at pH 3 and pH 11, however at pH 11 it was eluted IgG in the first and second elution step and with higher concentration than at pH 3. The amount of support used is not enough to bind all IgG used in the assay, which is confirmed by the presence of the IgG bands in all washes. Once again the inertness of the MNP_Dex but this time against the Mabs was confirmed by the gel on Figure 5.11. This gel shows the presence of concentrated bands in the flowthrough, almost equivalent to the bands of the loading, which is indicative that the protein did not bind to the support and was collected in the flowthrough. Furthermore there is any band in the elution lanes which is indicative that there are any proteins bound to the support to be eluted.

For both cases that have been studied the elution conditions at pH 3 did not reveal to be as good as at pH 11 as Teng and co-workers studied (Teng *et al.*, 2000). This might be explained by the fact that the particles are chemically unstable at acidic pH through leaching of the iron, as already discussed, which effect the properties of the matrix and have direct influence in the elution of the product to be purified (Hermanson *et al.*, 1992).

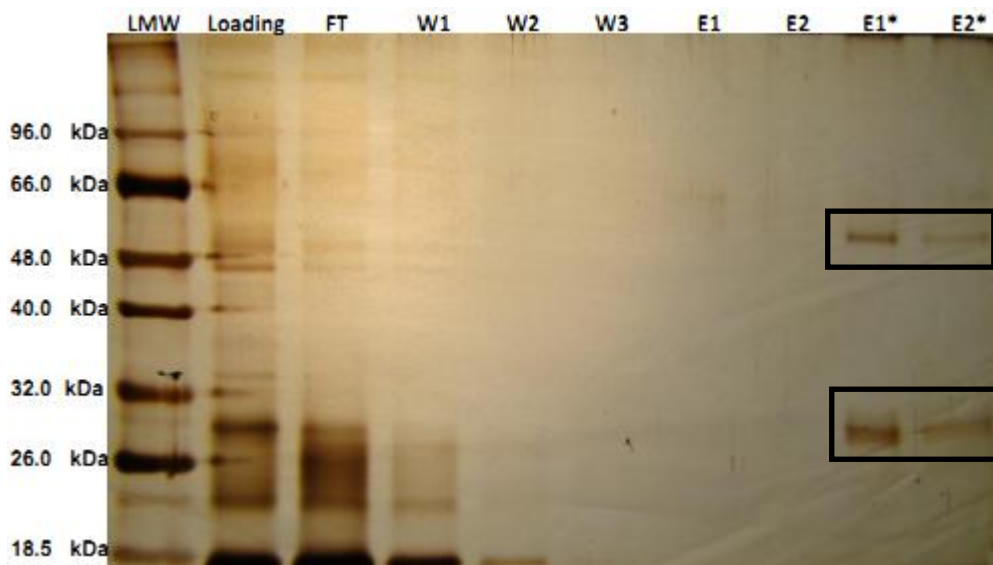


Figure 5.8 Electrophoreses gel 12,5 % in denaturation conditions to verify the binding capacity and the best elution conditions for ScFv from the MNP_Dex_{22/8}. LMW (Low Molecular Weight); Loading (Sample of the crude extract incubated with the adsorbent); FT (Flowthrought); W₁ (First Wash with Binding Buffer); W₂ (Second Wash with Binding Buffer); W₃ (Third Wash with Binding Buffer); E₁ (First Elution with 50 mM Glycine – HCl, pH 3); E₂ (Second Elution with 50 mM Glycine – HCl, pH 3); E₁* (First Elution with 50 mM Glycine – HCl, pH 11); E₂* (Second Elution with 50 mM Glycine – HCl, pH 11).

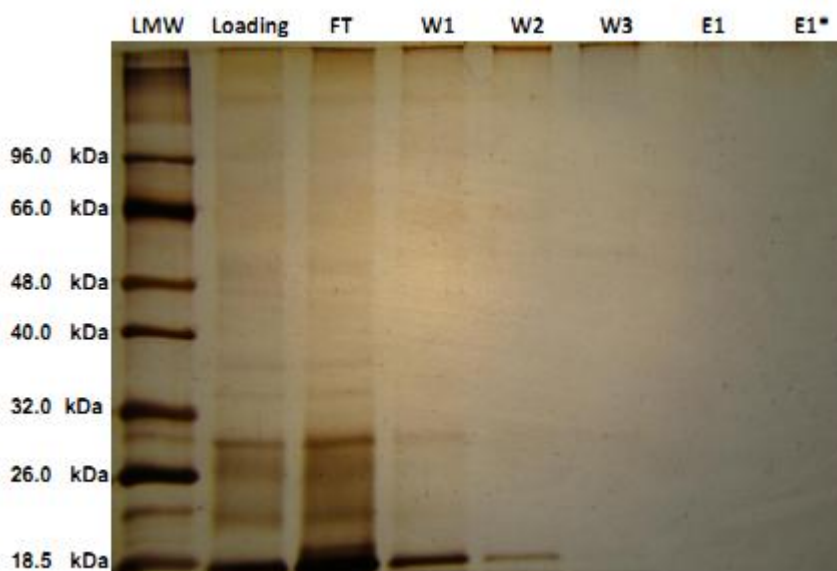


Figure 5.9 Electrophoreses gel 12,5 % in desnaturating conditions to verify the inertness of MNP_Dex for ScFv. LMW (Low Molecular Weight); Loading (Sample of the crude extract incubated with the adsorbent); FT (Flowthrought); W₁ (First Wash with Binding Buffer); W₂ (Second Wash with Binding Buffer); W₃ (Third Wash with Binding Buffer); E₁ (First Elution with 50 mM Glycine – HCl, pH 3); E₁* (First Elution with 50 mM Glycine – HCl, pH 11).

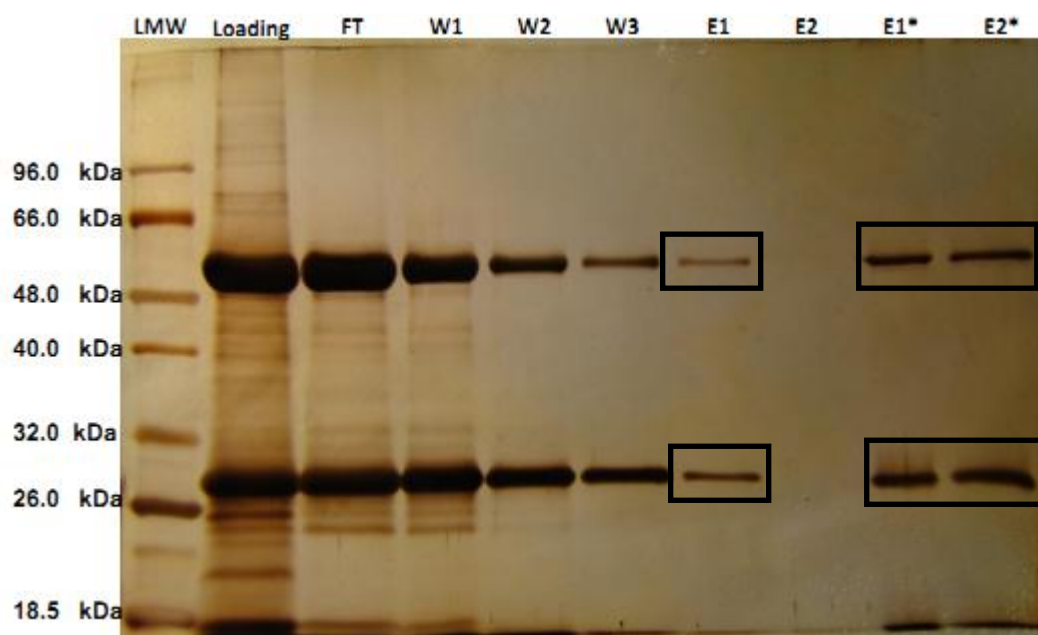


Figure 5.10 Electrophoreses gel 12,5 % in denaturation conditions to verify the inertness of MNP_Dex for Mabs. LMW (Low Molecular Weight); Loading (Sample of the crude extract incubated with the adsorbent); FT (Flowthrough); W₁ (First Wash with Binding Buffer); W₂ (Second Wash with Binding Buffer); W₃ (Third Wash with Binding Buffer); E₁ (First Elution with 50 mM Glycine – HCl, pH 3); E₁* (First Elution with 50 mM Glycine – HCl, pH 11).

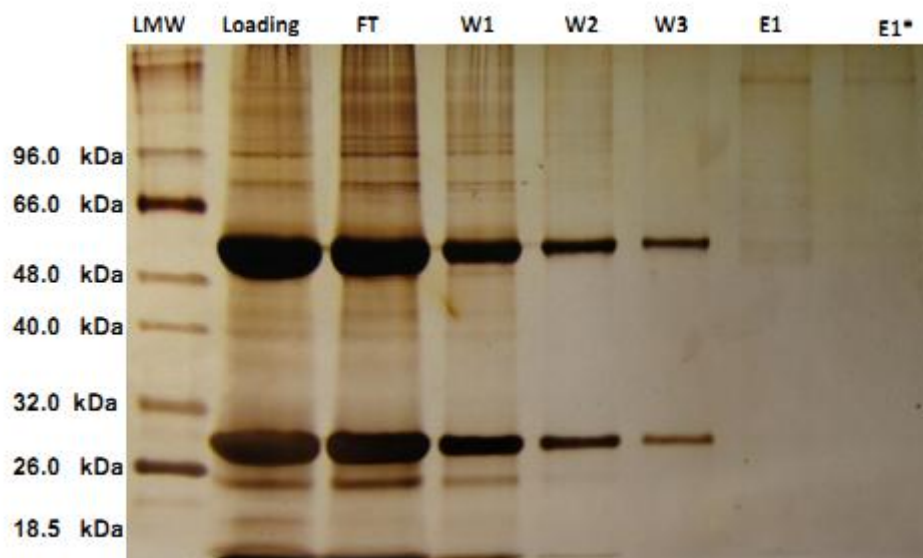


Figure 5.11 Electrophoreses gel 12,5 % in denaturation conditions to verify the inertness of MNP_Dex for Mabs. LMW (Low Molecular Weight); Loading (Sample of the crude extract incubated with the adsorbent); FT (Flowthrough); W₁ (First Wash with Binding Buffer); W₂ (Second Wash with Binding Buffer); W₃ (Third Wash with Binding Buffer); E₁ (First Elution with 50 mM Glycine – HCl, pH 3); E₁* (First Elution with 50 mM Glycine – HCl, pH 11).

After confirmation by SDS-PAGE electrophoresis of the binding and elution capacity of the support in both crude extracts studied, the samples collected were quantified by the BCA method in order to determine the amount of protein bound to and eluted from the support. However, in any of the cases, it was not possible to quantify the amount of protein bound and eluted. This might be explained by the fact that was not used a blank control with the exactly same composition of the culture media where each antibody was expressed. In addition, the crude extracts used in its composition may have substances that cause interference to the method of quantification. For example, in the case of ScFv crude extract has in its composition glycerol and methanol that are substances that causes interference in the BCA Method.

In terms of future works it is important to quantify the amount of protein bound to and eluted from the support. However, through BCA method it was not possible to determine theses values, so the methods that could be used to confirm and quantify the amount of antibody bond and eluted it is a Western Blot technique which separates the proteins of a certain lane of the SDS-PAGE by mass and an ELISA assay which is a technique used to quantify antibodies.

5.3 Conclusions

The modification of the different magnetic supports, studied in the chapter 3, with the ligand 22/8 was performed with success. From all immobilization methods performed the best method turned out to be Method C, which consists in the direct synthesis of the ligand 22/8 on the support based on the triazine scaffold. Whereas the best support reveal to be the iron oxide MNPs coated with Dextran. This support was chosen as the best one since it was the support with the best relation of high specificity and low nonspecific adsorption of hIgG from pure solutions. Moreover the affinity constant of this new adsorbent for hIgG is superior to the results obtained for agarose with ligand 22/8 immobilized and comparable to the ones of Protein A also immobilized on agarose beads, which proves once again how promising this support can be. As for the studies of this support with crude extracts here the binding and elution capacities of scfV and Mabs were confirmed. However these assays require further optimization in terms of increasing the binding capacity of the support to bind all the antibodies available in the assay and also in terms of the ability to quantify the amount of protein bound to and eluted from the support.

Overall it is possible to conclude that MNPs coated with biopolymers and immobilized with ligand 22/8 were found to have promising characteristics for the application of these adsorbents in bioseparation processes, particularly in antibody purification.

6 CONCLUDING REMARKS AND FUTURE DIRECTIONS

This chapter delivers a summary of the work performed. It then provides further development highlights, which are improvements and features that should be taken into consideration.

In this work magnetic particles were investigated as a support for the immobilization of an enzyme, Enterokinase (EK), used for cleavage of fusion proteins after protein purification. Bioseparation studies were also conducted by making use of the same magnetic supports modified with an affinity synthetic ligand (Ligand 22/8) used for the purification of antibodies.

MNPs were synthesized by the co-precipitation method and coated with different biopolymers (gum Arabic - Ga, dextran - Dex and extracellular polysaccharide - EPS) by an *in-situ* coating strategy. The quantity of biopolymer surrounding the particles was analyzed by the anthrone method and compared with the binding profiles for each biopolymer. EPS coating appeared as the less optimized method. The stability of magnetic supports towards storage and modification was also studied, showing high stability of the biopolymer coating in all supports. When MNPs are coated with biopolymers the hydrodynamic size increased for values between 1000 – 3000 nm, which indicates agglomeration of the particles. Besides that, the zeta potential also varies according to the charge of the polymer used. In the future, optimization of the MNP_EPS synthesis should be performed as well as more studies on characterization and stability of the supports, perhaps solvent, pH and temperature resistance.

To study the application of magnetic nanoparticles to the biocatalysis field the three supports synthesized were immobilized with EK by two different chemistries (EDC and Sulfo Coupling) and the enzyme activity was tested with a synthetic substrate. A preliminary study with two recombinant fusion proteins was also performed.

The immobilization methods used were selected according to the percentage of total groups available on the surface of the enzyme by molecular structure analysis. The quantity of EK immobilized was lower for the EDC coupling due to possible crosslinking effects, which reduce the quantity of enzyme available to be immobilized. However, the EDC coupling presented higher activity retention, 28.5%, compared with the 10.5% for the Sulfo coupling. The Sulfo coupling yielded supports with higher conversions but also higher nonspecific adsorption. However, when analyzing only the first cycle of reaction the EDC coupling presented higher conversion, but a loss of enzymatic activity for both methods was observed when compared with soluble EK. The loss of enzymatic activity upon covalent immobilization is well studied and reported (Buchholz *et al.*, 2005). It is known that several effects contribute for the loss of activity, namely conformational (alterations on the enzyme structure), inaccessibility of the active site, and mass transfer limitations caused by the heterogeneous catalysis and perhaps by the polymeric net coating the MNPs that can

create “porous” structures that limit the accessibility of the substrate. This loss of activity was compensated by the re-utilization of the immobilized enzyme up to ten times. The results show that the MNP_Dex was the best support for both chemistries showing high activity retention and less nonspecific adsorption. Therefore, the methods of immobilizing EK were optimized and tested once again for more five cycles with the synthetic substrate. The best support for EK immobilization was the MNP_Dex by the EDC coupling with an activity retention comparable to the results obtained in the literature (Kubitzki *et al.*, 2008). Preliminary cleavage of fusion recombinant proteins, were then performed with this support. However from the SDS-PAGE gels it was not possible to conclude about the enzymatic activity of the immobilized support. Different reaction conditions, such as, higher concentration of the fusion recombinant proteins, a gel with a different reticulation degree, different reaction time and a higher quantity of enzyme immobilized in the support should be tested. Enterokinase appears as a very unstable enzyme, which is confirmed by the low activity presented by its soluble form, which causes the immobilization of this enzyme on solid supports difficult and challenging, as shown by the very few reports on the immobilization of EK. Previous work conducted at Biomolecular Engineering Lab has shown that MNPs are very suitable for immobilization of lipase.

Finally, the applicability of the magnetic nanoparticles for bioseparation processes was tested through immobilization of the synthetic ligand 22/8, by three different methods.

All the supports were successfully modified with the synthetic affinity ligand, however the MNP_Dex with ligand 22/8 immobilized by triazine-based strategy (Method C) was the most promising support. It revealed a binding capacity of 130 ± 5 mg hIgG bound/g MNP and an elution capacity of 60.1 ± 0.7 mg hIgG eluted/g MNP for pure hIgG. In addition, this support also showed less nonspecific adsorption in the presence of BSA. The estimated values for maximum binding capacity and affinity constant for ligand 22/8 were comparable with protein A and ligand 22/8 immobilized on agarose. Also to prove the binding capacity of this support in real conditions a preliminary test using two different crude extracts containing different antibody species (Mabs and scFv) was conducted. These results proved the specificity and binding capacity of the support in the presence of a raw mixture of different proteins expressed by different systems. More studies need to be conducted in future in order to confirm the binding capacity of these supports and the purity of the recovered proteins.

Overall, iron oxide magnetic nanoparticles revealed to be a promising alternative in biocatalysis and bioseparation processes, specifically for antibody purification.

7 BIBLIOGRAPHY

- Amin, R., Hwang, S., et al., *Nanobiotechnology: An interface between nanotechnology and biotechnology*, Nano, **2011**, 6, 101-111.
- Arnau, J., Lauritzen, C., et al., *Current strategies for the use of affinity tags and tag removal for the purification of recombinant proteins*, Protein Expression and Purification, **2006**, 48, 1-13.
- Babes, L., Denizot, B., et al., *Synthesis of Iron Oxide Nanoparticles Used as MRI Contrast Agents: A Parametric Study*, Journal of Colloid and Interface Science, **1999**, 212, 474-482.
- Bäckström, M., Link, T., et al., *Recombinant MUC1 mucin with a breast cancer-like O-glycosylation produced in large amounts in Chinese-hamster ovary cells*, Biochem. J., **2003**, 376, 677-686.
- Batalha, I. L., Hussain, A., et al., *Gum Arabic coated magnetic nanoparticles with affinity ligands specific for antibodies*, Journal of Molecular Recognition, **2010**, 23, 462-471.
- Bhushan, B. (2004). Springer Handbook of Nanotechnology, Springer - Verlag.
- Birch, J. R. and Racher, A. J., *Antibody production*, Advanced Drug Delivery Reviews, **2006**, 58, 671-685.
- Bosse-Doenecke, E., Weininger, U., et al., *High yield production of recombinant native and modified peptides exemplified by ligands for G-protein coupled receptors*, Protein Expression and Purification, **2008**, 58, 114-121.
- Boyer, C., Whittaker, M. R., et al., *The design and utility of polymer-stabilized iron-oxide nanoparticles for nanomedicine applications*, NPG Asia Materials, **2010**, 23-30.
- Bucak, S., Jones, D. A., et al., *Protein Separations Using Colloidal Magnetic Nanoparticles*, Biotechnology Progress, **2003**, 19, 477-484.
- Buchholz, K., Bornscheuer, U. T., et al., **2005**, *Biocatalysts And Enzyme Technology*. WILEY-VCH Verlagsgesellschaft mbH.
- Clonis, Y. D., *Affinity chromatography matures as bioinformatic and combinatorial tools develop*, Journal of Chromatography A, **2006**, 1101, 1-24.
- Corchero, J. L. and Villaverde, A., *Biomedical applications of distally controlled magnetic nanoparticles*, Trends in Biotechnology, **2009**, 27, 468-476.
- Cunha, A. E., Clemente, J. J., et al., *Methanol induction optimization for scFv antibody fragment production in Pichia pastoris*, Biotechnology and Bioengineering, **2004**, 86, 458-467.
- De, M., Ghosh, P. S., et al., *Applications of Nanoparticles in Biology*, Advanced Materials, **2008**, 20, 4225-4241.
- deMello, A. J. and Woolley, A. T., *Nanotechnology*, Current Opinion in Chemical Biology, **2010**, 14, 545-547.

- Dias, A. M. G. C., Hussain, A., et al., *A biotechnological perspective on the application of iron oxide magnetic colloids modified with polysaccharides*, Biotechnology Advances, **2011**, 29, 142-155.
- Ditsch, A., Laibinis, P. E., et al., *Controlled Clustering and Enhanced Stability of Polymer-Coated Magnetic Nanoparticles*, Langmuir, **2005**, 21, 6006-6018.
- Ditsch, A., Yin, J., et al., *Ion-Exchange Purification of Proteins Using Magnetic Nanoclusters*, Biotechnology Progress, **2006**, 22, 1153-1162.
- Dziadek, S., Hobel, A., et al., *A Fully Synthetic Vaccine Consisting of a Tumor-Associated Glycopeptide Antigen and a T-Cell Epitope for the Induction of a Highly Specific Humoral Immune Response*, Angewandte Chemie International Edition, **2005**, 44, 7630-7635.
- Fang, C. and Zhang, M., *Multifunctional magnetic nanoparticles for medical imaging applications*, Journal of Materials Chemistry, **2009**, 19, 6258-6266.
- Fatehi, L., Wolf, S., et al., *Introduction: designing nanobiotechnology oversight*, Journal of Nanoparticle Research, **2011**, 13, 1341-1343.
- Faust, R. M., Hallam, G. M., et al., *Degradation of the parasporal crystal produced by Bacillus thuringiensis var. kurstaki*, Journal of Invertebrate Pathology, **1974**, 24, 365-373.
- Fonseca, P. and Light, A., *Incorporation of bovine enterokinase into synthetic phospholipid vesicles*, Biophysical journal, **1982**, 37, 44-45.
- Fonseca, P. and Light, A., *Incorporation of bovine enterokinase in reconstituted soybean phospholipid vesicles*, Journal of Biological Chemistry, **1983**, 258, 3069-3074.
- Franzreb, M., Siemann-Herzberg, M., et al., *Protein purification using magnetic adsorbent particles*, Applied Microbiology and Biotechnology, **2006**, 70, 505-516.
- Freitas, F., Alves, V. D., et al., *Characterization of an extracellular polysaccharide produced by a Pseudomonas strain grown on glycerol*, Bioresource Technology, **2009**, 100, 859-865.
- Gasparian, M. E., Bychkov, M. L., et al., *Strategy for improvement of enteropeptidase efficiency in tag removal processes*, Protein Expression and Purification, **2011**, 79, 191-196.
- González, Y., Ibarra, N., et al., *Expanded bed adsorption processing of mammalian cell culture fluid: comparison with packed bed affinity chromatography*, Journal of Chromatography B, **2003**, 784, 183-187.
- Grillo, M. E., Finnis, M. W., et al., *Surface structure and water adsorption on Fe₃O₄ (111): Spin-density functional theory and on-site Coulomb interactions*, Physical Review B, **2008**, 77, 075407.

- Guillier, F., Orain, D., et al., *Linkers and Cleavage Strategies in Solid-Phase Organic Synthesis and Combinatorial Chemistry*, Chemical Reviews, **2000**, 100, 2091-2158.
- Gupta, A. and Gupta, M., *Synthesis and surface engineering of iron oxide nanoparticles for biomedical applications*, Biomaterials, **2005**, 26, 3995-4021.
- Hermanson, G. T., Mallia, A. K., et al., **1992**, *Immobilized Affinity Ligand Techniques*. San Diego, Academic Press.
- Hong, R. Y., Feng, B., et al., *Synthesis, characterization and MRI application of dextran-coated Fe₃O₄ magnetic nanoparticles*, Biochemical Engineering Journal, **2008**, 42, 290-300.
- Horák, D., Babič, M., et al., *Preparation and properties of magnetic nano- and micro-sized particles for biological and environmental separations*, Journal of Separation Science, **2007**, 30, 1751-1772.
- Hradil, J., Pisarev, A., et al., *Dextran-modified iron oxide nanoparticles*, China Particuology, **2007**, 5, 162-168.
- Hu, S.-M., Wang, A. H. J., et al. (2001). Expression Tags for Protein Production. eLS, John Wiley & Sons, Ltd.
- Hubbuck, J. J., Matthiesen, D. B., et al., *High gradient magnetic separation versus expanded bed adsorption: a first principle comparison*, Bioseparation, **2001**, 10, 99-112.
- Huber, D. L., *Synthesis, Properties, and Applications of Iron Nanoparticles*, Small, **2005**, 1, 482-501.
- Jenny, R. J., Mann, K. G., et al., *A critical review of the methods for cleavage of fusion proteins with thrombin and factor Xa*, Protein Expression and Purification, **2003**, 31, 1-11.
- JianHan, X., Hui, S., et al., *Surface chemistry of nanoscale Fe₃O₄ dispersed in magnetic fluids*, Science in China Series B: Chemistry, **2007**, 50, 754-758.
- Jonasson, P., Liljeqvist, S., et al., *Genetic design for facilitated production and recovery of recombinant proteins in Escherichia coli*, Biotechnology and Applied Biochemistry, **2002**, 35, 91-105.
- Kievit, F. M., Veisheh, O., et al., *PEI-PEG-Chitosan-Copolymer-Coated Iron Oxide Nanoparticles for Safe Gene Delivery: Synthesis, Complexation, and Transfection*, Advanced Functional Materials, **2009**, 19, 2244-2251.
- Kim, D. K., Mikhaylova, M., et al., *Starch-Coated Superparamagnetic Nanoparticles as MR Contrast Agents*, Chemistry of Materials, **2003**, 15, 4343-4351.
- Kim, J., Grate, J. W., et al., *Nanostructures for enzyme stabilization*, Chemical Engineering Science, **2006**, 61, 1017-1026.

- Kitamoto, Y., Yuan, X., et al., *Enterokinase, the initiator of intestinal digestion, is a mosaic protease composed of a distinctive assortment of domains*, Proceedings of the National Academy of Sciences, **1994**, 91, 7588-7592.
- Kriangkum, J., Xu, B., et al., *Development and characterization of a bispecific single-chain antibody directed against T cells and ovarian carcinoma.*, Hybridoma, **2000**, 19, 33-41.
- Kubitzki, T., Minör, D., et al., *Application of immobilized bovine enterokinase in repetitive fusion protein cleavage for the production of mucin 1*, Biotechnology Journal, **2009**, 4, 1610-1618.
- Kubitzki, T., Noll, T., et al., *Immobilisation of bovine enterokinase and application of the immobilised enzyme in fusion protein cleavage*, Bioprocess and Biosystems Engineering, **2008**, 31, 173-182.
- Kuchibhatla, S., Karakoti, A., et al., *Colloidal stability by surface modification*, JOM Journal of the Minerals, Metals and Materials Society, **2005**, 57, 52-56.
- Labrou, N. E., *Design and selection of ligands for affinity chromatography*, Journal of Chromatography B, **2003**, 790, 67-78.
- Laurent, S., Forge, D., et al., *Magnetic Iron Oxide Nanoparticles: Synthesis, Stabilization, Vectorization, Physicochemical Characterizations, and Biological Applications*, Chemical Reviews, **2008**, 108, 2064-2110.
- Li, J., Staver, M. J., et al., *Expression and functional characterization of recombinant human HDAC1 and HDAC3*, Life Sciences, **2004**, 74, 2693-2705.
- Li, R., Dowd, V., et al., *Design, synthesis, and application of a Protein A mimetic*, Nat Biotech, **1998**, 16, 190-195.
- Li, Y. and Spencer, H. G., *Adsorption of dextrans on spherical TiO₂ particles*, Colloids and Surfaces, **1992**, 66, 189-195.
- Light, A. and Janska, H., *Enterokinase (enteropeptidase): comparative aspects*, Trends in Biochemical Sciences, **1989**, 14, 110-112.
- Liu, W.-T., *Nanoparticles and their biological and environmental applications*, Journal of Bioscience and Bioengineering, **2006**, 102, 1-7.
- Lowe, C. R., Lowe, A. R., et al., *New developments in affinity chromatography with potential application in the production of biopharmaceuticals*, Journal of Biochemical and Biophysical Methods, **2001**, 49, 561-574.
- Lu, A.-H., Salabas, E. L., et al., *Magnetic Nanoparticles: Synthesis, Protection, Functionalization, and Application*, Angewandte Chemie International Edition, **2007**, 46, 1222-1244.
- Lu, D., Fütterer, K., et al., *Crystal structure of enteropeptidase light chain complexed with an analog of the trypsinogen activation peptide*, Journal of Molecular Biology, **1999**, 292, 361-373.

- Lu, D., Yuan, X., et al., *Bovine Proenteropeptidase Is Activated by Trypsin, and the Specificity of Enteropeptidase Depends on the Heavy Chain*, Journal of Biological Chemistry, **1997**, 272, 31293-31300.
- Ma, H.-I., Qi, X.-R., et al., *Preparation and characterization of superparamagnetic iron oxide nanoparticles stabilized by alginate*, International Journal of Pharmaceutics, **2007**, 333, 177-186.
- Marcos, A. S. (2010). Magnetic Nanoparticles coated with EPS. Lisbon, New University of Lisbon, Faculty of Science and Technology.
- Marty, C., Scheidegger, P., et al., *Production of Functionalized Single-Chain Fv Antibody Fragments Binding to the ED-B Domain of the B-isoform of Fibronectin in Pichia pastoris*, Protein Expression and Purification, **2001**, 21, 156-164.
- Nixon, L., Koval, C. A., et al., *Preparation and characterization of novel magnetite-coated ion-exchange particles*, Chemistry of Materials, **1992**, 4, 117-121.
- Powers, D. B., Amersdorfer, P., et al., *Expression of single-chain Fv-Fc fusions in Pichia pastoris*, Journal of Immunological Methods, **2001**, 251, 123-135.
- Qi, D., Lu, J., et al., *Magnetically Responsive Fe₃O₄@C@SnO₂ Core-Shell Microspheres: Synthesis, Characterization and Application in Phosphoproteomics*, The Journal of Physical Chemistry C, **2009**, 113, 15854-15861.
- Ramsden, J. J., *What is nanotechnology?*, Nanotechnology Perceptions, **2005**, 1, 3-17.
- Roco, M. C., *Nanoscale Science and Engineering: Unifying and Transforming Tools*, AIChE Journal, **2004**, 50, 890-897.
- Roque, A. C. A., Bicho, A., et al., *Biocompatible and bioactive gum Arabic coated iron oxide magnetic nanoparticles*, Journal of Biotechnology, **2009**, 144, 313-320.
- Roque, A. C. A. and Lowe, C. R., *Advances and applications of de novo designed affinity ligands in proteomics*, Biotechnology Advances, **2006**, 24, 17-26.
- Roque, A. C. A., Lowe, C. R., et al., *Antibodies and Genetically Engineered Related Molecules: Production and Purification*, Biotechnology Progress, **2004**, 20, 639-654.
- Roque, A. C. A., Silva, C. S. O., et al., *Affinity-based methodologies and ligands for antibody purification: Advances and perspectives*, Journal of Chromatography A, **2007**, 1160, 44-55.
- Roque, A. C. A., Taipa, M. Â., et al., *Synthesis and screening of a rationally designed combinatorial library of affinity ligands mimicking protein L from Peptostreptococcus magnus*, Journal of Molecular Recognition, **2005a**, 18, 213-224.

- Roque, A. C. A., Taipa, M. Â., et al., *An artificial protein L for the purification of immunoglobulins and Fab fragments by affinity chromatography*, Journal of Chromatography A, **2005b**, 1064, 157-167.
- Roque, A. C. A. and Wilson Jr, O. C., *Adsorption of gum Arabic on bioceramic nanoparticles*, Materials Science and Engineering: C, **2008**, 28, 443-447.
- Rossi, L. M., Quach, A. D., et al., *Glucose oxidase–magnetite nanoparticle bioconjugate for glucose sensing*, Analytical and Bioanalytical Chemistry, **2004**, 380, 606-613.
- Safarik, I. and Safarikova, M., *Magnetic nano- and microparticles in biotechnology*, Chemical Papers, **2009**, 63, 497-505.
- Shoseyov, O. and Levy, I. (2008). *NanoBiotechnology - BioInspired Devices and Materials of the Future*, Springer - Verlag.
- Sturmfels, A., Götz, F., et al., *Secretion of human growth hormone by the food-grade bacterium *Staphylococcus carnosus* requires a propeptide irrespective of the signal peptide used*, Archives of Microbiology, **2001**, 175, 295-300.
- Suh, C. W., Park, S. H., et al., *Covalent immobilization and solid-phase refolding of enterokinase for fusion protein cleavage*, Process Biochemistry, **2005**, 40, 1755-1762.
- Sun, X. and Li, Y., *Colloidal Carbon Spheres and Their Core/Shell Structures with Noble-Metal Nanoparticles*, Angewandte Chemie International Edition, **2004**, 43, 597-601.
- Teng, S. F., Sproule, K., et al., *Affinity chromatography on immobilized “biomimetic” ligands: Synthesis, immobilization and chromatographic assessment of an immunoglobulin G-binding ligand*, Journal of Chromatography B: Biomedical Sciences and Applications, **2000**, 740, 1-15.
- Teng, S. F., Sproule, K., et al., *A strategy for the generation of biomimetic ligands for affinity chromatography. Combinatorial synthesis and biological evaluation of an IgG binding ligand*, Journal of Molecular Recognition, **1999**, 12, 67-75.
- Terpe, K., *Overview of tag protein fusions: from molecular and biochemical fundamentals to commercial systems*, Applied Microbiology and Biotechnology, **2003**, 60, 523-533.
- Wagner, B., Robeson, J., et al., *Horse cytokine/IgG fusion proteins – mammalian expression of biologically active cytokines and a system to verify antibody specificity to equine cytokines*, Veterinary Immunology and Immunopathology, **2005**, 105, 1-14.
- Wang, W., Singh, S., et al., *Antibody structure, instability, and formulation*, Journal of Pharmaceutical Sciences, **2007**, 96, 1-26.
- Wang, Z., Xiao, P., et al., *Synthesis and characteristics of carbon encapsulated magnetic nanoparticles produced by a hydrothermal reaction*, Carbon, **2006**, 44, 3277-3284.

- Waugh, D. S., *Making the most of affinity tags*, Trends in Biotechnology, **2005**, 23, 316-320.
- West, J. L. and Halas, N. J., *Applications of nanotechnology to biotechnology: Commentary*, Current Opinion in Biotechnology, **2000**, 11, 215-217.
- Williams, D., Gold, K., et al., *Surface Modification of Magnetic Nanoparticles Using Gum Arabic*, Journal of Nanoparticle Research, **2006**, 8, 749-753.
- Wilson Jr, O. C., Blair, E., et al., *Surface modification of magnetic nanoparticles with oleylamine and gum Arabic*, Materials Science and Engineering: C, **2008**, 28, 438-442.
- Won, Y.-H., Aboagye, D., et al., *Core/shell nanoparticles as hybrid platforms for the fabrication of a hydrogen peroxide biosensor*, Journal of Materials Chemistry, **2010**, 20, 5030-5034.
- Wu, W., He, Q., et al., *Magnetic Iron Oxide Nanoparticles: Synthesis and Surface Functionalization Strategies*, Nanoscale Research Letters, **2008**, 3, 397-415.
- Xu, X. Q., Shen, H., et al., *Core-shell structure and magnetic properties of magnetite magnetic fluids stabilized with dextran*, Applied Surface Science, **2005**, 252, 494-500.
- Zhao, Y., Qiu, Z., et al., *Preparation and Analysis of Fe₃O₄ Magnetic Nanoparticles Used as Targeted-drug Carriers*, Chinese Journal of Chemical Engineering, **2008**, 16, 451-455.